Taxus Cell Culture to Delivery System:

A Novel Approach to Administer Paclitaxel

A Major Qualifying Project

Submitted to the Faculty of Worcester Polytechnic Institute

in partial fulfillment of the requirement for the Degree in Bachelor of Science

in

Chemical Engineering

By

_____

Dasia Aldarondo

_____

Donald Dione

_____

Adele Werner

Date: April 25th, 2019

Project Advisors:

_____

Susan C. Roberts, Advisor

_____

Jeannine Coburn, Advisor

Abstract

Paclitaxel (PTX) is one of the leading chemotherapy drugs available for various solid tumor cancers and is most commonly administered systemically in a solution consisting of dehydrated alcohol and Cremophor EL. This project investigated the potential for a *Taxus* suspension culture derived local delivery system of PTX. For this purpose, increased cell-associated PTX accumulation, DNA removal, and release kinetics were investigated. PTX was retained throughout a piloted decellularization process at an average of 0.68 mg/L with greater than 80% DNA removal. The decellularized biomass allowed for almost complete drug release within 72 hours of suspension in 4 % bovine serum albumin solution. Initial release rate could be sustained when encapsulated in calcium alginate microbeads, suggesting this to be a feasible approach for PTX delivery. Moving forward, increasing the amount of PTX produced by Taxus culture through alternative elicitation methods and maximizing the PTX retained through processing is imperative to the feasibility of a cell culture-based drug delivery system.

Acknowledgements

Our team would like to thank those who have contributed to this project's success this past year. We extend gratitude to our project advisors and professors Susan C. Roberts and Jeannine M. Coburn for their insight and guidance, Michelle McKee for her ongoing support and patience, Lexi Crowell for keeping the lab fun, and to the members the Coburn lab for their cooperation over the course of this project.

Table of Contents

Table of Figures

Table of Tables

Chapter 1: Introduction

Cancer is one of the most prominent diseases in the world. The International Agency for Research on Cancer estimates there will be 18.1 million new cancer cases in 2018 and 9.6 million cancer deaths worldwide Bray, Ferlay [1]. Advancing treatments for cancer patients drives a large portion of the health field. In 2017, the NIH put $6.3 billion of its $33.1 billion budget towards cancer research [2]. Along with the development of new treatment options, traditional treatments are continuously being improved. In particular, chemotherapy, one of the three main treatment methods for solid tumors (along with surgery and radiation therapy), results in many negative side effects and is therefore continually being refined [3]. Paclitaxel (PTX), one of the most effective chemotherapy drugs has been a target for such advancements [4].

Currently, the majority of PTX is synthesized from a precursor molecule, 10-deacetylbaccatin III, extracted from the renewable twigs and leaves of yew trees (*Taxus*), a natural source of PTX [5]. *Taxus* suspension cell culture has the potential to be an alternative source of the drug. Methods to increase the production of PTX in these cultures have been studied [6]. At present, once PTX is synthesized and purified, harsh solvents are necessary to systemically deliver the hydrophobic drug to the patient [7]. Alternative delivery systems, such as liposome encapsulation and impregnation in solid materials for direct (local) delivery are under development in order to circumvent the need for these solvents [8, 9].

Investigations have been performed on the use of whole-plant treatments which can exploit synergistic effects of the naturally produced drug and other compounds present in the plant material [10]. Whole-plant treatments do, however, have design challenges that differ from the traditional drug-only approach. The use of total *Taxus* cell culture is potentially compatible with

several direct drug delivery techniques, such as injectable gels, liposomes, and scaffolds. Utilizing total cell culture as a direct delivery system may reduce or eliminate dangerous side effects associated with current delivery methods, bypass the need for purification from culture, which is very complex, and reduce the total amount of drug required compared to systemic delivery. Additionally, the cultures' ability to produce assorted taxanes and other specialized metabolites could change the efficacy of the drug through synergistic effects.

This Major Qualifying Project studied processed *Taxus* suspension culture as part of a delivery system for local PTX delivery. It piloted the decellularization process of *Taxus* and examined the retention of PTX and other specialized metabolites while quantifying DNA removal. This study explores the potential of a total *Taxus* cell culture derived drug delivery system through the investigation of three aims:

Aim 1: Identify strategies to increase the concentration of cell-associated PTX *in vitro* to prepare the plant cell for use as a drug delivery system.

Aim 2: Optimize the decellularization of plant cell culture to develop a biomaterial capable of delivering PTX.

Aim 3: Quantify the feasibility of the biomaterial through evaluation of its release profile in protein-saturated liquid both alone and encapsulated in a protective hydrogel.

Chapter 2: Background

2.1. Paclitaxel

2.1.1 History

PTX is an anti-tumor drug discovered through the plant and natural products screening program conducted by the National Cancer Institute (NCI) and United States Department of Agriculture between 1960 and 1981 [11]. PTX, trademarked as Taxol®, was first isolated from the bark of the Pacific Yew tree, *T. brevifolia,* and moved into the NCI drug development program [12]. Today, PTX, a highly cytotoxic compound, remains a popular chemotherapy agent, used in the treatment of breast, ovarian, lung, and prostate cancers and other solid tumor cancers [13]. In addition to the treatment of cancers, PTX has been studied to treat other health afflictions including psoriasis [14] and to minimize restenosis after coronary stenting [15]. Overall, PTX acts as a non-proliferative and immunosuppressive agent with many applications in the medical field.

2.1.2 Biosynthesis, Structure, and Mechanism

Biosynthesis and Structure

PTX is a member of the taxane family, a class of diterpenes. Like all taxanes, it contains a taxadiene three-ring core [16]. Currently, its biosynthetic pathway is not completely understood, though it is predicted to contain nineteen steps, many of which have yet to be characterized [4]. Figure 1 depicts the steps of the currently-known biosynthetic pathway of PTX in *Taxus.* Several notable compounds along the pathway are geranylgeranyl diphosphate, an important precursor for all diterpenoids, taxadiene, the foundation of all taxanes that provides the characteristic three-ring base structure, as well as baccatin III and 10-deacyclbaccatin III which are important precursors used for semi-synthesis of PTX [17, 18].

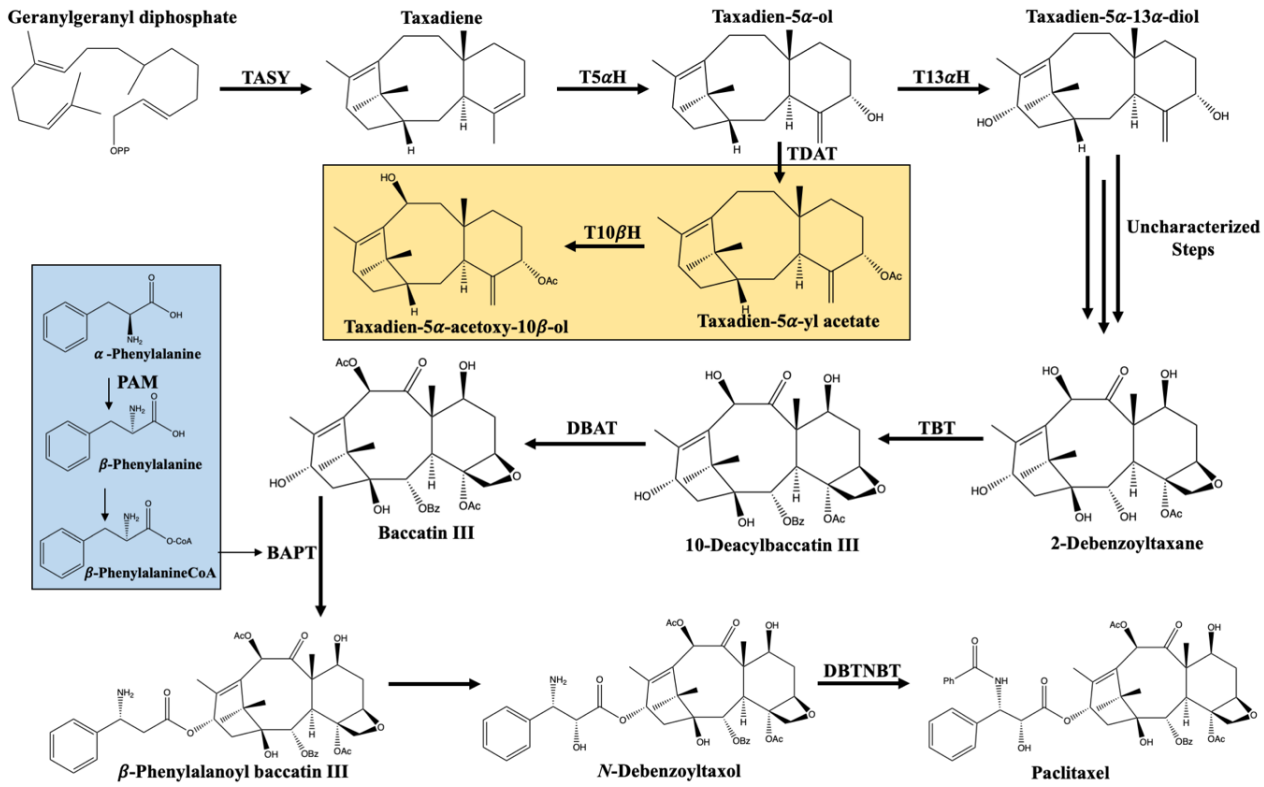

Figure 1: The hypothesized biosynthetic pathway of PTX within *Taxus*. The blue box shows the synthesis of the precursor BAPT while the yellow box shows another path which Taxadien-5α-ol can take which does not lead to PTX production. Note that there are a number of uncharacterized steps between the taxadiene alterations of the synthesis and the creation of 2-debenzoyltaxane. Adapted from [17].

Other Taxanes

Taxanes other than PTX as well as PTX precursors have shown significant bioactivity making them compounds of interest [19]. Many of these taxanes produced in *Taxus* cell culture have yet to be isolated, identified, or tested for activity due to the low quantities at which they naturally accumulate [19]. It is important to note that these taxanes of interest and the PTX precursors are produced both naturally by whole plants as well as in plant cell culture.

Docetaxel, a synthetic analog of PTX, is a taxane that boasts higher aqueous solubility and therefore higher bioavailability [20]. Cabazitaxel, a commercially available semi-synthetic taxoid derivative, is used for the treatment of prostate cancer. These synthesized alternatives retain the

base mechanism of which PTX is most effective and show promising results as alternative treatments to the natural compound [21, 22]. It is important to note that these analogs are by definition synthetic and therefore are not produced naturally via *Taxus* culture or otherwise. These compounds' structures as well as PTX are pictured in Figure 2 [21].

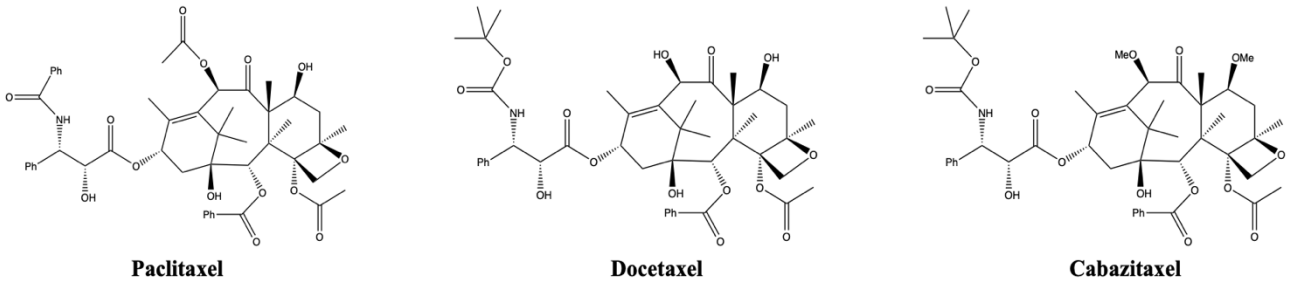

Figure 2: The relative structures of paclitaxel, docetaxel, and cabazitaxel. Note the consistency of the basic three ring structure and the differences in the 'tail' between paclitaxel and the two semi-synthetics.

Mechanism of Action

PTX interrupts cell function by altering microtubule stability within cancer cells. Through excessive promotion of tubulin polymerization, PTX treatment results in microtubules that are overly stable and therefore dysfunctional [4]. This stability directly interferes with the ability of a cell to successfully form the mitotic spindle during division, inevitably inducing cell death [23]. It is suggested that PTX produces stable microtubules due to increased dimer contacts of axial tubulin and a rearrangement of density in α-tubulin subunits [24]. As a result of its mechanism of action, PTX has an intensified effect on cells that are rapidly proliferating, such as cancer cells.

Additionally, studies have investigated other mechanisms through which PTX may affect cell function. One study found that in the presence of the P-53 tumor suppressor gene, PTX can stimulate the lipopolysaccharide signaling pathway in murine macrophages which can cause the secretion of cytokines interleukin 1β and tumor necrosis factor α, the latter of which can induce

apoptosis [25]. This mechanism is independent of microtubule production and may be due to an increase in the activity of NADPH oxidase, which increases the generation of reactive oxygen species which may participate in P53-independent apoptosis [23]. In small doses PTX has been shown to stimulate the immune system partially due to its ability to enhance the activation of human dendritic cells independent of TLR4 binding [26]. Overall, PTX is effective in decreasing tumor viability because of its ability to influence various cells processes leading to cell death.

2.1.3 Production

The drug PTX was originally isolated from extracts from the bark of yew trees. Extraction of PTX uses an organic solvent, typically an alcohol, to obtain a crude product which is then put through several purification steps to arrive at an applicable concentration of the drug (typically 6 mg/ml) [27]. Some common purification procedures include filtration, n-hexane extraction (which favors PTX), and various forms of liquid chromatography [28]. However, this process is not practical for large-scale production for several reasons. Namely, the amounts of PTX produced naturally are too low for natural harvest to be useful with nearly 3,000 full-grown trees required to make one kilogram of the drug [29]. This amounts to approximately 8 adult yew trees to treat one cancer patient [30]. Considering that the harvesting process requires the complete processing and sacrifice of the tree, the number of trees, space, and time needed to keep up with today's demands would be astronomical, and therefore not feasible. Additionally, the accumulated concentrations of the drug in the natural plant has been shown to vary seasonally, further complicating the ability for consistent production [31].

Due to the difficulties associated with the use of extraction methods for large-scale production of PTX, numerous efforts have been made to develop alternatives that are more sustainable and consistent. Various pathways for the complete synthesis of PTX were first

published in 1994. These groups included the Houlton group, which designed a linear synthesis pathway with the precursor patchoulol [32], and the Nicolaou group who started from mucic acid [33]. Despite their success, these processes were outshined by a semisynthetic process which uses the natural product 10-deacetylbaccatin III which accumulates in the yew at a much higher rate than PTX. The natural product is extracted, protected, and then reacted with 3R,4S-N-benzoyl-3-(1-ethoxy-ethoxy)-4-phenyl-2-azetidinone which adds the requisite tail [18].

10-Deacetylbaccatin III can be isolated from the twigs and leaves of the yew (both more renewable sources) in quantities sufficient for processing, decreasing the impact of extraction on the trees themselves [18]. This process, trademarked by Bristol-Myer Squib, is the primary source of the commercialized form of PTX (Taxol®), utilized today. This semi-synthesis is favorable to complete synthesis for its decreased number of reaction steps and reduced environmental impact as compared to a purely natural extraction [18].

2.1.4 *Taxus* Suspension Cultures for Paclitaxel Production

The development of suspension cultures of *Taxus* for use as production systems stems from the challenges of the other available methods of production. By providing opportunity for sustained production, higher yields, and more efficient processing, plant cell culture is a promising production avenue for plant derived metabolites that are otherwise difficult to procure [6]. The process begins with the needles of the *Taxus brevefolia* which are sterilized by suspending in a 1% aqueous hypochlorite solution for ten minutes [34]. Next, the needles are removed from the solution washed with sterile water, then cut into small pieces and plated onto solid media [34]. Every four weeks, the calli are transferred to new solid media until there is enough callus mass to create a liquid suspension culture [34]. To create a liquid suspension, approximately 5 grams of friable calli is disaggregated using a spatula and transferred into liquid media. Then, a pipette is

used to shear calli into smaller aggregates [34]. *Taxus* suspension cultures have a doubling rate of about 4 to 8 days [35] so a 5 grams of calli takes significant time to accumulate. Liquid cultures are transferred every 14 days. This process is long and requires exceptional sterility due to the culture's high susceptibility to fungal and bacterial contamination [34].

The method of liquid suspension production is notably not available for synthetic alternatives to PTX, presenting an opportunity unique to the natural drug. Plant cultures also produce an assortment of other natural products associated with plant cell function including proteins, a variety of specialized metabolites (formerly secondary metabolites), and other taxanes; all of which can be impacted by the culture's response to stimuli. In *Taxus*, these metabolites primarily include phenolics, flavonoids, and other taxanes. These cell cultures can display a large degree of heterogeneity particularly in size, shape, and metabolic function which can cause wide variation in the production of PTX in cultures [35, 36].

2.1.5 Delivery of Paclitaxel

PTX's natural hydrophobicity requires it be bound or dissolved in specialized solvents before being used as a therapeutic. There are two main forms in which PTX is currently used for chemotherapeutic applications. The first is the traditional solvent-based variety. In this form, PTX is administered using Cremophor EL, a non-ionic surfactant mainly composed of oxylated triglycerides of ricinoleic acid soluable in water, and dehydrated ethanol as a drug delivery formulation [37, 38]. Treatment with this formulation often results in toxic side effects, due not only to PTX itself, but also the associated solvents [37]. The second form, albumin bound PTX (nab-paclitaxel), has recently gained popularity, as the protein bound PTX has greater solubility in water and higher biocompatibility, thus reducing toxicity and making it an atrractive alternative. Due to the reduced toxicity increased dosages of PTX can be achieved resulting in more effective

treatments and higher survival rates. In a 2012 study, nab-paclitaxel nanoparticle formulation was shown to significantly increase the proportion of early stage breast cancer patients achieving a pathologically complete response rate [39].

The development of alternative PTX delivery methods is currently a research topic of increasing interest. Current studies have investigated the use of emulsions, co-solvents or surfactants to increase the solubility of PTX [40]. The development of prodrugs, or inactive derivatives of parent drugs that convert into the bioactive compound in the body also show promise. Significant research has been done on prodrugs developed with an addition of ester groups to the C-2' and C-7' hydroxyl groups as well as additions of carbonates and carbamates to the C-2' group [41]. While these prodrugs create compounds with the ability to dissolve in water, a current challenge in their development is the tuning of their *in vivo* stability so they can convert to the parent drug readily [41]. Other studies have looked at the delivery of PTX encapsulated in delivery vessels such as liposomes, nanoparticles, or thin films [40].

2.2 Drug Delivery Systems

A multitude of drug delivery systems (DDSs) are utilized in everyday life: from intramuscular flu shot vaccinations to topical antibacterial ointment applied to abrasions. Successful drug delivery systems must be designed with the targeted system of interest in mind and effective at releasing the drug in the desired concentration at the desired rate. Systems vary vastly in design: some as simple as a solvent for the drug to be delivered systemically, while others use specialized materials to control the release of a drug over time to target locations.

Drug delivery systems can be classified into two broad categories, systemic and local, both of which can be augmented to target specific cells within the body. In systemic delivery, the drug is transported throughout the body through the circulatory system after being administered in various methods some of which include intravenous, oral, and pulmonary delivery [42].

2.2.1 Local Drug Delivery Systems

Local DDS, drugs are delivered by placing them physically in, on, or near the target treatment site. Examples of these includes solids, wafers, particles, powders, pastes foams, gels, membranes, and films [8, 9]. One of the many benefits of direct delivery systems is that they do not require the drug to travel through the entire circulatory system, this allows for the use of smaller concentrations of the drug because there are fewer opportunities for degradation or metabolism before the drug reaches the target area. Additionally, direct delivery avoids the distribution of the drug to other sites where it may potentially have harmful effects. A concern of direct delivery is the necessity to be physically placed on or near the target site which can be difficult or even impossible depending on site accessibility. One example of an effective direct delivery system available today is the Gliadel® Wafer, a carmustine-loaded polymer wafer made by MGI Pharma used to treat malignant glioma, a common type of brain tumor in adults [43].

Local delivery methods call for rate-controlled release of the drug to the target site governed by principles of mass transfer. Factors such as the concentration of a drug in a delivery system and temperature can influence release rate [44]. Delivery methods may also incorporate physical targeting methods, such as pH dependent or enzymatic release [10].

A common problem with direct delivery systems is the formation of a fibrous capsule around the DDS, hindering transfer of drug to the target [45], but fibrous capsule development can

be controlled with anti-inflammatories such as dexamethasone [46]. Transfer of cancer drugs to tumors has been demonstrated to be aided by the implantation of the delivery system inside the tumor [45]. One study examined implantation methods of doxorubicin loaded polymer millirods in tumorous rat livers [47]. It was found that ablation, or breaking, of tissue prior to insertion resulted in a maximum concentration of drug in tumor tissue of approximately four times than that of non-ablated tissue [47]. Unfortunately, ablated tissue can develop fibrous capsule over time which has been shown to decrease drug transfer into tumor cells, but treatment of ablated tissue with an anti-inflammatory can reduce fibrous capsule development [47]. Additionally, tumor reoccurrence at the boundaries of ablation is a common issue [48]. As PTX has anti-inflammatory properties, fibrous capsule formation may be inhibited in the case of a PTX loaded implantation device [8].

Another example of local delivery is the incorporation of PTX and polyethylene glycol (PEG) into thin poly(lactic acid-co-glycolic acid) (PGLA) films [49]. The rate of PTX release correlates to the crystallinity and its affiliation with the PEG present in the film due to phase separation of crystalline PEG, creating pores that allow for diffusion of PTX from the system. PEG higher in crystallinity resulted in faster release of PTX but was also attributed with lower tensile strength of the film after phase separation [49].

Local drug delivery systems are not without challenges, and may, for example, face rejection from the body and inadequate drug diffusion and bioavailability. However, they offer an alternate method for drug delivery that could significantly increase the efficacy of a drug if designed with these issues in mind.

2.2.2 Properties of Successful Local Drug Delivery Systems

In solid delivery systems, physical integrity and flexibility are important factors in successful designs. Scaffolds are often used as a supportive structure which allows solid delivery systems to maintain their form and functionality. These scaffolds can be composed of various materials including electro-spun mats, lyophilized sponges, hydrogels, and collagen [8, 50]. Collagen and decellularized skin (human, porcupine, or bovine) are particularly appealing scaffold materials due their natural and similar components to the tissues they interact with when implanted as well as their strength and flexibility increasing their biocompatibility [8, 50]. With these structural properties in mind various solid drug delivery systems are currently being investigated for their use in the treatment of various ailments. This research includes the investigation of films, wafers, stents, and thermogels (a polymer solution which forms a gel at a specific concentration and temperature).

Silk films have been a potential candidate for the delivery and sustained release of anticancer agent doxorubicin as well as platinum-based drugs [51, 52]. Bilayer silk films can provide time dependent delivery to target cells through the exploitation of physical properties, such as hydrophobicity and charge [53]. In comparison, homogeneously-made (constant concentration of drug throughout material) Gliadel® wafers utilize a copolymer matrix made of 1,3-bis(*p*-carboxyphenoxy) propane and sebacic acid in a 20:80 molar ratio to deliver carmustine, an anticancer agent, directly to tumor cells [54]. Although wafers and films stay in place and provide localized treatment, they generally tend to develop a buildup of tissue around them (fibrous capsule formation), which can hinder drug delivery due to the additional physical barrier [45].

For the development of PTX eluting stents, various polymers have been studied. One stent, TAXUS^{TM} Express^{2} ® (Boston Scientific, Marlborough, MA) uses the polymer translate

[poly(styrene-b-isobutylene-b-styrene)] as an inactive carrier of PTX [55]. Unfortunately, this polymer has appeared to result in inflammation of surrounding tissue and potential blood clotting [7]. An alternative polymer, poly(ethylene carbonate) was studied separately as a PTX eluting stent coating. This PTX coating is released in the presence of inflammation of the blood vessel when the stent is under stress in order to treat the inflammation and allow the stent to continue to function properly [7].

The use of low-dose PTX-loaded thermogels on the surface of implantable medical devices has been studied to reduce the formation of fibrous capsules around silicone implants and avoid interruption of drug delivery over time [56]. PTX was of interest in these studies due to its capacity to inhibit collagen synthesis, fibroblast growth, inflammation, and fibrosis at low doses [7].

Local drug delivery systems have the capability to bypass many of the challenges of drug delivery, and investigations into the design of such devices are widespread, with only a few examples being introduced above. One avenue for the further development of these drug delivery systems is the use of naturally derived drug delivery systems.

2.2.3 Benefits of Natural Drug Delivery Systems

Effective drug treatment regimens elicit minimal immune response. An immune response can present as irritation and/or inflammation of the tissue, and it can be quantified by the population of cells containing elevated concentrations of macrophages and lymphocytes [8]. Some polypeptides have already been investigated and found to be accepted by the immune system. These include collagen, albumin, elastin, and gelatin [45]. Additionally, tolerable natural polymers (tested *in vivo*) include polysaccharides such as alginate, hyaluronic acid, dextran, and chitosan [45]. Naturally produced systems are desirable for drug delivery due to a variety of properties,

including a generally lower cost, high availability, capacity to be modified chemically, biocompatibility, and, in some cases, biodegradability [10].

The biocompatibility and somewhat complex nature of naturally-derived DDSs makes them of increasing interest in new drug delivery strides. For instance, natural silk has been found to be an effective material to construct a DDS for anti-cancer drugs [57]. Silk's ability to alter its crystallinity and interact with hydrophobic, hydrophilic, or charged particles has a significant effect on drug retention and release [51]. In one study, a pH dependent release system for doxorubicin, a natural product from bacteria Streptomyces peucetius, was created using silk nanoparticles in which the surface of the nanoparticles were altered to have an overall negative charge [58, 59]. Studies on self-assembling silk hydrogels have also highlighted that the ability to self-assemble aided in the ability to be physically implanted [60].

2.2.4 Plant Cell-Derived Delivery System

Plant-derived polymers are diverse in their application: matrix systems, implants, films, beads, microparticles, nanoparticles, inhalable, injectable, and viscous liquids are all different ways in which they can be utilized [10].

The use of total plant cell culture as a drug delivery system is appealing field of investigation due to many potential benefits. The culture is readily available, relatively inexpensive, and relatively easy to produce and maintain. It can be more environmentally friendly than the extraction from the naturally occurring plant. The minimization of downstream processing can also decrease cost by removing purification steps and decreasing production time [61]. Culture derived delivery systems also have potential for enhanced performance through synergistic effects of other plant metabolites that can increase drug efficacy [62, 63].

Plants produce many different classifications of specialized metabolites (small organic molecule not essential for cell growth), organic compounds that potentially have different pharmaceutical advantages [64]. Using total plant cell culture for drug delivery would capitalize on the unique properties of all present metabolites. Some metabolite classes are described in Table 1.

Table 1: Specialized Metabolites

A chart of common specialized metabolites produced in plant cell culture and their pharmaceutical advantages. Note that various metabolites have properties that would aid in the effectiveness of a plant cell derived DDS. *Adapted from:(Kabera, 2014* [65]*).*

Metabolite Classification	Description	Pharmaceutical Usages
Phenolics	- Synthesized by fruits, vegetables, teas, cocoa, and other plants that possess certain health benefits	- Anti- inflammatory - Protect from oxidative stress - Bactericidal - Antiseptic - Anthelmintic
Flavonoids	- Water-soluble pigments found in the vacuoles of plant cells - May act as (in plants): chemical messengers physiological regulators cell cycle inhibitors	- Anti-allergic, anti-cancer, anti-inflammatory, anti-viral - Some relive fevers, eczema, asthma, and sinusitis - Reduce the risk of atherosclerosis - Reduce risk of heart disease
Terpenoids	- Composed of the most important active compounds of plant cells – why? - A tool for communication between plants and other organisms	- Disease treatment - Antimicrobial and antiviral - Steroids
Essential Oils	- Natural aromatic and volatile compounds - Provide protection to the plant from predators and disease	- Aromatherapy - Antibacterial, antifungal, and antiviral
Tannins	- Phenolic compounds that precipitate proteins - Water soluble	- Astringent against diarrhea - A diuretic against stomach and duodenal tumors - Anti-inflammatory
Glycosides	- Phenols, alcohols, or sulfur containing compounds - Contain sugar and non-sugar portion - Inactive until hydrolyzed by enzyme	- Prodrugs - Anticancer agents - Expectorants - Sedatives - Digestion aids
Saponins	- Produce colloidal solutions in water - Precipitate cholesterol - Can lower surface tension acting as detergent	- Antimicrobial - Hemolytic
Alkaloids	- Contain basic nitrogen atoms - May also contain oxygen, sulfur, chlorine, bromine, and/or phosphorous - Produced by bacteria, fungi, animals, and plants	- Narcotics - Anti-cancer, anti-inflammatory, anti-bacterial, anti-viral - Treatments against malaria - Immune effects - Neurotoxins

An example of applying whole-plant metabolites as medicine is the success of whole plant *Artemisia annua* to treat malaria [66]. Recently there has been an emergence of drug resistant parasites which have made typical malaria treatment less effective. *Artemisia annua* produces the drug artemisinin which can interfere with heme detoxification, a requirement for parasite survival [66]. A recent study examined the effects of using the whole plant as an oral drug delivery system and found that it increases the efficacy and bioavailability of artemisinin [66]. This augmentation is likely because non-artemisinin metabolites with the whole plant inhibits the high metabolic breakdown of artemisinin by hepatic and intestinal cytochrome P enzymes which can reduce the bioavailability of the drug. There are also probable synergistic effects from the flavonoids in the whole plant which can potentiate the activity of the artemisinin [66]. Other studies have explored the use of bananas and other crops as a method to produce and deliver vaccines [67]. Along with a decrease in production costs using whole plants such as bananas, tobacco, carrots, and rice, these oral vaccines can increase efficacy because they mimic the natural infection, as well as increase both systemic and mucosal effects [67].

Examples of these synergistic effects can be seen in various other whole plant applications. Liquorice is often used as an aid in detoxification as it can alter the absorption in the stomach [68]. For treatment of multiple sclerosis patients, processing whole cannabis plants allows for the retention of cannabidiol (CBD) which can increase the effects of tetrahydrocannabinol (THC), the psychoactive constituent, to reduce anxiety and enhance the antispastic traits [68]. It has also been determined that CBD has anticonvulsant effects which are also augmented by the anticonvulsant effects caused by THC making it an effective treatment for epilepsy [69]. *Taxus* cell cultures produces various taxanes as well as other specialized metabolites provide the potential to induce synergistic effects such as aforementioned natural compounds.

2.3. Research Plan: *Taxus* Cell Culture as a Drug Delivery System for Paclitaxel

Overall, the desire to improve treatments and patient outcomes continues to drive innovation in the field of cancer treatment. How can treatments be made more effective and feasibly scalable, while minimizing the negative side effects often associated with cancer treatments? *Taxus* cell culture provides a promising avenue for developing alternative delivery methods for PTX.

The use of total *Taxus* cell culture as drug delivery system offers various possibilities of different solid local drug delivery options, such as injectable gels, liposomes, or scaffolds. PTX is a hydrophobic compound that poses a problem for the use of purified PTX used in current PTX drug delivery. Harsh solvents need to be used for PTX to be delivered which can have severe negative effects on the patient. Using total cell culture, a decrease in the dangerous and cytotoxic side effects often associated with current delivery methods may be achieved and lower doses of the drug may be delivered by increasing the amount of the drug in proximity to a tumor. Local contact within tumor sites limits the cytotoxic effects of PTX to the affected areas decreasing side effect cytotoxicity throughout the body. Along with this, the cultures' ability to produce various taxanes and specialized metabolites could increase the efficacy of the drug through synergistic effects. This study explores the potential of a total *Taxus* cell culture derived drug delivery system through the completion of the following aims:

Aim 1: Identify strategies to improve the concentration of cell-associated PTX *in vitro* to prepare the plant cell for use as a drug delivery system.

Aim 2: Optimize the decellularization of plant cell culture to develop a biomaterial capable of delivering PTX.

Aim 3: Quantify the feasibility of the biomaterial through evaluation of its release profile in protein-saturated liquid both alone and encapsulated in a protective hydrogel.

Chapter 3: Improve Uptake and Retention of Cell-Associated Paclitaxel

Achieving an effective concentration of cell-associated PTX is necessary for the success of the targeted drug delivery system. Currently, intravenous solutions are supplied at a concentration of 6 mg/mL and diluted for the needs of the patient which is not feasible to achieve using modern cell culture methods although current research has focused on increasing PTX concentrations *in vitro* [70].

3.1. Background

3.1.1. Elicitation of Paclitaxel Production and Culture Treatment

Obtaining PTX in cell culture can be difficult with naturally low production rates. The production of the drug is determined by a complex interaction of various steps with a multiplicity of rate limiting factors which makes it difficult to achieve desirable concentrations [71]. This project explored two methods to increase the amount of PTX in culture: elicitation with methyl jasmonate (MeJA) and the addition of exogenous PTX.

Methyl Jasmonate (MeJA) Elicitation

MeJA is a natural plant hormone which elicits the production of PTX by the *Taxus* cells. Elicitors signal environmental stresses which can stimulate the production of defense-related compounds and proteins including PTX, a specialized metabolite most likely used to protect the plant [72]. A study found that the introduction of 100 μM MeJA in culture can increase the production of PTX by more than 50% yielding a concentration of 1.1 mg/L two days after elicitation [72]. Another study found that

cells elicited on day 8 of suspension culture with the same 100 μM MeJA addition can achieve concentrations as high as 14.4 mg/L 10 days after elicitation [73]. Response to the hormone varies greatly between cell line, affecting the increase in PTX production observed, due to this an investigation into the response of the cell lines needed for this project is necessary [73].

Treating Cultures with Exogenous Paclitaxel

Exogenously adding purified PTX to cultures is an effective and calculated method to control the total amount of PTX in a culture and to observe how different concentrations of PTX can affect cell growth and behavior [71].

Both methods increase the concentration of PTX in culture, but there are additional, potentially more effective methods that could be used. Other alternative methods have been explored for increased PTX production including the addition of silver-based compounds and/or other plant hormones [74].

A wide variety of methods and agents have been studied to increase cellular production of PTX. Some abiotic elicitors include metal ions and inorganic compounds such as silver complexes, copper sulphate, and cobalt complexes [74, 75]. Many silver containing compounds function as anti-ethylene agents, thought to increase PTX production [74]. Biotic elements functionable as elicitors include fungi, bacteria, viruses, cell wall components, and various chemicals such as jasmonates (anti-ethylene agents), arachidonic acid, and salicyclic acid, synthesized by the plant at sites of attack from pathogens or herbivores [75]. Recently, cyclodextrin and coronatine have been noted as successful elicitation agents [76]. Coronatine, a bacterium produced toxin can reduce growth capacity of cells and elicit PTX production in *Taxus* [76]. Cyclodextrin can counteract the reduced growth induced by coronatine and induce a cellular defense response through PTX

production [76]. Additionally, cyclodextrin can complex with poorly soluble compounds to facilitate in cellular excretion [76]. Combining cyclodextrin with MeJA has shown to increase PTX elicitation than either compound used alone [76]. Metabolic engineering of the *Taxus* genome could be employed to fine tune the biosynthetic pathway to promote PTX production, but this approach is difficult partially due to the slow growth of *Taxus* and the difficulty of genome editing [75].

For this project, along with an increase in PTX production and increase in the concentration of cell-associated PTX, is also necessary to retain sufficient PTX for accurate quantification throughout decellularization, as well as for the development of a feasible DDS. The processed biomass should contain enough PTX to be effective in tumor treatment. A beneficial approach to further facilitate PTX cell association would be to block PTX transport from the cell and accumulate the drug intracellularly.

PTX is a specialized metabolite within the terpeoid classification so while the exact transport mechanisms of PTX within the cells are unknown, studies on the transport of related metabolites in other plant species offer insight into the potential transport mechanism of PTX. It is suspected that PTX transport is facilitated in part by ATP-binding cassette (ABC) transport proteins, but continued research into specialized metabolite transport suggests that there could be multiple PTX transport mechanisms [77, 78]. ATPase inhibitors are also useful because they block the ATP proton pumps which provide the energy necessary for transport [64]. These concepts are important to take into consideration as they could affect *Taxus* cell culture and PTX transport when attempting to obtain improved cell-associated accumulation.

3.1.2. Preliminary Inhibition Research

Prior studies conducted within the Roberts' lab have investigated the effects of inhibitors on the transport of PTX in the *Taxus* cell culture. One study conducted during a 2017-2018 MQP looked at the effects of various transports inhibitors which covered two groups: ABC transport inhibitors and an ATPase inhibitor [79]. This study was conducted over the course of 24 hours with the short-term effects of verapamil increasing the concentration of cell-associated PTX (Figure 3).

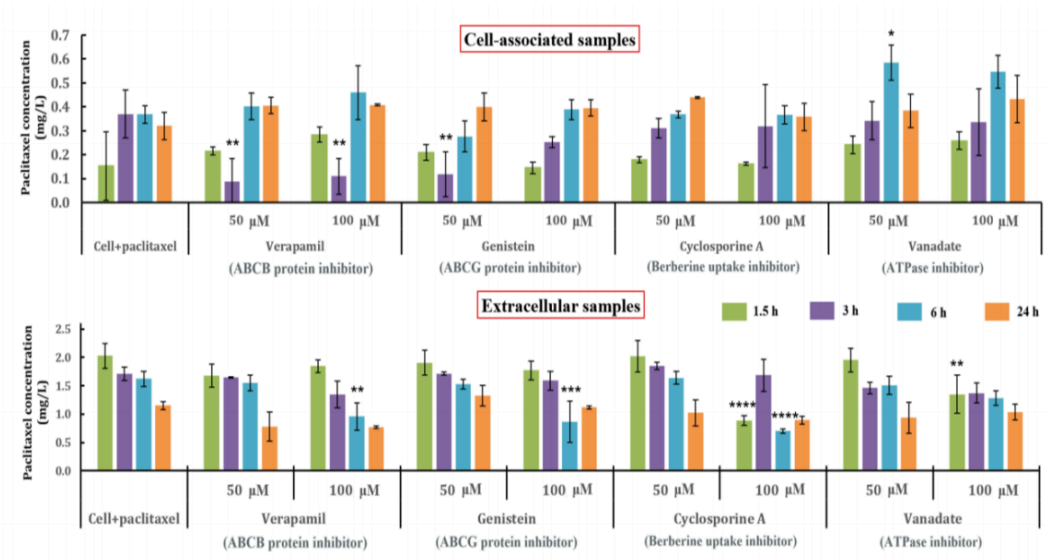

Figure 3: The effect of inhibitor concentration (50µM and 100µM) on PTX concentration in P093X *Taxus* culture over time. Inhibitors tested were verapamil, genistein, cyclosporine A, and vanadate. Cell associated and extracellular (media) PTX was tested (mg/L) after inhibitor addition at 1.5, 3, 6, and 24 hours *=p<0.0332, **=p<0.0021, ***=p<0.0002 and ****=p<0.0001 [79].

Following this study, a summer research project by Dasia Aldarondo studied the effects that extended exposure to verapamil could have on a culture's PTX transport. This study was conducted on both elicited cells and unelicited cells (treated with a 20 mg/L concentration of PTX). Various concentrations of verapamil were investigated in staggered additions. Results from this study concluded that verapamil could not only increase the amount of cell associated PTX in the

cell but could also increase the total PTX in the media of culture as well. This is represented in Figures 4 and 5.

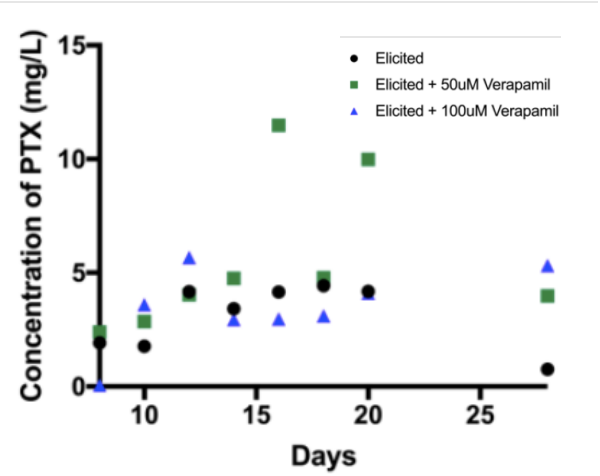

Figure 4: Concentration of accumulated PTX measured over 27 days in elicited 21260C culture with various amounts of verapamil (0µM, 50µM, and 100µM).

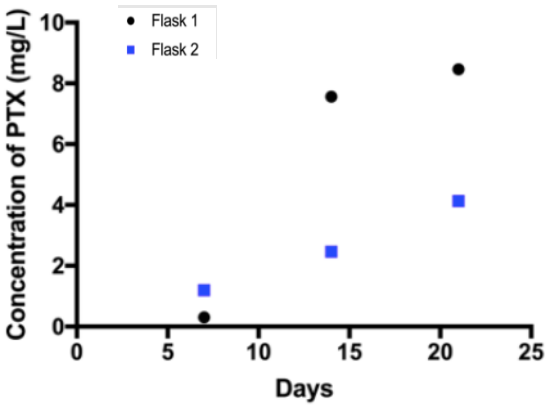

Figure 5: Concentration of accumulated PTX measured over 21 days of elicited 21260C suspension cultures treated with 50 µM verapamil. Flask 1 and Flask 2 represent two biologically different flask under the same treatment.

These data align with another study recently published that looked at the effects of different inhibitors on the production of isoflavones in *Trifolium pratense* L. cells [80]. This study concluded that verapamil (ABC protein inhibitor) increased the concentration of genistin both inside and outside of the cells [80].

3.1.3. *Taxus* Culture Characteristics

Overall culture health, viability, and general characteristics are factors to explore in bioprocess development. Healthy cultures are essential to ensure that bioproduction of a delivery system is feasible. One method to assess cell viability is through propidium iodide (PI) staining. PI binds to the DNA of dead cells but is incapable permeating the cell wall of living cells and thus is a beneficial qualitative tool to measure cell death. An effective approach to study the viability of cell culture is to tract cell growth and culture biomass [81]. *Taxus* cell culture grows in

aggregates and so analysis of individual cell size is very difficult and correlations of volume to dry weight can be used to measure cell mass [81].

In the scope of this project cell viability is important for increased PTX production but following PTX accumulation cells must be dried for further processing. A common method utilized to dry cells is lyophilization, or freeze drying under a vacuum [82]. While lyophilization kills the cells, it allows for the retention of nonvolatile specialized metabolites such as PTX [82].

3.2. Methods

To increase the amount of cell-associated PTX concentrated in the final lyophilized product to serve as a DDS, two approaches were explored.

1. Manipulating cellular PTX transport mechanisms
2. Exploiting PTX's hydrophobic properties

Experimental procedures for each approach are outlined in this chapter.

3.2.1 Plant Cell Culture Maintenance

21260C (*Taxus chinensis*) and 48-82-A (*Taxus cuspidata)* cells were grown and maintained in 50 mL liquid suspension cultures and transferred every 14 days. Media consisted of 20 g/L sucrose (Caisson Laboratories, Smithfield UT), 3.21 g/L Gamborg-B5 (PhytoTechnology Laboratories, Lenexa KS), 120 µL/L benzyl adenine (Sigma-Aldrich, St. Louis MO), 2.7 mL/L 1-napthalenacetic acid (Sigma-Aldrich, St. Louis MO). The final solution was brought to pH 5.5 using 1 M sodium hydroxide before being aliquoted and autoclaved in 125 mL Erlenmeyer flasks containing 40 mL of media at 121 °C for 30 minutes. *Taxus* cell cultures are transferred every 14 days to new media; day seven in culture is when the *Taxus* reaches stationary, non-growth phase,

which is when most PTX is produced [83]. To transfer cultures, 10 mL of day 14 cell culture was transferred in a sterile environment using serological pipettes to fresh media supplemented with 2.5 mL of filter-sterilized antioxidant solution containing 2.5 mg/mL ascorbic acid (Fisher Scientific, Hampton NH), 2.5 mg/mL citric acid (PhytoTechnology Laboratories, Lenexa KS), and 14.6 mg/mL L-glutamine (Caisson Laboratories, Smithfield UT). Cultures were incubated at 23 °C in the dark and shaken at 125 RPM.

3.2.2 Manipulating Transport Mechanisms

Inhibitor Study

To examine the effects of three ABC transport inhibitors and one ATPase inhibitor on PTX concentration in cultures over 21 days, cultures were elicited with methyl jasmonate (MeJA) (Sigma-Aldrich, St Louis MO, 392707) and treated with inhibitors as described in Table 2. Two ABC transporter inhibitors: cyclosporine A (Cayman Chemical, Ann Arbor MI, 12088) and verapamil (Acros Organics, Geel (Belgium), 329330010) were investigated alongside the ATPase inhibitor vanadate (MP Biomedicals, Solon OH, 218058). Inhibitors were selected from preliminary data from a previous MQP that examined the effects of inhibitors over a 24-hour time span (Section 3.1.2).

Table 2: Inhibitor Test Groups

The experimental test group names and the treatment conditions

Test Groups (Inhibitor)	Conditions
Control	No treatment
Elicited	200 μM MeJA
Elicited +Verapamil	200 μM MeJA 50 μM Verapamil (ABC Transport Inhibitor)
Elicited + Cyclosporine A	200 μM MeJA 50 μM Cyclosporine A (ABC Transport Inhibitor)
Elicited + Vanadate	200 μM MeJA 50 μM Vanadate (ATPase Transport Inhibitor)
Elicited + Verapamil and Vanadate	200 μM MeJA 50 μM Verapamil (ABC Transport Inhibitor) 50 μM Vanadate (ATPase Transport Inhibitor)

All test groups, apart from the control group, were treated with MeJA and their respective inhibitors on day seven of culture. On this day, the culture was divided into 50 mL flasks containing 25 mL of culture (conditioned media and cells). MeJA was utilized to increase the natural production of PTX as well as other specialized compounds to be investigated for the delivery system. Verapamil and vanadate were combined to determine if inhibiting both types of transport mechanisms could result in a significant increase of cell-associated PTX.

Two 1 mL samples of the total cultures and two 1 mL samples of media of each condition were taken 7 and 14 days after treatment with inhibitors. Samples were weighed and stored at -20°C for later UPLC processing and quantification (Section 3.2.4). Culture aggregate size distribution of total culture samples (2 mL, one sample per treatment flask) were analyzed with the Coulter Counter (Section 2.2.5) to determine effects of inhibitors on culture growth and aggregation on days 7 and 14 after treatment. Finally, cell viability was qualitatively assessed microscopically with total culture samples from each treatment stained with 2.5 µL of propidium iodide on days 7 and 14 after treatment.

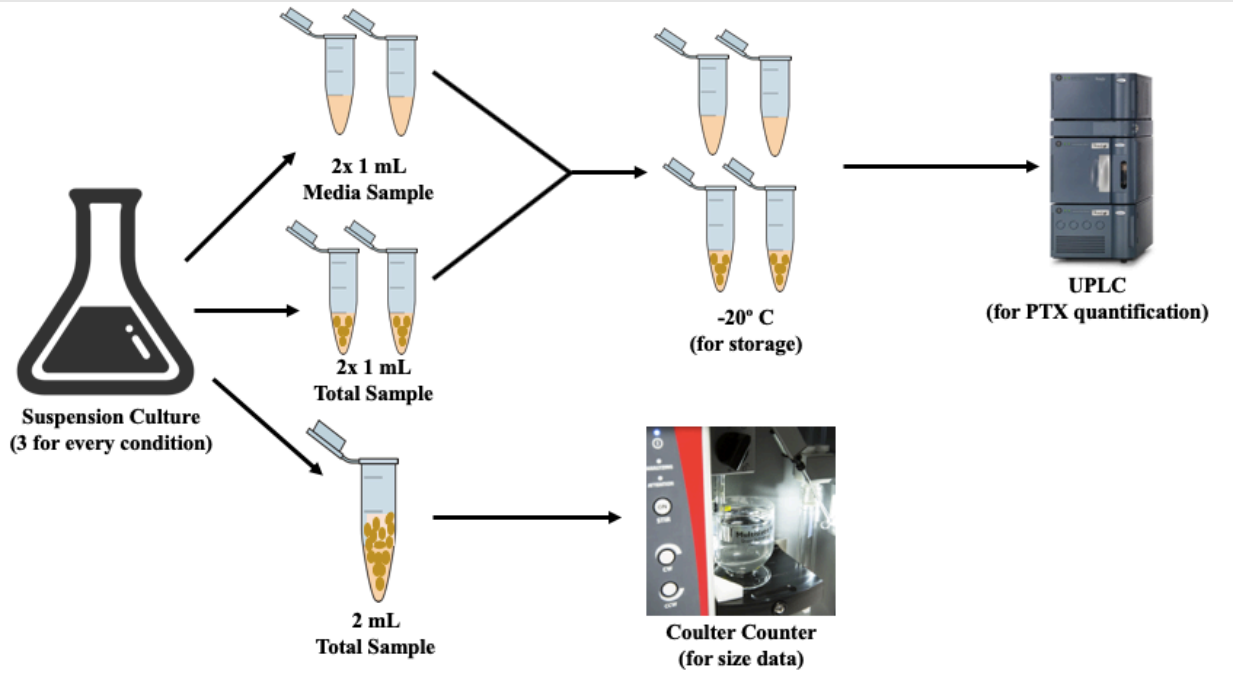

Figure 6: Flow chart of the sampling procedure for testing inhibitor effects.

3.2.3 Exploiting Paclitaxel's Insolubility

Two experiments were performed to determine the effect of lyophilization and washing on *Taxus* cultures and PTX retention throughout the process. The preliminary experiment was to compare changes in weight during the lyophilization and washing of total culture versus the lyophilization and washing of only cells. The second experiment aimed to determine if and where

PTX was retained throughout the lyophilization process as well as changes in weight throughout the process.

Lyophilization Study: Changes in Weight

This experiment was conducted to ensure that there was no significant final mass difference between lyophilization of a complete culture sample (media and cells) and a cell sample (cells only) post washing. To execute this experiment, two 50 mL conical tubes were filled with equal volumes of well mixed culture and weighed. From one tube, the media was removed, and the remaining contents of the tube were washed with deionized (DI) water three times and reweighed. The other sample tube was left untreated. Both tubes were flash frozen using liquid nitrogen then lyophilized overnight on a shelf lyophilizer (VirTis BenchTop Pro with Omnitonics, SP Scientific, Stone Ridge, NY) and weighed. Finally, both samples tubes were washed again with DI water, dried using Buchner funnel vacuum filtration, and weighed.

Lyophilization Study: PTX Association

To determine if PTX would remain associated with samples throughout the lyophilization and washing process, the following experiment was performed. Samples were analyzed for PTX with UPLC at three points in the process: before lyophilization, after lyophilization, and after lyophilization and washing.

A total of five treatments were tested using 48-82A-32 (*Taxus cuspidata)*. Three of the treatments included samples from elicited cells (elicited with MeJA on day 7 of culture then sampled 14 days later): total culture, cells only, and media only. Two of the treatments were from unelicited total culture samples loaded with 20 mg/L PTX (Alfa Aesar, Ward Hill, MA) at different

time points: two hours before flash freezing, and immediately before flash freezing. An outline of these treatments can be seen in Table 3.

Table 3: Lyophilization Treatments

The experimental test group names and the treatment conditions.

Treatment	Condition
PTX 0	20 mg/L PTX (added directly before lyophilization)
PTX 2	20 mg/L PTX (added 2 hours before lyophilization)
Elicited Total Culture	200 μM MeJA
Elicited Cells Only	200 μM MeJA (Media Removed)
Elicited Media Only	200 μM MeJA (No Cells Sampled)

Nine 1 mL samples were taken for each treatment into pre-weighed 1.5 mL microcentrifuge tubes, outlined in Figure 7. Total culture samples were taken using a 1 mL cut pipette tip, the culture flask was stirred as the sample was taken. For cell only samples, a 1 mL well mixed total culture sample was taken and weighed. They were centrifuged at 15,000 rpm for 5 minutes, and media was removed with a 200 μL pipette tip and the samples were weighed again. Media only samples were taken with a 1 mL pipette tip from culture flasks that had been allowed to settle so that only media was removed. All samples were then flash frozen with liquid nitrogen before being stored in a –20 °C freezer until lyophilization or processing.

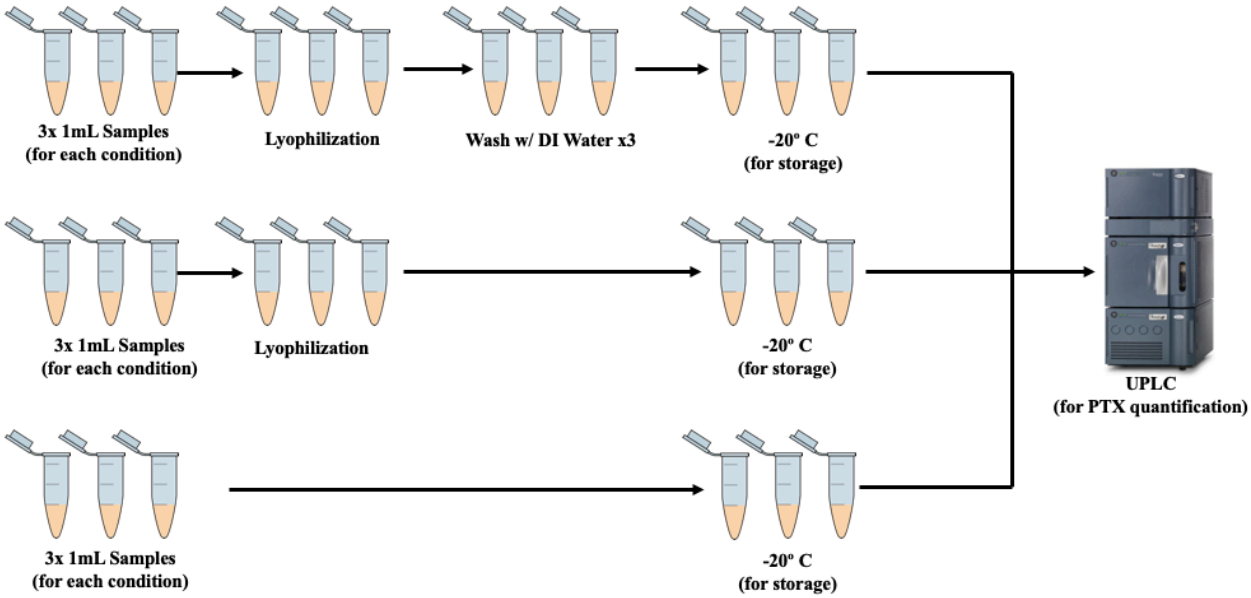

Figure 7: Flow chart of the sampling procedure for lyophilization experiment.

Samples were freeze dried with a shelf lyophilizer for 16 hours. After lyophilization, all samples were weighed and stored at -80 °C. Samples that were not lyophilized were stored at -20 °C.

Relevant samples were washed (post-lyophilization) before UPLC processing. To do this, 1 mL of deionized water was added and vortexed briefly. The samples were then centrifuged (Eppendorf, Hamburg Germany, Model 5418R) for 4 minutes at 15,000 RPM. The remaining liquid was removed with a 200 µL pipette tip. This washing process was repeated three times. After, the samples were re-weighed and stored at -80 °C. All samples were analyzed for PTX quantification following the procedure in Section 3.2.4.

3.2.4 UPLC Preparation Procedure

To prepare samples for UPLC processing, they underwent an organic extraction to remove PTX from the culture matter. Samples were first placed in an evaporative centrifuge (Vacufuge

plus, Eppendorf, Hamburg Germany) overnight (approximately eight hours) under aqueous evaporation conditions (1400 rpm, suction capacity: 1.8 m^3/h). After samples were completely dried, they were resuspended in 1 mL acidified methanol (0.01% acetic acid in methanol) briefly vortexed, then sonicated (Aquasonic 75HT, VWR, Radnor PA) for 30 minutes on ice. After sonication, large particulates that remained in the samples were manually broken using a spatula combined with vortexing. Samples were sonicated on ice again (20 minutes), incubated on a shaker (20 minutes), and centrifuged at 15,000 RPM (20 minutes). The supernatant (800 µL) was removed with a 1 mL pipette and transferred into a new microcentrifuge tube. These samples were returned to the evaporative centrifuge for approximately 2 hours until samples were dry using alcohol evaporating conditions (1400 rpm, suction capacity: 1.8 m^3/h). Finally, samples were stored in a –20 °C freezer until preparation for UPLC quantification.

UPLC samples were dissolved in 25 µL methanol, 35 µL acetonitrile, and 40 µL nano-pure water. Between each addition of solvent, the samples were briefly vortexed and sonicated. When the sample was fully dissolved, it was filtered through a 0.22 µm polyvinylidene difluoride filter using a 1 mL syringe into a low volume UPLC vial. A cap was crimped onto the top of the vial and any air trapped in the sample was removed. Samples were then analyzed by UPLC (Waters, Milford MA, Acquity UPLC H-Class), which consisted of one 10 µL injection and a 6-minute separation time in which molecules are separated in a 70:30 (v:v) water-acetonitrile solvent in a C 18 2.1x50mm, 1.7µm column. The chromatograms were analyzed at a wavelength of 228 nm and compared to a standard curves produced by 0, 12.5, 25, 50, and 100 mg/L standards containing PTX, baccatin III, and 10-deacetylbaccatin III (Alfa Aesar, Ward Hill, MA) in 70:30 (v:v) water: acetonitrile.

3.2.5 Coulter Counter Methods

The size distribution of aggregates present in culture were measured with a Multisizer 3^{TM} Coulter Counter (Beckman, Brea CA). The analysis procedure for the Coulter Counter was adapted from that of Kolewe et. al. [81]. From each sample, 2 mL of total cell and media sample was taken with a 5 mL cut pipette tip and put into a round bottom 500 mL Coulter Counter flask. The flask was then brought to volume with the diluent, a 65:35 water to glycerol solution (v:v) (Thermo Fischer Scientific, Waltham MA, A16205-0D) with 6.34 g/L sodium chloride (Sigma-Aldrich, St Louis MO, S5886) and 0.32 g/L sodium azide (Acros, New Jersey, 19038-1000). The diluent and sample were stirred and analyzed for size distribution by the Coulter Counter. The size distribution data collected from each sample was further processed in Microsoft Excel to approximate dry weight of each sample using a correlation between total volume and volume percent developed by Kolewe [81].

3.3 Results and Discussion

3.3.1 Manipulating Transport Mechanisms

Inhibitor study:

Results from the inhibitor study were inconclusive with only 23% of 144 samples containing identifiable levels of PTX. Samples that did show PTX were in low yields in comparison to past results. Imaging and Coulter Counter data (Figures 9-11) showed that most of treated flasks were no longer viable within the first 7 days of the treatment (day 14 of culture). Visual observations suggested viability decrease even earlier at day 2 for some of the treated cells indicated by dark green/brown culture as shown in Figure 8.

Figure 8: Examples of unviable cultures observed after vanadate treatment.

Microscope images of propidium iodine stained samples on days 14 and 21 of cell culture (days 7 and 14 of treatment) gave qualitative evidence of cell death within cultures, as shown in Figure 9. This cell death could be attributed to various reasons including contamination or devastating stress induced by elicitation.

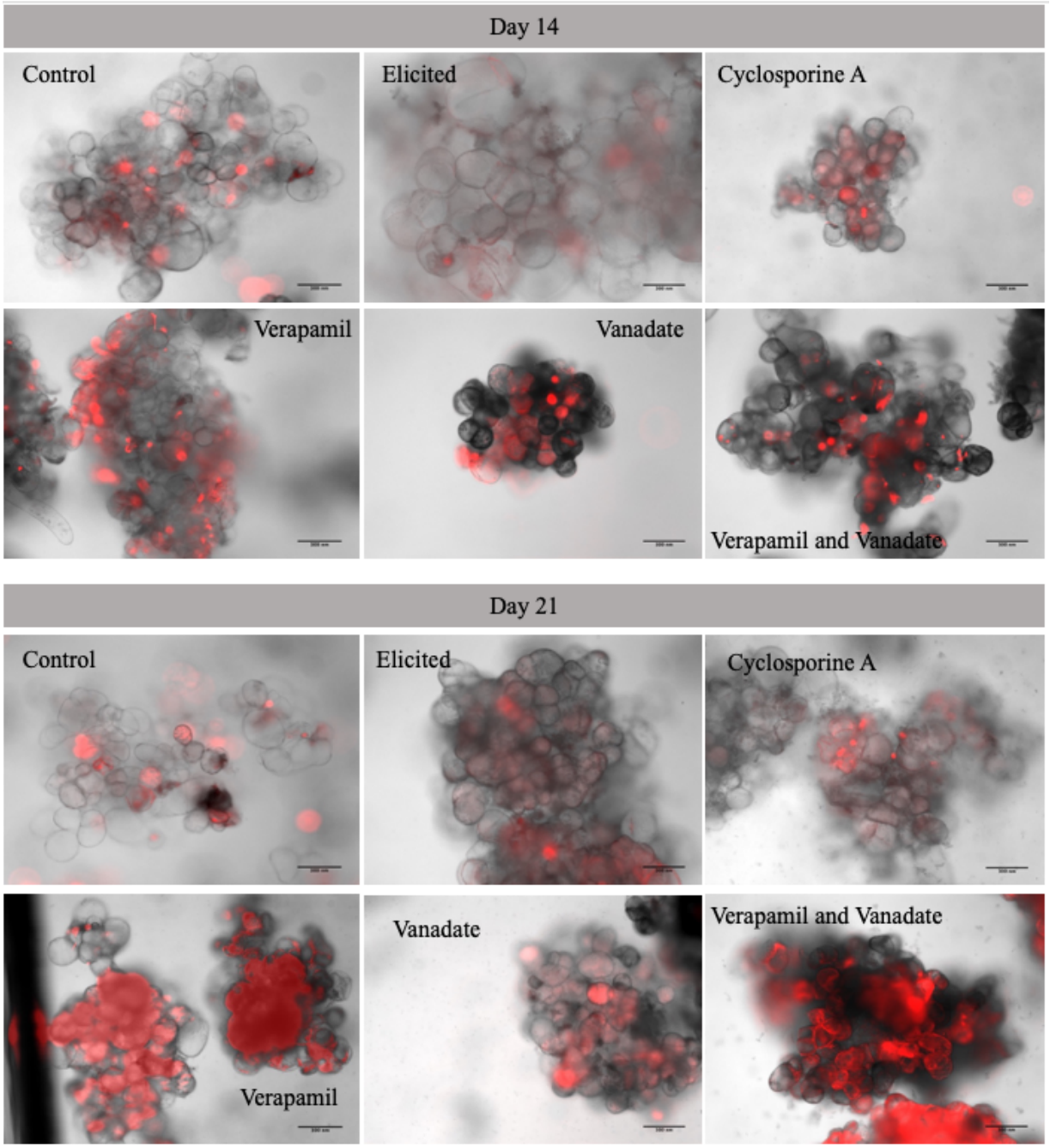

Figure 9: Shows a qualitative analysis of the viability of cultures for each treatment at days 14 and 21 of cell culture (days 7 and 14 after treatment). The red staining indicates a dead nucleus, increased red depicts a culture with poor cell viability. Many flasks show a considerable amount of PI fluorescence by day 14 of culture (day 7 of treatment) an indication of culture death with the exception of the control cells which showed the anticipated low concentration of dead nuclei.

Coulter Counter analysis was used to further understand these observations at the same time samples for UPLC and microscope images were taken. The Coulter Counter data were used to approximate correlated dry weight of the cells through particle diameter. Figure 10 shows the average particle diameter of each treatment at both days.

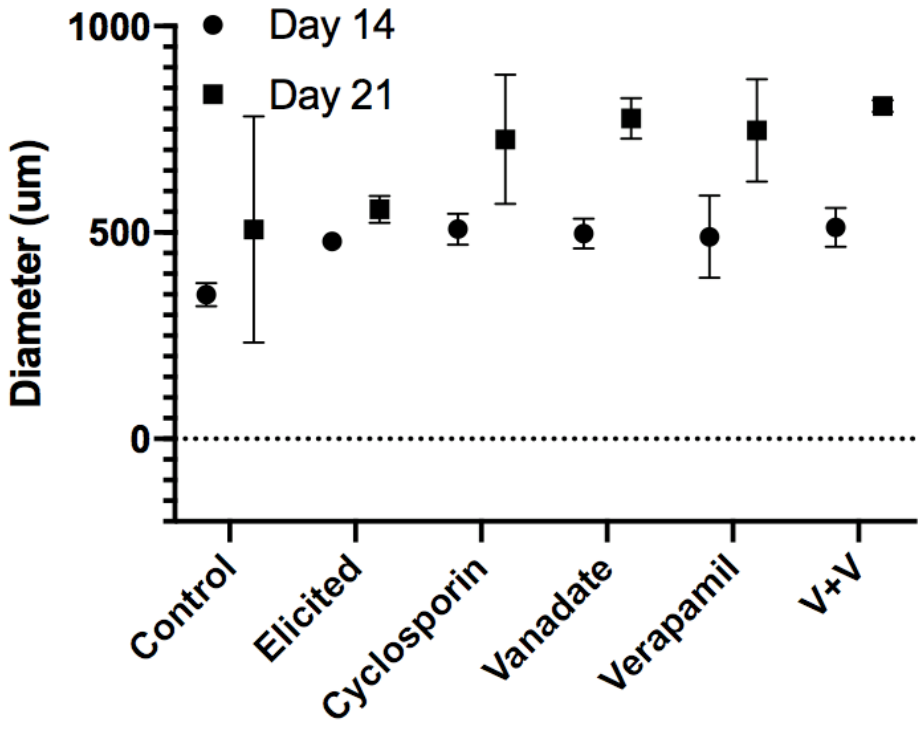

Figure 10: Shows the mean particle diameter of each treatment at days 14 and 21 after treatment, where V+V represents vanadate and verapamil. The error bars represent the standard deviation of each of the three flasks from each other, where one trial per flask was performed.

In all cases, the mean particle diameter increases over time. It was observed that the treated cells have larger diameters compared to control cells. This could be an indication of cell death caused by stresses that cause cell plasma membrane rupture and is preceded by the swelling of various organelles, increasing particle diameter [84]. This hypothesis would support the quantitative observations made from the PI stained microscopy pictures.

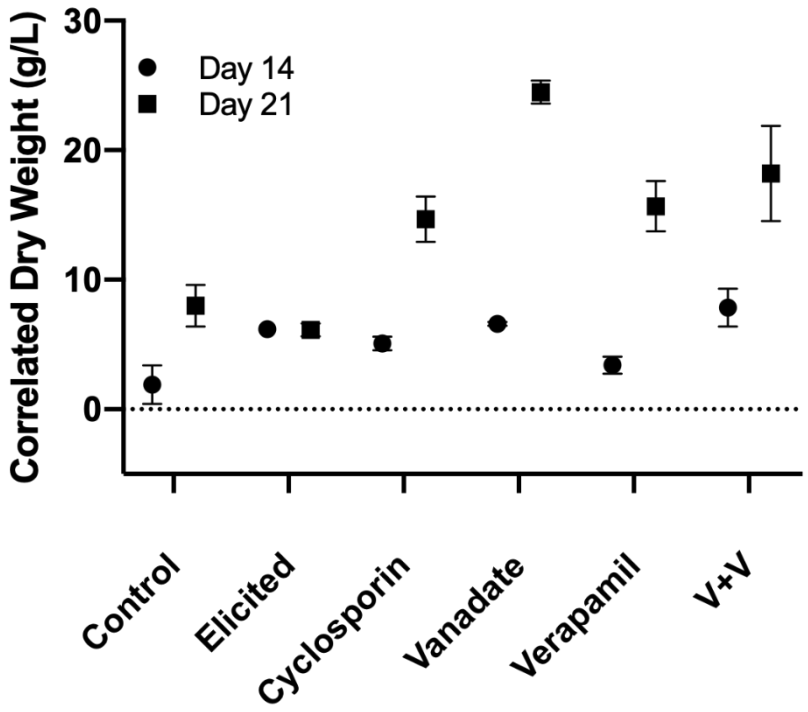

Figure 11: Shows the correlated dry weight calculated from the mean particle diameter data using a relationship developed by Kolewe et al. [81], shown above in Figure 10. The error bars represent standard deviation of the three samples tested for at each data point. As before, V+V represents the vanadate and verapamil treatment.

Like the mean particle diameter, correlated dry weight increased with time. Deviations in trends may be due to the dry weight calculation accounting for the number of particles in each sample. Both treating the cells and time scale of culture can affect the average dry weight.

3.3.2 Exploiting Paclitaxel's Insolubility

Initial results were utilized to determine if the lyophilization of total culture (both cells and media, well mixed) followed by washing significantly affected the resulting mass. Data show that there was no significant difference in final weights between samples washed after lyophilization or those washed prior to lyophilization as shown in Figure 12. With this knowledge all further experiments used cells lyophilized in media (total culture). Also using these data, a correlation between the mass of the total lyophilized culture and cells only was determined so the 2 mg

samples of cells necessary for all the following experiments could be achieved. It was determined that four times (8 mg) the mass of total culture sample is necessary to yield the desired amount of cell biomass (2 mg). This correlation was used for following experiments that used cell lyophilized in media.

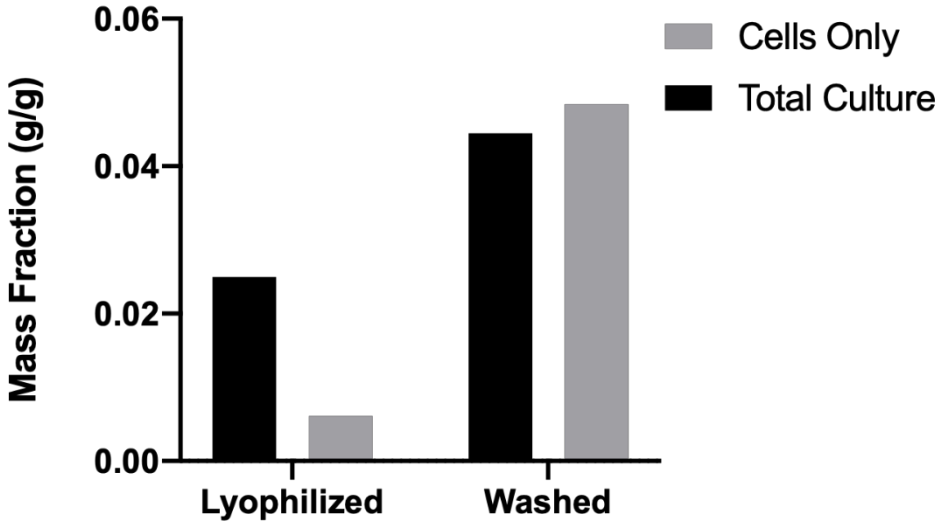

Figure 12: Shows mass fraction on a gram per gram basis of two 20 mL total culture samples normalized to initial total culture mass. The lyophilized mass fractions represent differences between the mass of washed cells (media removed) and total culture sample after lyophilization. The washed mass fractions represent mass fractions after lyophilization and washing, leaving only wet biomass.

Lyophilization Study:

The goal of the lyophilization study was to determine if lyophilizing total culture could increase the amount of cell associated PTX within a sample. To determine the impact that both cells and media had on the concentrations of PTX, elicited culture samples of only cells, only media, and both cells and media were compared prior to lyophilization, after lyophilization, and after washing with deionized (DI) water. Results were used to verify a mass balance on PTX through the various steps in the process and to determine if any PTX was lost during any point of process. Along with the comparison of the concentration for sample type there is also a comparison to the theoretical total to fulfill the mass balance. Results were not consistent with this expected

mass balance. The results also demonstrated no significant variation in total PTX between each step of the lyophilization process, as shown in Figure 12. A significant decrease in total PTX after washing the cells post-lyophilization was observed. This loss is undesirable for product development both from a monetary and feasibility perspective. The elimination of any unnecessary post-lyophilization wash steps or using alternative methods of washing could maximize PTX retention.

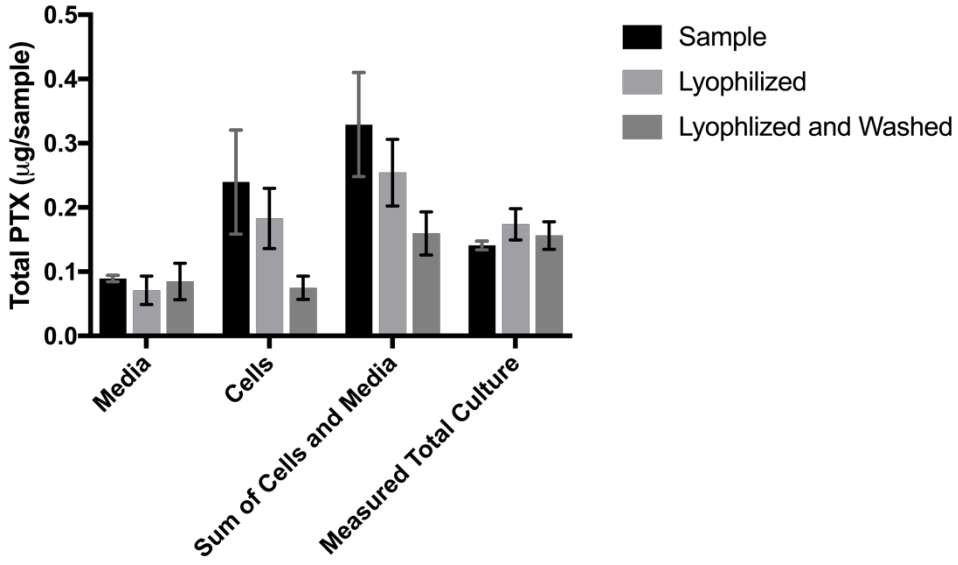

Figure 13: Concentration of PTX in a 1 mL sample. These data shows the comparison of PTX at each stage of the cell lyophilization process for an elicited culture both in total and split into cell and media components. The error bars represent standard deviation amongst three biological replicates.

The total PTX amount for samples of cultures that had additions of PTX 2 hours and 0 hours before lyophilization was also compared. This set of samples demonstrated a significant decrease in the amount of PTX post-washing. This could be due to a lower degree of cell-association of the PTX when added extracellularly or the binding of PTX to extracellular materials that result in PTX removal during the wash steps. The two time points chosen did not show a significant difference in concentration of PTX, so it is unclear if time influences the association of

PTX with the sample (Figure 14). An in-depth absorption study is required to better understand the kinetics.

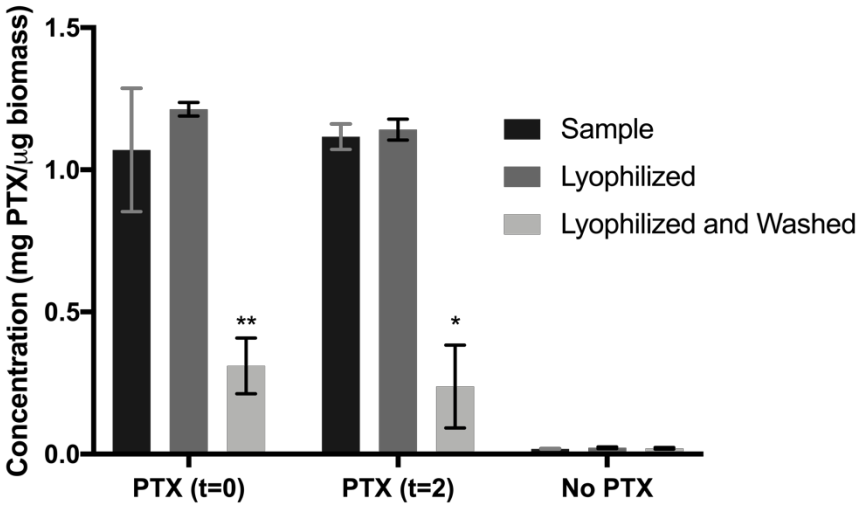

Figure 14: Concentration of PTX/biomass of cells (mg/µg) in a 1 mL sample. These data show the comparison of PTX at each stage of the cell lyophilization process for a culture with the addition of PTX (20 mg/L) 2 hours (t = 2) and at the time of lyophilization (t = 0) in comparison to an elicited culture (No PTX). Error bars represent standard deviations amongst three biological replicates. *=$p<0.03$, **=$p<0.007$ in comparison to the lyophilized and washed No PTX samples.

3.3.3 Conclusions

These studies suggest that the best method to yield significant amounts of PTX in culture to develop an effective delivery system is using MeJA elicited culture that is subsequently treated with 20 mg/L PTX (or even potentially higher concentrations) in culture prior to lyophilization. It is understood that this method does not optimize the process, as the best process would utilize only the PTX produced by the plant cell suspension cultures and maintain its concentration after washing. There are currently ongoing efforts to increase PTX production and accumulation, some of which are discussed further in Section 6.1.1. With this conclusion in mind all subsequent experiments were executed using cells that were both MeJA elicited and treated with 20 mg/L PTX.

Chapter 4: Preparation of a Drug Delivery System

4.1. Background

In applications where foreign biological material is introduced to mammalian tissue, it is important that foreign DNA is not brought in to the system as to avoid an immune response [85]. In delivery systems stemming from living organisms or cells, decellularization (the removal of DNA) is necessary in order to prevent this issue [85]. This is the case for a *Taxus* cell derived drug delivery system, requiring the decellularization of the cell aggregates to remove DNA which may be harmful to healthy human tissue [85]. This must be executed while also ensuring that a large enough concentration of PTX is maintained to ensure effective treatment.

4.1.1. *Taxus* Cell Culture Processing

The use of PTX as a therapy presents some unique challenges, mainly due to its low solubility in aqueous solutions [41]. It is believed that PTX retention in processed culture will aid in bypassing this challenge by permitting direct delivery, but it raises concern about the mechanism in which the PTX will be released from the system upon placement on or in the tumor tissue (explored in Chapter 5). Biocompatibility of the drug delivery system with mammalian tissue is an important consideration to avoid an immune response.

Specialized metabolites produced by plants are of interest in the medical field because of their bioactive properties; PTX being an example of this. In some cases, synergistic effects between metabolites can help overcome cases of drug resistance and improve treatment [65]. Additional effects of specialized metabolites that could potentially be found in plant cell culture

as previously discussed. Lyophilization of plant material generally preserves the chemicals within it, especially those that are non-volatile, protecting the medicinal value [82].

4.1.2. DNA and Drug Delivery

Decellularization minimizes the effect of foreign DNA on mammalian tissue. DNA has a strong negative charge and is susceptible to nucleases in mammalian tissue [86]. Foreign DNA can elicit a cascade of responses by the immune system including the proliferation of B cells, white blood cells, and dendric cells [87]. In humans, nonparenchymal liver cells work to clear foreign DNA from circulation in the bloodstream [86]. *Taxus* suspension culture cell lines contain varying amounts of DNA that can change over time due to chromosomal rearrangements [88]. Based on studies that used flow cytometry, nuclear DNA content of *Taxus* cells varies between 21.06 and 62.30 pg/cell [88, 89]. DNA can be enzymatically degraded with deoxyribonuclease I. DNase cleaves DNA randomly in the presence of Mg^{2+} ions and uniformly in the presence of Mn^{2+} ions [90].

4.1.3. DNA Quantification

DNA quantification of cells through PicoGreen Assay requires lysing of the cell wall. This can be done with cell-wall degrading enzymes such as cellulase, hemicellulase, and macerozyme. Cellulase (derived from *Trichoderma verde*) functions through breaking down cellulose present in the cell wall by hydrolization of its 1,4-glucosidic linkages [91]. Hemicellulase (derived from *Aspergillus niger)* is a combination of glycolytic enzymes that break down sugars present in hemicellulose making up the cell wall [92]. Hemicellulase usually contains xylanases that degrades xylan, a component of hemicellulose and mannanases, enzymes that degrade mannans, also present in hemicellulose [93, 94]. Macerozyme (derived from *Rhizopus sp.*) is a blend of pectinases that cleave pectins in the cell wall by hydrolysis [95]. It is important to note that PTX may be affiliated

with the cell wall, as the use of cell-wall degrading enzymes has been seen to release PTX in surrounding cell media [96]. Therefore, degradation of the cell wall is mainly important to DNA quantification, not the decellurazation process itself in the context of this project.

4.2 Methods

This study aimed to investigate the capacity for cultures to retain PTX and other specialized metabolites through decellularization, the elimination of DNA. The following procedure describes the decellularization process and the steps taken to analyze content of DNA, PTX, flavonoids, and phenolics throughout processing of *Taxus* cultures.

4.2.1 Quantifying DNA Removal

The first goal was to quantify total DNA in untreated samples. Lyophilized (2 mg, washed before lyophilization) culture samples were treated with three enzymes and one control, as described in Table 4.

Table 4: DNA Removal Test Groups

Enzymatic test group names and amounts of treatment added. The primary addition was added to triplicates of 2 mg lyophilized cells (washed preceding lyophilization) and incubated for one hour at room temperature before the secondary addition was added.

Treatment (in triplicates)	Primary Addition (200 µL)	Secondary Addition
Hemicelluase	5% Hemicelluase in PBS	200 µL Nuclear Lysis Buffer 0.10 g Bullet Blender Beads
Celluase	5% Celluase in PBS	
Macerozyme	5% Macerozyme in PBS	
Buffer Only (Control)	PBS	

Each of the four treatments tested 2 mg of washed then lyophilized cell samples in triplicate. The three enzymes tested: hemicellulase (Sigma-Aldrich, St Louis MO, H-2125), cellulase (bioWORLD, New York NY 21500003-1), and macerozyme (ICN Biomedicals Inc, Aurora OH, 152340) were mixed in 0.1 M phosphate buffered saline (1x PBS) (Fisher Scientific, Hampton NH, BP2944-100) for a 5% (w:v) solution. Nuclear lysis buffer was made from a solution of Tris EDTA (TE) buffer containing 0.1% Triton X-100 detergent (Sigma-Aldrich, St Louis MO, 9002-93-1). A flow chart of the experimental process can be seen in Figure 15.

A primary addition of 200 µL of each enzyme solution (or PBS in the Buffer Only treatment) was added to each lyophilized cell sample in triplicates and incubated for one hour. Following incubation, each sample was diluted with 200 µL nuclear lysis buffer and approximately 0.10 g of 0.5 mm diameter zirconium silicate beads (Next Advance, Troy NY). Samples were ground in a Bullet Blender (Next Advance, Troy NY) for 8 minutes. After grinding, samples were centrifuged at 15,000 RPM for 8 minutes, and 20 µL of the supernatant was analyzed via the PicoGreen Assay (Section 4.2.3). The treatment that provided the greatest DNA release was used preceding the following PicoGreen Assays.

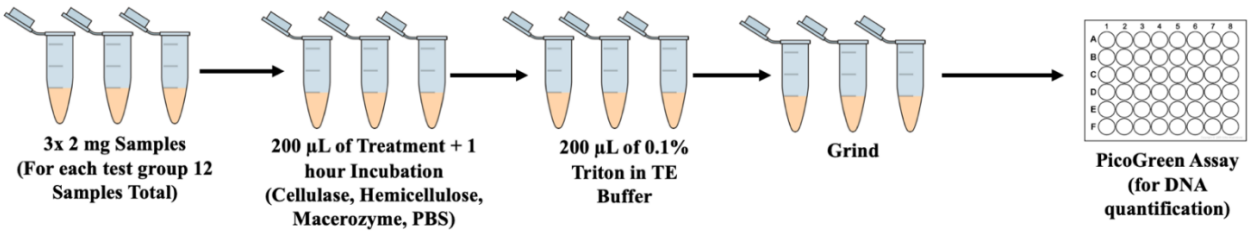

Figure 15: Flow chart of the steps for the experiment to determine which method is the best for DNA extraction.

4.2.2. DNAse Treatment to Degrade DNA

This study investigated two test groups of 21260C (*Taxus chinensis*), untreated (control) and MeJA elicited + 20 mg/L PTX (treated). On day 21 of culture, 1 mL mechanically homogenized (BioSpec Products, Inc., Bartlesville OK, Tissue Tearor^{TM}) culture samples were taken in triplicate from both test groups and stored at stored at -20 °C until processing. All the remaining cell culture was then lyophilized and stored at -80 °C until further processing.

Eight milligrams of treated and lyophilized total culture samples were weighed into 1.5 mL microcentrifuge tubes. Samples were treated with DNase, and triplicates were used for both DNA and PTX quantification. DNA quantified samples followed the DNA extraction procedure outlined in Section 4.2.1 followed by the PicoGreen Assay (procedure in Section 4.2.3) and PTX quantified samples were processed with UPLC. One DNase+ treated sample was reserved for imaging. All treatments were compared to triplicates of samples incubated in a buffer absent of DNase and triplicates of samples which underwent no treatment at all. These procedures are presented in Figure 16.

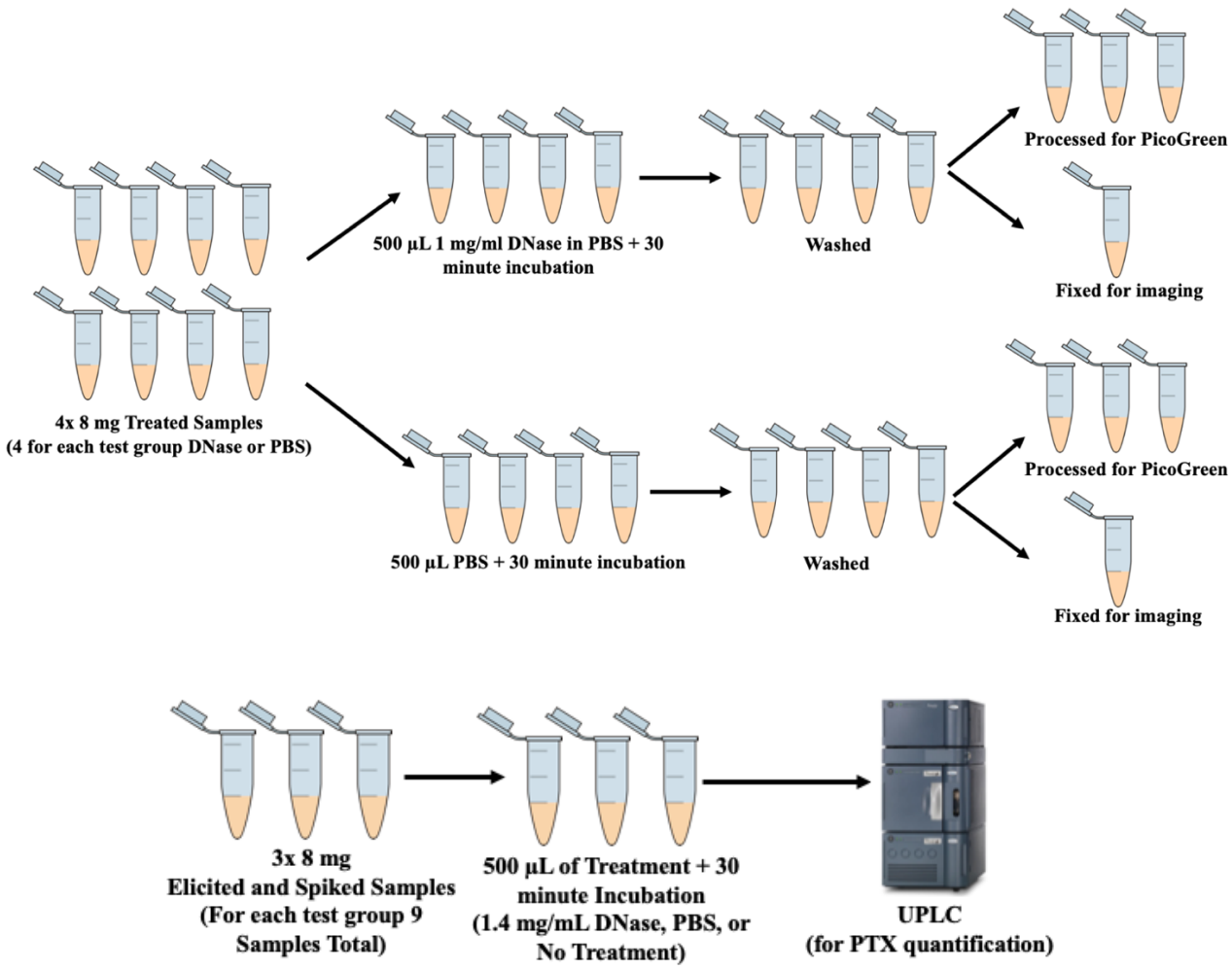

Figure 16: Flow chart of the steps for the DNase experiment split into elicited and unelicited cells.

Additionally, 6 (8 mg) total lyophilized culture samples of both *Treated* and *Control* cells were designated for the phenolics and flavonoids assays described in Section 3.2.4.

The decellularization procedure was designed to remove DNA from the lyophilized cells followed by DNA quantification steps to ensure that the DNA was degraded. A DNase buffer consisted of DNase enzyme, (Sigma-Aldrich, St. Louis MO, D5025) and Dulbecco's PBS (DPBS), PBS with Ca^{2+} and Mg^{2+} (Thermo Fisher Scientific, Waltham MA, 14080-055) to create a 1 mg DNase/mL solution. DNase buffer (500 µL) was added to each 8 mg sample and degassed under

house vacuum with a desiccator until gas trapped in samples was removed. Samples that were not treated with DNase were treated with 500 µL of DPBS. +DNase and –DNase samples were all incubated for 30 minutes at 37 °C. The samples were centrifuged (15,000 RPM for two minutes) and the initial supernatant was removed and saved for UPLC quantification. Samples were washed four times with PBS (volumes of 500 µL, 700 µL, 900 µL, 900 µL), centrifuged (15,000 RPM for two minutes) between each wash.

4.2.3 PicoGreen Assay Procedure

DNA concentration of samples were quantified using fluorometric assay with the Quant-iT™ PicoGreen™ dsDNA Assay Kit (Thermo Fisher Scientific, Waltham MA, P11496). Samples were prepared through the DNA release protocol outlined in Section 4.2.1. A stock solution of 98.2 µg/mL purified genomic plant DNA was diluted in 0.01% Triton X-100 TE buffer for DNA standards of the concentrations: 0, 0.0049, 0.015, 0.044, 0.131, 0.394, 1.183, and 3.556 µg/mL. The working assay solution was prepared by adding 16 µL of PicoGreen Assay reagent to 3.72 mL of 1X TE Buffer. In a black 96 well plate, 50 µL of the working assay solution and 50 µL of each sample supernatant or standard was added to individual wells. The plate was incubated at room temperature for 5 minutes, then the florescence was read with a F535 emission filter on a Victor3 1420 Multilabel Plate Reader (PerkinElmer, Waltham, MA).

4.2.4 Flavonoid and Phenolic Assay Procedures

Sample Preparation

For both the phenolics and flavonoids assays the following sample preparation steps were taken. For samples taken from suspension, 1 mL well mixed samples were taken and stored at -80 °C. For lyophilized cultures, 8 mg of cell sample was weighed out into a microcentrifuge tube, and half were washed with DI water. The day before the assay was run, all samples were dried

overnight via evaporative centrifuge on the aqueous evaporation setting (V-AQ). Both the dried suspension cultures and the lyophilized samples were resuspended in 500 µL of acidified methanol (0.01% acetic acid). The samples were then vortexed and broken up mechanically with a spatula, similarly to the protocol for UPLC preparation. The samples were then centrifuged at 15,000 RPM for 10 minutes.

Phenolics Assay

The following components were combined in a microcentrifuge tube; 4 µL of the sample supernatant,16 µL of acidified methanol, 40 µL 0.2M Folin-Ciocalteau reagent, and 160 µL 700 mM sodium carbonate (Fischer Scientific, Hampton NH, S263-500). The assay was incubated for 10 minutes at room temperature, and then centrifuged at 15,000 RPM for one minute. For each sample, 200 µL of the supernatant was transferred to a 96 well plate and the colorimetric absorbance was read at 750 nm on a colorimetric plate reader (Accuskan Go, Fisher Scientific, Hampton NH). These readings were quantified to phenolic concentration using gallic acid as a standard at 0.0 mg/mL, 0.025 mg/mL, 0.05 mg/mL, 0.075 mg/mL, 0.10 mg/mL, and 0.20 mg/mL.

Flavonoids Assay

The following reagents were placed directly into 96 well plates: 25 µL of the sample supernatant, 50 µL water, and 75 µL sodium nitrite (Acros, New Jersey, 42435-5000) (6 g/L). These were incubated for 30 seconds. Next, 75 µL aluminum chloride (Sigma-Aldrich, St Louis MO, 7784-13-6) (22 g/L $AlCl_3 \cdot 6H_2O$) was added, followed by another two minutes incubation. Finally, 75 µL 0.8 M sodium hydroxide (Sigma-Aldrich, St Louis MO, 1310-73-2) was added to each well and the colorimetric absorbance was read at 490 nm. These readings were

compared to standards of catechin (Cayman Chemical, Ann Arbor MI, 70940) at 0.0 mg/mL, 0.1 mg/mL, 0.2 mg/mL, 0.4 mg/mL, 0.6 mg/mL, 0.8 mg/mL, and 1.0 mg/mL.

4.2.5 Nuclear DNA Imaging Procedure

Three 8 mg samples of lyophilized 21260C (*Taxus chinensis)* culture that had been elicited with MeJA (200 μM seven days preceding lyophilization) and loaded with PTX (20 mg/L) preceding lyophilization were taken for nuclear DNA imaging with Hoechst Stain (Hoechst 33342, Tocris Bioscience, Bristol United Kingdom, 5517) to visualize the effect of DNase treatment on DNA concentration. Treatments examined were lyophilized only (as a control), DNase+, and DNase-. DNase+/- treatments were performed as described in Section 4.2.2. After appropriate processing steps, each sample was formalin fixed by adding 0.5 mL of 4% paraformaldehyde (PFA) (Acros, New Jersey, 30525-89-4) in PBS to each sample and incubating for 2 hours. Samples were centrifuged briefly, and the PFA supernatant was replaced with 0.5 mL PBS and stored at 4° C until imaging.

For staining, 0.5 μL of 2 μg/mL Hoechst stain in PBS was added to each sample and incubated for 30 minutes in the dark at room temperature. Preliminary images did not appear to show as many nuclei as expected, so 0.1 μL of Hoechst stain (2 μg/mL) was added to each sample and incubated for approximately three additional minutes. Images were taken at 20x magnification at brightfield (exposure time of 500 milliseconds) and fluorescence (exposure time of 250 milliseconds) on a Nikon Eclipse E600 microscope (MVI, Avon MA). The exposure time was modified as necessary for image clarity.

4.3 Results

4.3.1 Determining DNA Release Protocol

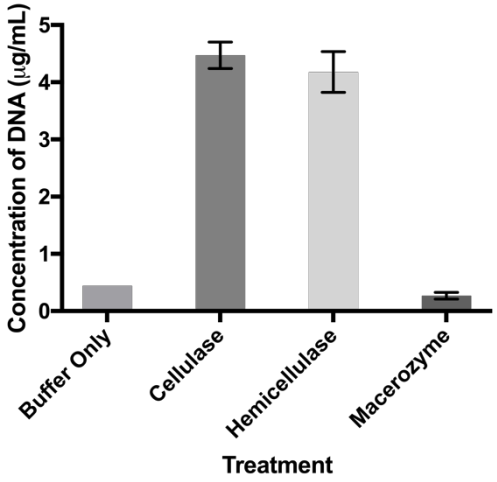

Figure 17: Concentration of DNA (µg/mL) in solution after non-elicited lyophilized plant cells were treated for DNA extraction. Error bars represent standard deviations of three biological samples which we each averaged from three technical replicates. The buffer only control lacks error bars because two of the biological replicates were lost during sampling.

Figure 17 represents the data collected to determine the best method to quantify the amount of DNA removed in future experiments. These data suggest that both cellulase and hemicellulase efficiently degraded the cell wall to release DNA. Cellulase was utilized in the remaining experiments to prepare samples for the PicoGreen Assay.

4.3.2 DNase Treatment Results

Treatment with DNase was effective in reducing DNA content of the lyophilized *Taxus* culture by approximately 82% (Figure 18). This indicated that the process piloted is an effective way to remove a significant portion of the DNA in preparation of the delivery system. DNA removal would ultimately reduce the amount of foreign DNA being introduced into the body, which lowers the risk of adverse reactions to the treatment. Further optimization of this process regarding the concentration and activity of DNase could increase the amount of DNA degraded in

a sample. Product labels suggest using an alternative solvent to a phosphate buffer and avoiding agitation to increase efficacy [90].

DNA removal:

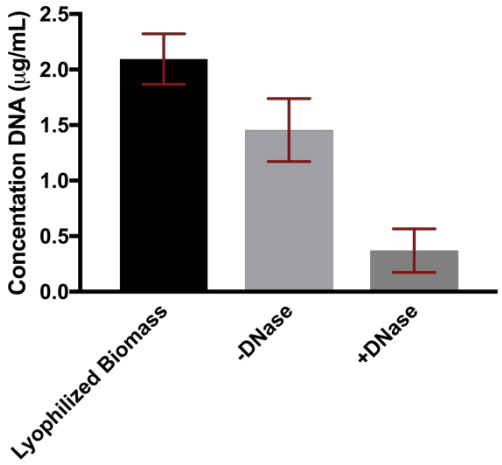

Figure 18: Concentration of DNA (µg/mL) in solution after elicited (200 µM MeJA) and treated (20 mg/L PTX addition) lyophilized plant cells were treated with DNase (+DNase), incubated in buffer only (-DNase), and samples which were not treated (lyophilized biomass) and processed for DNA extraction. Error bars represent standard deviations of three biological samples which were each averaged from three technical replicates.

DNA Staining

Fluorescent DNA staining with Hoechst stain allowed for visualization and qualitative confirmation of DNA reduction after treatment with DNase (Figure 19). DNA containing nuclei are highlighted by the blue fluorescent punctates; remaining blue fluorescence was regarded as autofluorescence. Samples that were lyophilized or treated with buffer only showed similar exhibition of nuclei, while the sample treated with DNase show fewer nuclei. The nuclei that remain in the DNase+ sample (notably slide C) reaffirm the PicoGreen data that not all DNA is removed. Larger cellular aggregates made attaining clear images somewhat difficult. A method to break down aggregates before slide preparation or analyze a singer layer of cells may be useful to clarify results.

DNA

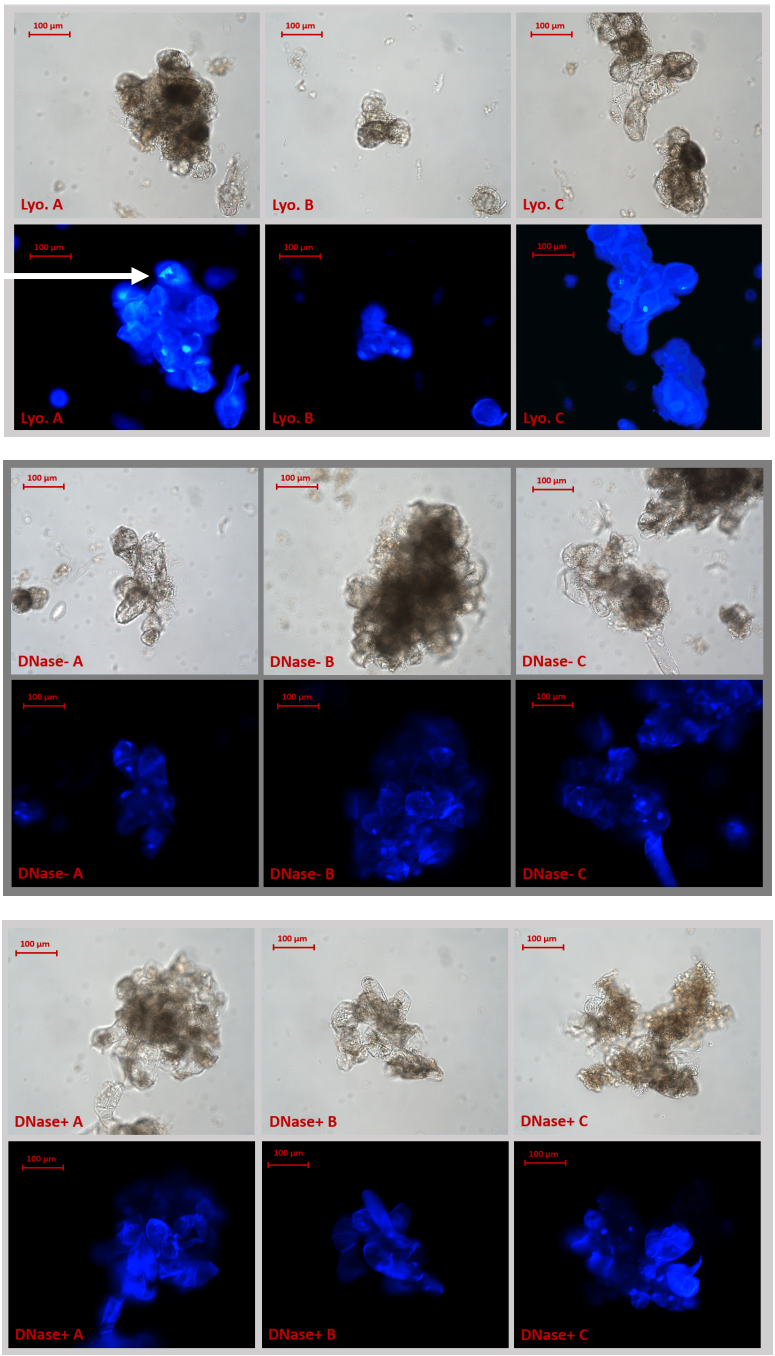

Figure 19: Images taken at 20x magnification of lyophilized 21260C (*Taxus chinensis*) culture elicited with MeJA and PTX displaying differences in DNA content between sample sets. DNA containing nuclei are highlighted by the blue fluorescent punctates, as indicated by the arrow in (Lyo. A). Treatments examined were DNase (DNase+), treatment with buffer only (DNase-), and lyophilized cells (Lyo). Each set of six images were from a single biological sample on the same microscope slide (A-C). Brightfield images are shown above fluorescent images in each treatment image group.

Paclitaxel Quantification:

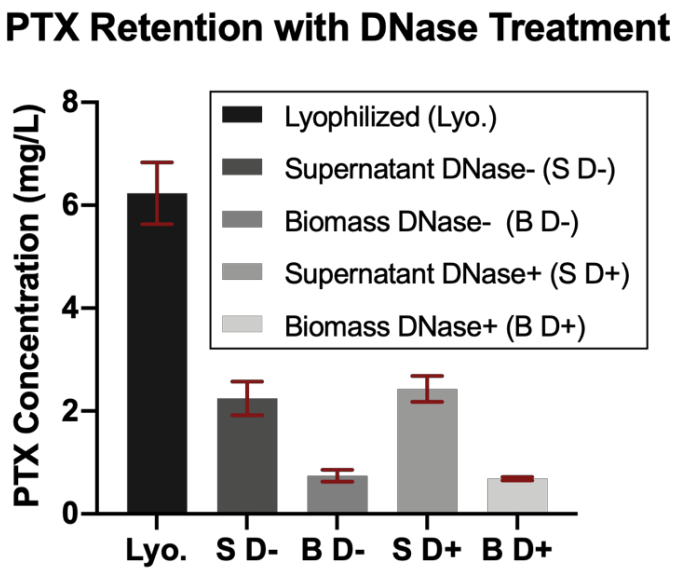

Figure 20: Concentration of PTX (mg/L) in solution after lyophilized plant cells elicited with 200 µM MeJA and treated with a 20 mg/L PTX addition were treated with DNase (+DNase), incubated in buffer only (-DNase) and samples which were not treated (lyophilized) supernatants were collected after DNase treatment to determine the amount lost to the buffer during treatment. Error bars represent standard deviations of three biological samples that were each averaged from three technical replicates.

The retention of PTX through the decellularization process is important to ensure that an adequate amount of PTX is retained for feasible treatment. Through the decellularization process a significant amount of the PTX is lost when compared to the lyophilized biomass (Figure 20). It is hypothesized the loss of PTX is attributed to the problem expressed in earlier experiments in which the PTX binds to water soluble proteins in the media and is therefore removed when washed with aqueous solutions. This observation is supported by the concentration of PTX found in the supernatant, which was removed directly after treatment, which accounts for a considerable amount of the PTX which is lost from the final biomass product. A complete mass balance was not achieved because the supernatants from all the wash steps were not processed. It is expected that if the quantity of PTX in the supernatant from each wash was summed, a greater convergence

to the original lyophilized product PTX concentration would be seen. A typical concentration of PTX for treatment by systemic delivery is 6 mg/mL which is then diluted to 0.2-1.2 mg/ml. This is presumably higher than would be required to be therapeutically significant in a localized delivery scenario because a majority of the drug would not be lost within the blood stream [97]. Further process optimization and better cell-associated PTX accumulation could produce a feasibly large concentration of PTX allowing for *in vitro* cell culture testing.

4.3.3 Flavonoid and Phenolic Quantification

Post-Lyophilization:

Flavonoid and phenolic production increases under MeJA elicitation, and these metabolites have the potential for increased effectiveness of the drug delivery system through synergistic interactions with PTX. Retention of flavonoids and phenolics was quantified through the lyophilization process and wash step for all three conditions (Figure 20).

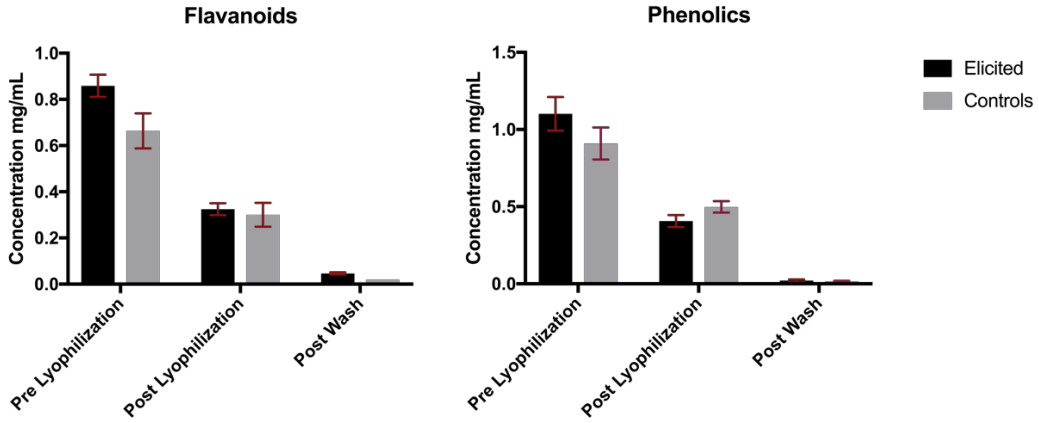

Figure 21: Concentration (mg/mL) of flavonoids and phenolics in both elicited and unelicited (control) samples. Samples tested were: Total Culture (Pre Lyophilization), Lyophilized (Post Lyophilization), and Lyophilized and Washed (Post Wash). Error bars represent standard deviation amongst three biological replicates.

A significant concentration of both flavonoids and phenolics are lost during lyophilization and wash steps. Cells elicited with MeJA have larger observable concentrations of the metabolites compared to cells that have not been elicited. This difference becomes smaller after lyophilization, which could be due to the high volatility of the metabolites. Due to the potential for synergistic effects from these and other specialized metabolites, further optimization of the retention of flavonoids and phenolics and determination of their effect on system efficacy could prove beneficial for future work.

Post-DNase Treatment:

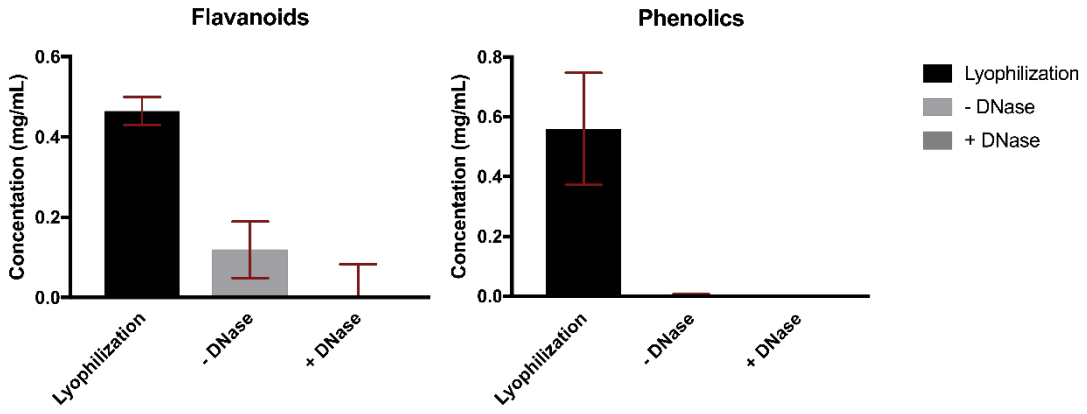

Figure 22: Concentration (mg/mL) of flavonoids and phenolics in +DNase (treated with DNase) -DNase (buffer only) and lyophilized biomass elicited samples. Error bars represent standard deviation amongst three biological replicates.

Following treatment with DNase, the same trend as the post lyophilization analysis can be seen in which the use of an aqueous solution during treatment significantly decreases the concentration of flavonoids and phenolics in the delivery system. The interest in the synergistic effects due to the presence of these metabolites is not relevant unless an increase in the retention is achieved. Because PTX is also a specialized metabolite optimization of the process for retention

of PTX may also result in higher retention of theses metabolite; future studies should explore this possibility.

4.3.4 Conclusions

DNase treatment of lyophilized *Taxus* culture was successful in removing upwards of 80% of the DNA present in a sample within a 30-minute incubation period while maintaining a detectable amount of PTX despite a significant decrease in the concentration when compared to the initial lyophilized sample. The other specialize metabolites screened for (flavonoids and phenolics) were not maintained through the decellularization process. Overall, with proper optimization of PTX retention the decellularization process could be utilized to develop the drug delivery system.

Chapter 5: Drug Delivery System Effectiveness

5.1 Background

5.1.1. Current Treatment of Cancer with Paclitaxel

PTX is an FDA-approved anticancer agent for several solid tumor types when accompanying neutrophil (white blood cell) counts are of at least 1000 cells/mm^3 [98]. It is administered as first-line treatment in non-small cell lung cancer and advanced ovarian carcinoma. In breast carcinoma and AIDS-Related Kaposi's Sarcoma, it is administered as second line treatment [98]. The effectiveness of the PTX as an anticancer agent varies between cell line and cancer type, and it is sometimes administered concurrently with other chemotherapy drugs [98].

PTX is toxic to humans above a threshold concentration of 175 mg/m^2 within 24 hours requiring proper dilution prior to delivery [99].

The current solvent used in treatment today is composed of ethanol, Cremophor EL, and water [41]. This solvent is associated with anaphylactic hypersensitivity, an undesirable reaction characterized by labored breathing, rash, chest pain, low blood pressure, swelling of the deep dermis, and hives [37]. These devastating side effects drive the current push to develop drug delivery systems that meet the requirements to provide effective treatment while also minimizing undesirable side effects caused by the damage to healthy, surrounding cells.

5.1.2. Simulating Paclitaxel Release Kinetics

Drug release kinetics play a large role in the effective delivery of a drug. PTX is hydrophobic and has an affinity for proteins, such as human serum albumin (abundantly found in

the blood) in aqueous environments [100]. Measuring the release of PTX from decellularized *Taxus* biomaterial in a protein-rich solution can be used to preliminarily model how the DDS might release PTX *in vivo.*

Drug stability over the expected length of time for delivery is essential to DDS efficacy. PTX has demonstrated variable stability dependent on temperature and solution composition, most commonly converting to 7-*epi*-taxol at higher temperatures, a thermodynamically more stable isomer [101]. Understanding PTX stability in the DDS and its release environment and release over time is important to maximize system efficacy and ensure that the patient receives a proper dose of drug.

Nanoparticles are commonly used in the delivery of hydrophobic drugs and their release kinetics are commonly studied *in vitro.* Several methods used to study the release of drugs from nanoparticles include dialysis bag suspension, a steady flow through dialysis bag, and suspension in solvent [102]. Often, multiple release mediums are studied, such as PBS, PBS with surfactant, and PBS with protein [102]. One study quantified the release kinetics of PTX loaded poly(lactic-co-glycolic acid) (PGLA) nanoparticles in various release mediums. Release studies such as these are intended to mimic release *in vivo* and are applicable to several DDSs.

5.1.3. Drug and Tumor Interaction

To create an effective drug delivery system, tumor pathology must also be considered. Tumors are not always of a single cell type and their composition is constantly changing. In conjunction with this, their surface marker phenotype may not be consistent across themselves or within subcultures [103]. Anti-cancer treatments are often not capable of penetrating tumor tissue which makes drug diffusion a concern [104]. There are several forms of direct injection that would

be desirable for a PTX total culture drug delivery system. These include microemulsions (mixtures of oil, water, and surfactant), hydrogels, and serums [73]. Examples include thermosensitive chitosan-based hydrogel that can be injected as a liquid to gel when heated to body temperature in order to control the local release of PTX over one month [44] as well as serums such as albumin which has been used in prior PTX studies [105].

5.2. Methodology

5.2.1 Biomass Release Profile

To determine the rate of release of PTX from the decellularized biomass, it was suspended in a PBS and bovine serum albumin (BSA) (Sigma-Aldrich, St Louis MO, 9048-46-8) solution. In triplicates, samples of decellularized biomass (procedure in Section 4.2.2) was suspended in 1 mL of 4% BSA-PBS solution (w:v) and degassed. Samples were incubated at 37 °C and shaken at approximately 150 RPM. Samples were taken 1, 6, 12, 24, 47, 72, 168 (7 days), and 480 (20 days) hours after initial suspension. During the sampling process, the sample tubes were centrifuged at 15,000 RPM for 12-20 minutes until all biomass pelleted, and a 900 µL supernatant sample was removed and replaced with 900 µL of the 4% BSA in PBS solution. Samples were processed for UPLC using the method outlined in Section 3.2.4.

5.2.2 Hydrogel Release Profile

The alginate beads for PTX delivery were prepared using 1.5% (w:v) sodium alginate (Willpowder, Miami Beach FL) aqueous solution which was used to study two different conditions. One solution contained the decellularized biomass incorporated in a 2 mg/mL concentration while the other was loaded with PTX at a 6.85 mg/L concentration. The sodium

alginate and biomass mixture was added dropwise to a 10 mM calcium chloride ($CaCl_2$) (Willpowder, Miami Beach FL) solution. After, the $CaCl_2$ solution was removed to dry the beads. Beads were measured using a ruler as an in-picture scale and Microsoft PowerPoint was used to make size estimates. The average diameter was determined to be approximately 0.3-0.4 cm.

The resulting microbeads were split evenly into 3 wells of a 6-well plate and suspended in 4% BSA-PBS solution. In triplicate, each set of beads (biomass loaded and PTX loaded) were suspended in 5 mL of PBS containing 4% (w:v) of BSA protein and incubated at 37 °C and shaken on an incubator (New Brunswick Scientific Co. Inc, Edison NJ, G24 Environmental Incubator Shaker) at approximately 120 RPM. Samples were taken at 1, 6, and 12 hours until beads were degraded and no longer visible. At each time point 3.4 mL of solution were taken for sampling and the remaining liquid was discarded and replaced with 5 mL PBS-BSA solution. Samples taken were processed for UPLC using the method outlined in Section 3.2.4.

5.2.3 Paclitaxel Degradation in Protein Solution

PTX powder (0.4 mg) was dissolved in 10 mL of PBS containing 4% BSA (w:v) and incubated at 37 °C on a 120 RPM shaker. A well-mixed sample (1 mL) was taken immediately before incubation to confirm initial PTX concentration. Following incubation, two 0.5 mL samples were taken every 48 hours for one week. All samples were stored at -20 °C until UPLC processing using the method outlined in Section 3.2.4.

5.3. Results

5.3.1 Release Profile from Processed Biomass in BSA

The acquired profile (Figure 22) for the decellularized drug delivery system indicates almost complete drug release from the biomass within 72 hours, with most of the PTX release

occurring in the first 24 hours. This establishes the feasibility of drug release to the intended site when placed in the body. Adjusting the initial concentration of PTX in the delivery system at implantation along with optimization of the drug release rate could prove to be an effective treatment for solid cancerous tumors.

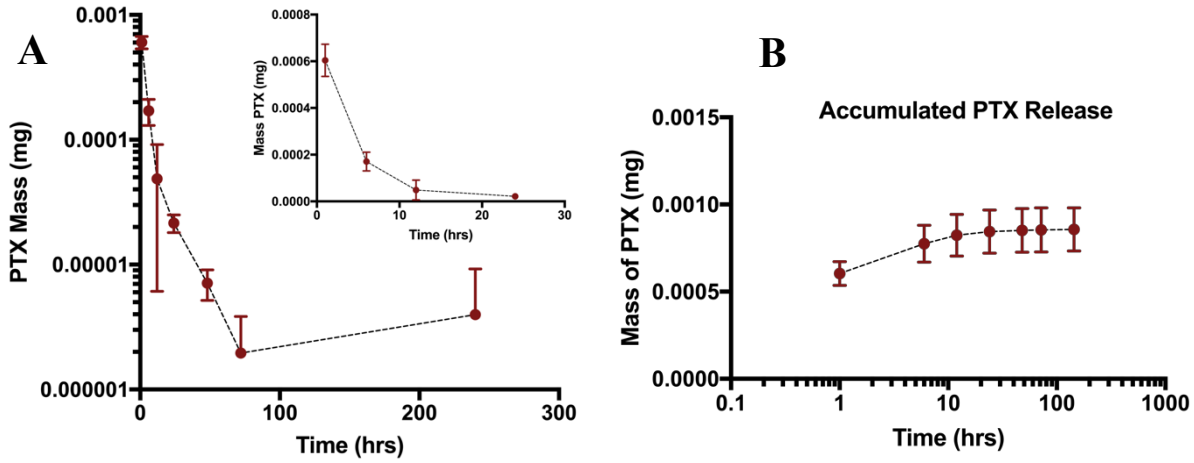

Figure 23: Mass of PTX (mg) released over time by samples after decellularized plant biomass is suspended in a 4 % BSA+PBS solution. F**(A)** Mass of PTX released **(B)** Accumulated PTX release. The mass of PTX in an initial sample is 0.00069 ± 0.00003496 mg. Error bars represent standard deviations of three biological samples.

5.3.2 Release Profile from Alginate in BSA

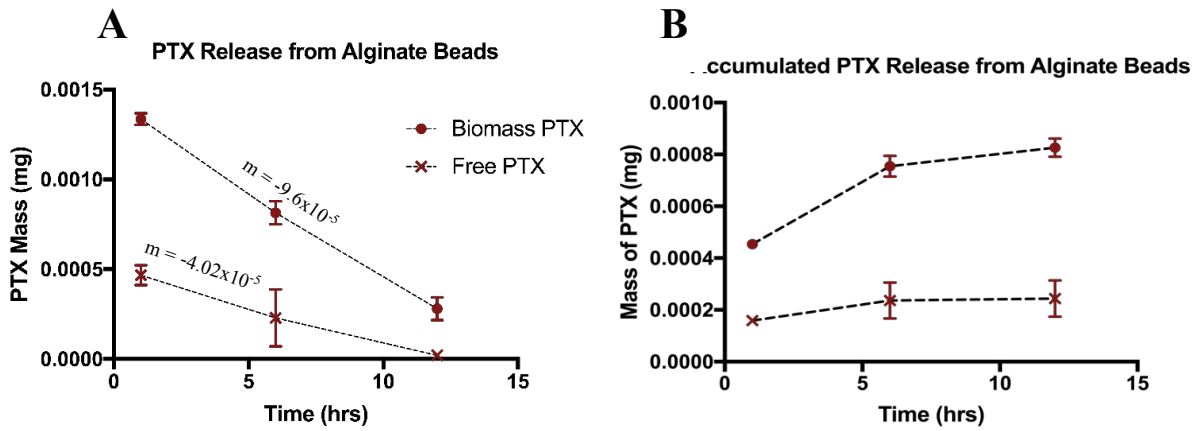

Figure 24: Mass of PTX (mg) released over time by samples after decellularized plant biomass and free PTX were suspended in calcium alginate beads and suspended in a 4 % BSA+PBS solution. (**A)** Mass of PTX released **(B)** Accumulated PTX release. The mass of PTX in an initial sample is 0.00343 ± 0.0001748 mg. Error bars represent standard deviations of three biological samples.

Suspending the biomass in calcium alginate beads resulted in an observable difference in the how long the initial rate of release was sustained. Biomass encapsulated in calcium alginate sustained an almost consistent release rate over the first twelve hours (Figure 23). In comparison, the free biomass has two distinct slopes between the hour 1 - 6 and hour 6-12 (Figure 22). This is an indication that biomass encapsulated in alginate can sustain release longer than free biomass and avoid a spike in release typically associated with uncontrolled treatments.

By comparing the release rate between the encapsulated biomass (biomass PTX) and free PTX by linear regression (Figure 23), the rate of release of free PTX is slower than that of biomass PTX. This could be attributed to a change in the diffusion coefficient of PTX with respect to microbead composition (Figure 24). Contact between biomass aggregates in the gel matrix could have resulted in a more porous structure of the beads, allowing for more diffusion of PTX and a higher diffusion coefficient. The study was not extended past 12 hours due to loss of structural integrity of the microbeads and subsequent homogenization with the PBS-BSA solution.

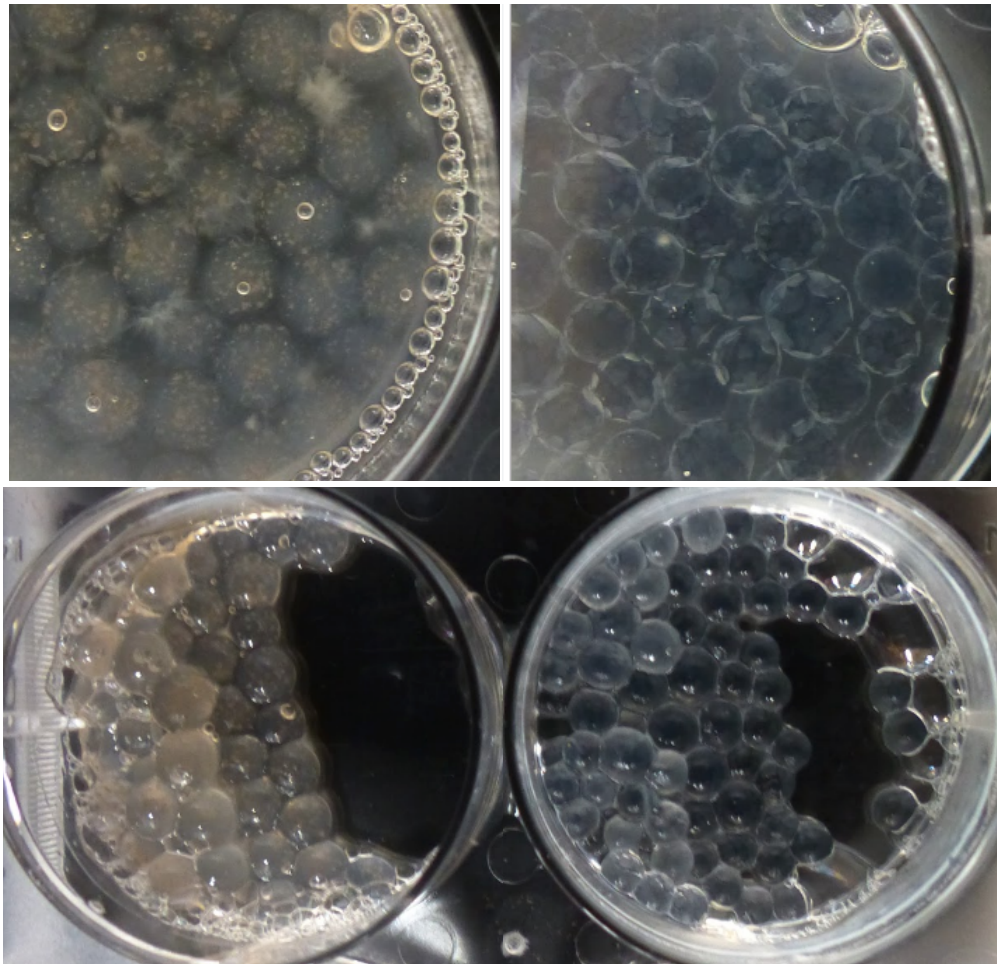

Figure 25: Visualization of alginate microbeads at hour 6 of release study. Biomass-PTX loaded alginate beads are shown on the left and free PTX microbeads on the right. Top images show microbeads submerged in BSA-PBS solution, while bottom images show the beads after solution was removed.

5.3.3 Conclusions

Overall, with proper optimization of preceding steps the drug delivery system has the capability to release PTX over time and thus has the potential for future development toward the goal of clinical applications. Further suspending the beads in a matrix hydrogel could increase the length of a sustained release rate for the which is desirable to increased control of drug dosage and length of treatment. Investigating this and other strategies for tuning PTX release will become imperative as this process develops further.

Chapter 6: Discussion

This Major Qualifying Project studied the potential for use of processed suspension *Taxus* culture in a direct delivery system for PTX. Experiments were conducted to identify how the properties and contents changed throughout processing. Properties analyzed included concentration and retention of PTX, DNA, flavonoids, and phenolics in the cell-culture-product throughout processing. Additionally, the release of PTX from processed cell culture, and process cell culture suspended in alginate beads was studied. The following section outlines the results as well as an overview of future direction to build upon these results.

6.1 Future Research

6.1.1. Production and Retention of Cell Produced Paclitaxel

Maximizing the amount of PTX retained through decellularization processing was a central consideration of this project. To determine fractional loss throughout processing steps, PTX was quantified at various points. PTX was initially introduced into the culture system through both natural production via elicitation with MeJA as well as direct addition of purified PTX to cultures. It was determined that the best method to gain an effective accumulation of PTX was through the use of cells which have both been elicited and treated with 20 mg/L PTX.

For a suspension-culture derived delivery system to be feasible in industry, the cells will need to be able to produce and retain sufficient levels of PTX for treatments to be effective. Additionally, uniformity and quality control of the production process is essential before transition to commercial scale. Elicitors, such as MeJA could be further studied to better understand and

promote the biosynthesis of PTX. Further research on potential transport mechanisms of PTX could help to identify potential modes of efflux that could provide avenues to impact the intracellular accumulation and/or retention of PTX throughout processing steps.

Further investigation of PTX production in suspension cultures could provide insight to methods that could increase the yield of PTX. Research done so far includes growth media tuning and elicitation agents [74]. Patented elicitation agents of taxanes include silver ions or complexes, jasmonic acids, auxin-related growth regulators, and phenylpropanoid pathway inhibitors [74]. Understanding the mechanisms by which these elicitation agents' function could bring further insight to understanding the biosynthetic pathway of PTX and strategies to manipulate it. Additionally, media composition containing levels of taxane precursor(s) α or β-phenylalanine, amino acids, or and sufficient sugars (act as carbon source) promotes the biosynthesis of taxanes [74]. Modification of the environment that cultures are grown in could also be considered. For instance, environmental oxygen can affect the rate of specialized metabolite synthesis and oxygen demands are not constant, varying across growth phases and upon MeJA elicitation [74]. Along with the optimization of the growth environment itself, investigations into multi-stage culture have shown promising results regarding PTX and specialized metabolite production [106].

Phenolic, flavonoid, and related compounds can hinder the growth, vitality, and production of cells when present in abnormal concentrations in culture [74]. Some of the negative effects of high concentrations of these compounds may be reduced with low concentrations of antioxidant agents, such as ascorbic acid in the media (10 ppb - 10 ppm) [74]. Additionally, media replenishment strategies, such as a flow bioreactor or simple media replacement, may alleviate these issues. On the contrary, the properties of specialized metabolites in higher than average concentrations, such as those of phenolic compounds (anti-inflammatory, oxidative stress

protection, anti-bacterial, anti-parasitic, and antiseptic) could act synergistically when retained within the DDS [65]. The potential synergistic effects of these compounds with PTX are one area which further research could identify the benefits or challenges of a full-cell based DDS.

6.1.2. Expansion of Specialized Metabolite Study

This project only examined flavonoid and phenolic production and retention throughout processing. Our preliminary results found that elicitation with MeJA increases the concentration of both metabolite classes in culture, although concentrations were significantly reduced with DDS processing steps. Identification and quantification of specific metabolites is important to research further so that potential synergistic effects between the DDS and tissue can be anticipated, or even manipulated. Future research could be geared towards determining conditions that promote the production of favorable metabolites in *Taxus* as well as identifying techniques to retain those desired metabolites throughout processing, such as phenolic compounds with anti-inflammatory properties [65].

Numerous other specialized metabolites such as terpenoids and alkaloids, some of the most common metabolites produced, are also likely present in *Taxus* culture [107]. Alkaloids are of pharmaceutical interest primarily due to their pain reliving, anti-malarial, anti-cancer, anti-inflammatory, anti-bacterial, anti-viral, and neurotoxic properties [65]. Although many of these properties could be beneficial, there is also many possible adverse reactions. Identifying compounds which could cause these and developing methods to remove or minimize their effects will be an important step in the further development of this project.

6.1.3. Further Study of Decellularization Process

DNA removal experiments used deoxyribonuclease I from bovine pancreas to digest DNA and the PicoGreen Assay to quantify the removal. Further research could be done on alternative

decellularization enzymes or methods that may allow for an increase retention of PTX or beneficial metabolites during the process. Further research into the ordering, number, and method of wash steps could be done to minimize PTX loss and make the process more efficient and scalable.

6.1.4. Determination of Cytotoxicity *in vitro*

It is common to use cytotoxicity against cancer cell lines to determine if the anticancer agent is effective [103]. There are a variety of assays that can be done to assess cytotoxicity and cell viability. The MTT assay is a colorimetric assay which uses a dye that is reduced by living cells and correlates the spectrophotometric absorbance to the amount of viable cells [108]. This assay, or comparable alternatives, can be performed on a cancer cell lines with various treatments to quantify cytotoxic effects of the DDS. The result of such tests would reflect the potential for the treatment to influence cancer *in vivo* [109].

6.1.5. Interaction of DDS with Tissue

The effectiveness of the DDS on tumors and biocompatibility of it with surrounding tissue is an important area of interest in this research that can be started with testing *in-vitro*. Biocompatibility of the DDS with healthy cells and with tumor cells should be investigated. Cytotoxicity and cell viability can be evaluated with assays such as the MTT, a colorimetric assay, and resazurin, a fluorometric assay [108, 109].

The release of the PTX from the DDS could be refined with a variety of methods. For instance, an impermeable layer or film could be introduced to one side of the DDS to inhibit drug transfer away from the site of interest. An extended release system, such as through steady degradation of a polymer matrix, could also be employed. Achieving a therapeutically relevant drug concentration in the surrounding tissue over the desired time frame will require significant

tuning of the DDS. The rate of release could also be studied under various circumstances such as material composition modifications or in environments that more accurately mimic *in vitro* conditions such as 3D cultures [15].

References

References

1. Bray, F., et al., *Global cancer statistics 2018: GLOBOCAN estimates of incidence and mortality worldwide for 36 cancers in 185 countries.* 2018.

2. Budget, O.o. *2017 Budget in Breif*. 2016 [cited 2018 10/13/2018]; Available from: https://www.hhs.gov/about/budget/fy2017/budget-in-brief/nih/index.html.

3. Gavhane, Y., et al., *Solid tumors: facts, challenges and solutions.* 2011. **2**(1): p. 1-12.

4. Singla, A.K., A. Garg, and D.J.I.j.o.p. Aggarwal, *Paclitaxel and its formulations.* 2002. **235**(1-2): p. 179-192.

5. Liu, W., T. Gong, and P.J.R.A. Zhu, *Advances in exploring alternative Taxol sources.* 2016. **6**(54): p. 48800-48809.

6. DiCosmo, F. and M.J.B.a. Misawa, *Plant cell and tissue culture: alternatives for metabolite production.* 1995. **13**(3): p. 425-453.

7. Zhang, Z., L. Mei, and S.-S.J.E.o.o.d.d. Feng, *Paclitaxel drug delivery systems.* 2013. **10**(3): p. 325-340.

8. Modulevsky, D.J., C.M. Cuerrier, and A.E.J.P.o. Pelling, *Biocompatibility of subcutaneously implanted plant-derived cellulose biomaterials.* 2016. **11**(6): p. e0157894.

9. Coburn, J., et al., *Implantable chemotherapy-loaded silk protein materials for neuroblastoma treatment.* 2017. **140**(3): p. 726-735.

10. Beneke, C.E., A.M. Viljoen, and J.H.J.M. Hamman, *Polymeric plant-derived excipients in drug delivery.* 2009. **14**(7): p. 2602-2620.

11. Żwawiak, J. and L.J.J.o.M.S. Zaprutko, *A brief history of taxol.* 2016. **83**(1): p. 47-52.

12. Weaver, B.A.J.M.b.o.t.c., *How Taxol/paclitaxel kills cancer cells.* 2014. **25**(18): p. 2677-2681.

13. Liebmann, J., et al., *Cytotoxic studies of paclitaxel (Taxol®) in human tumour cell lines.* 1993. **68**(6): p. 1104.

14. Ehrlich, A., et al., *Micellar paclitaxel improves severe psoriasis in a prospective phase II pilot study.* 2004. **50**(4): p. 533-540.

15. Park, S.-J., et al., *A paclitaxel-eluting stent for the prevention of coronary restenosis.* 2003. **348**(16): p. 1537-1545.

16. Croteau, R., et al., *Taxol biosynthesis and molecular genetics.* 2006. **5**(1): p. 75-97.

17. Howat, S., et al., *Paclitaxel: biosynthesis, production and future prospects.* 2014. **31**(3): p. 242-245.

18. Ojima, I., et al., *New and efficient approaches to the semisynthesis of taxol and its C-13 side chain analogs by means of β-lactam synthon method.* 1992. **48**(34): p. 6985-7012.

19. Schneider, B., et al., *Taxane analysis by high performance liquid chromatography–Nuclear magnetic resonance spectroscopy of Taxus species.* 1998. **9**(5): p. 237-244.

20. Clarke, S.J. and L.P.J.C.p. Rivory, *Clinical pharmacokinetics of docetaxel.* 1999. **36**(2): p. 99-114.

21. De Bono, J.S., et al., *Prednisone plus cabazitaxel or mitoxantrone for metastatic castration-resistant prostate cancer progressing after docetaxel treatment: a randomised open-label trial.* 2010. **376**(9747): p. 1147-1154.

22. Omlin, A., et al., *Analysis of side effect profile of alopecia, nail changes, peripheral neuropathy, and dysgeusia in prostate cancer patients treated with docetaxel and cabazitaxel.* 2015. **13**(4): p. e205-e208.

23. Alexandre, J., et al., *Accumulation of hydrogen peroxide is an early and crucial step for paclitaxel-induced cancer cell death both in vitro and in vivo.* 2006. **119**(1): p. 41-48.

24. Reuther, C., A.L. Diego, and S.J.N.n. Diez, *Kinesin-1 motors can increase the lifetime of taxol-stabilized microtubules.* 2016. **11**(11): p. 914.

25. Lanni, J.S., et al., *p53-independent apoptosis induced by paclitaxel through an indirect mechanism.* 1997. **94**(18): p. 9679-9683.

26. Weir, G.M., R.S. Liwski, and M.J.C. Mansour, *Immune modulation by chemotherapy or immunotherapy to enhance cancer vaccines.* 2011. **3**(3): p. 3114-3142.

27. Ketchum, R.E., et al., *Efficient extraction of paclitaxel and related taxoids from leaf tissue of Taxus using a potable solvent system.* 1999. **22**(11): p. 1715-1732.

28. Hong, S.-S., et al., *Method for purifying taxol from taxus biomass*. 1999, Google Patents.

29. Schippmann, U., *Medicinal Plants Significant Trade Study: CITES Project S-109, Plants Committee Document PC9 9.1. 3 (rev.)*. 2001: BfN.

30. Malik, S., et al., *Production of the anticancer drug taxol in Taxus baccata suspension cultures: a review.* 2011. **46**(1): p. 23-34.

31. Hook, I., et al., *Seasonal variation of neutral and basic taxoid contents in shoots of European Yew (Taxus baccata).* 1999. **52**(6): p. 1041-1045.

32. Holton, R.A., et al., *First total synthesis of taxol. 1. Functionalization of the B ring.* 1994. **116**(4): p. 1597-1598.

33. Nicolaou, K., et al., *Total synthesis of taxol.* 1994. **367**(6464): p. 630.

34. McClenahan, S.R. and W.M. Rogers, *Investigation of DNA Methylation and Paclitaxel Production Levels in Taxus Cell Cultures.* 2018.

35. Naill, M.C. and S.C. Roberts, *Cell cycle analysis of Taxus suspension cultures at the single cell level as an indicator of culture heterogeneity.* Biotechnology and bioengineering, 2005. **90**(4): p. 491-500.

36. Parmar, V.S., et al., *Constituents of the yew trees.* 1999. **50**(8): p. 1267-1304.

37. Gelderblom, H., et al., *Cremophor EL: the drawbacks and advantages of vehicle selection for drug formulation.* 2001. **37**(13): p. 1590-1598.

38. Scripture, C.D., et al., *Paclitaxel chemotherapy: from empiricism to a mechanism-based formulation strategy.* 2005. **1**(2): p. 107.

39. Untch, M., et al., *Nab-paclitaxel versus solvent-based paclitaxel in neoadjuvant chemotherapy for early breast cancer (GeparSepto—GBG 69): a randomised, phase 3 trial.* 2016. **17**(3): p. 345-356.

40. Nicolas, J., et al., *Design, functionalization strategies and biomedical applications of targeted biodegradable/biocompatible polymer-based nanocarriers for drug delivery.* 2013. **42**(3): p. 1147-1235.

41. Terwogt, J.M., et al., *Alternative formulations of paclitaxel.* 1997. **23**(2): p. 87-95.

42. Wang, B., L. Hu, and T.J. Siahaan, *Drug delivery: principles and applications*. 2016: John Wiley & Sons.

43. Perry, J., et al., *Gliadel wafers in the treatment of malignant glioma: a systematic review.* 2007. **14**(5): p. 189.

44. Ruel-Gariépy, E., et al., *A thermosensitive chitosan-based hydrogel for the local delivery of paclitaxel.* 2004. **57**(1): p. 53-63.

45. Wolinsky, J.B., Y.L. Colson, and M.W.J.J.o.c.r. Grinstaff, *Local drug delivery strategies for cancer treatment: gels, nanoparticles, polymeric films, rods, and wafers.* 2012. **159**(1): p. 14-26.

46. Blanco, E., et al., *Local release of dexamethasone from polymer millirods effectively prevents fibrosis after radiofrequency ablation.* 2006. **76**(1): p. 174-182.

47. Blanco, E., et al., *Effect of fibrous capsule formation on doxorubicin distribution in radiofrequency ablated rat livers.* 2004. **69**(3): p. 398-406.

48. Siperstein, A., et al., *Laparoscopic radiofrequency ablation of primary and metastaticliver tumors.* 2000. **14**(4): p. 400-405.

49. Steele, T.W., et al., *The effect of polyethylene glycol structure on paclitaxel drug release and mechanical properties of PLGA thin films.* 2011. **7**(5): p. 1973-1983.

50. Willard, J.J., et al., *Plant-derived human collagen scaffolds for skin tissue engineering.* 2013. **19**(13-14): p. 1507-1518.

51. Coburn, J.M., E. Na, and D.L.J.J.o.C.R. Kaplan, *Modulation of vincristine and doxorubicin binding and release from silk films.* 2015. **220**: p. 229-238.

52. Qu, J., et al., *Silk fibroin nanoparticles prepared by electrospray as controlled release carriers of cisplatin.* 2014. **44**: p. 166-174.

53. Chiu, B., et al., *Surgery combined with controlled-release doxorubicin silk films as a treatment strategy in an orthotopic neuroblastoma mouse model.* 2014. **111**(4): p. 708.

54. Dang, W., et al., *Effects of GLIADEL® wafer initial molecular weight on the erosion of wafer and release of BCNU.* 1996. **42**(1): p. 83-92.

55. Scientific, B., *TAXUS Express2 and TAXUS Express2 Atom.* 2012.

56. Luan, J., et al., *Thermogel Loaded with Low-Dose Paclitaxel as a Facile Coating to Alleviate Periprosthetic Fibrous Capsule Formation.* 2018. **10**(36): p. 30235-30246.

57. Seib, F.P., et al., *Focal therapy of neuroblastoma using silk films to deliver kinase and chemotherapeutic agents in vivo.* 2015. **20**: p. 32-38.

58. Thorn, C.F., et al., *Doxorubicin pathways: pharmacodynamics and adverse effects.* 2011. **21**(7): p. 440.

59. Seib, F.P., et al., *pH-dependent anticancer drug release from silk nanoparticles.* 2013. **2**(12): p. 1606-1611.

60. Seib, F.P., E.M. Pritchard, and D.L.J.A.f.m. Kaplan, *Self-assembling doxorubicin silk hydrogels for the focal treatment of primary breast cancer.* 2013. **23**(1): p. 58-65.

61. Avachat, A.M., R.R. Dash, and S.N.J.I.J.P.E.R. Shrotriya, *Recent investigations of plant based natural gums, mucilages and resins in novel drug delivery systems.* 2011. **45**(1): p. 86-99.

62. Adwan, G. and M.J.M.-E.J.o.S.R. Mhanna, *Synergistic effects of plant extracts and antibiotics on Staphylococcus aureus strains isolated from clinical specimens.* 2008. **3**(3): p. 134-139.

63. Verma, S.P., et al., *Curcumin and genistein, plant natural products, show synergistic inhibitory effects on the growth of human breast cancer MCF-7 cells induced by estrogenic pesticides.* 1997. **233**(3): p. 692-696.

64. Monfil, V.O. and S. Casas-Flores, *Molecular mechanisms of biocontrol in Trichoderma spp. and their applications in agriculture*, in *Biotechnology and biology of Trichoderma*. 2014, Elsevier. p. 429-453.

65. Kabera, J.N., et al., *Plant secondary metabolites: biosynthesis, classification, function and pharmacological properties.* 2014. **2**: p. 377-392.

66. Elfawal, M.A., et al., *Dried whole plant Artemisia annua as an antimalarial therapy.* 2012. **7**(12): p. e52746.

67. Sharma, M. and B. Sood, *A banana or a syringe: journey to edible vaccines.* World Journal of Microbiology and Biotechnology, 2011. **27**(3): p. 471-477.

68. Williamson, E.M.J.P., *Synergy and other interactions in phytomedicines.* 2001. **8**(5): p. 401-409.

69. Gaston, T.E., D.J.E. Friedman, and Behavior, *Pharmacology of cannabinoids in the treatment of epilepsy.* 2017. **70**: p. 313-318.

70. *Paclitaxel-Drug Summary*. [cited 2018 9/30/2018]; Available from: http://www.pdr.net/drug-summary/Paclitaxel-paclitaxel-1299.4045.

71. Venkataraman Bringi, P.G.K., Christopher L. Prince, Braden L. Roach *Enhanced production of taxol and taxanes by cell cultures of Taxus species*.

72. Mirjalili, N. and J.C.J.B.p. Linden, *Methyl jasmonate induced production of taxol in suspension cultures of Taxus cuspidata: ethylene interaction and induction models.* 1996. **12**(1): p. 110-118.

73. Ketchum, R.E., et al., *The kinetics of taxoid accumulation in cell suspension cultures of Taxus following elicitation with methyl jasmonate.* 1999. **62**(1): p. 97-105.

74. Bringi, V., et al., *Enhanced production of taxol and taxanes by cell cultures of Taxus species*. 1995, Google Patents.

75. Cusido, R.M., et al., *A rational approach to improving the biotechnological production of taxanes in plant cell cultures of Taxus spp.* 2014. **32**(6): p. 1157-1167.

76. Ramirez-Estrada, K., et al., *Changes in gene transcription and taxane production in elicited cell cultures of Taxus× media and Taxus globosa.* 2015. **117**: p. 174-184.

77. Marsh, S., et al., *Pharmacogenetic analysis of paclitaxel transport and metabolism genes in breast cancer.* 2007. **7**(5): p. 362.

78. Nour-Eldin, H.H. and B.A.J.C.o.i.b. Halkier, *The emerging field of transport engineering of plant specialized metabolites.* 2013. **24**(2): p. 263-270.

79. Addai, M., M.K.R. Bidon, and Y. Opare-Sem, *Development of a High-Througput Screening System to Assess the Effect of Plant Extracts on Mammalian Cancer Cells.* 2018.

80. Kubes, J., et al., *Vanadium elicitation of Trifolium pratense L. cell culture and possible pathways of produced isoflavones transport across the plasma membrane.* 2019: p. 1-15.

81. Kolewe, M.E., M.A. Henson, and S.C.J.P.c.r. Roberts, *Characterization of aggregate size in Taxus suspension cell culture.* 2010. **29**(5): p. 485-494.

82. Abascal, K., et al., *The effect of freeze-drying and its implications for botanical medicine: a review.* 2005. **19**(8): p. 655-660.

83. Bourgaud, F., et al., *Production of plant secondary metabolites: a historical perspective.* 2001. **161**(5): p. 839-851.

84. Van Doorn, W., et al., *Morphological classification of plant cell deaths.* 2011. **18**(8): p. 1241.

85. Flintoft, L.J.N.R.G., *Cellular defence: Human cells clear foreign DNA.* 2010. **11**(3): p. 172.

86. Wang, B., T. Siahhan, and R. Soltero, *Drug Delivery: Principles and Applications*. 2005, Hokoben, New Jersey
Canada: John Wiley & Sons, Inc.

87. Klinman, D.M.J.N.R.I., *Immunotherapeutic uses of CpG oligodeoxynucleotides.* 2004. **4**(4): p. 249.

88. Baebler, Š., et al., *Establishment of cell suspension cultures of yew (Taxus× media Rehd. and assessment of their genomic stability.* 2005. **41**(3): p. 338-343.

89. Gaurav, V., A. Shavit, and S.C. Roberts, *Nuclear DNA and protein content evaluation in Taxus plant cell cultures using multiparameter flow cytometry.* 2009.

90. *Deoxyribonuclease I from bovine pancreas [product information], Sigma-Aldrich Co. LLC, St. Louis, MO.* 2017.

91. bioWORLD. *Celluase (Trichoderma)*. 2019; Available from: https://www.bio-world.com/productinfo/2_31/140927/Cellulase.html.

92. Sigma-Aldrich, *Hemicellulase from Aspergillus niger: Product Specification Sheet*, in *https://www.sigmaaldrich.com/catalog/product/sigma/h2125?lang=en&region=US*.

93. Beg, Q., et al., *Microbial xylanases and their industrial applications: a review.* 2001. **56**(3-4): p. 326-338.

94. Chauhan, P.S., et al., *Mannanases: microbial sources, production, properties and potential biotechnological applications.* 2012. **93**(5): p. 1817-1830.

95. Biomedicals, M. *Macerozyme Application Notes*. 9032-75-1 2018; Available from: https://www.mpbio.com/0215234010-macerozyme-cf.

96. Roberts, S., et al., *A simple method for enhancing paclitaxel release from Taxus canadensis cell suspension cultures utilizing cell wall digesting enzymes.* 2003. **21**(12): p. 1217-1220.

97. Hodgson, B.B. and R.J. Kizior, *Saunders nursing drug handbook 2013*. 2012: Elsevier Health Sciences.

98. Company, B.-M.S., *TAXOL® (paclitaxel) INJECTION [package insert]*. 2011.

99. Administration, U.F.a.D., *TAXOL® (paclitaxel) Injection Label*. 2011.

100. Paál, K., J. Müller, and L.J.E.j.o.b. Hegedûs, *High affinity binding of paclitaxel to human serum albumin.* 2001. **268**(7): p. 2187-2191.

101. MacEachern-Keith, G., L. Wagner Butterfield, and M.J.A.c. Incorvia Mattina, *Paclitaxel stability in solution.* 1997. **69**(1): p. 72-77.

102. Abouelmagd, S.A., et al., *Release kinetics study of poorly water-soluble drugs from nanoparticles: are we doing it right?* 2015. **12**(3): p. 997-1003.

103. Bae, Y.H. and K.J.J.o.c.r. Park, *Targeted drug delivery to tumors: myths, reality and possibility.* 2011. **153**(3): p. 198.

104. Trédan, O., et al., *Drug resistance and the solid tumor microenvironment.* 2007. **99**(19): p. 1441-1454.

105. Kratz, F. and B.J.J.o.C.R. Elsadek, *Clinical impact of serum proteins on drug delivery.* 2012. **161**(2): p. 429-445.

106. Khosroushahi, A.Y., et al., *Improved Taxol production by combination of inducing factors in suspension cell culture of Taxus baccata.* 2006. **30**(3): p. 262-269.

107. Jiang, Z., C. Kempinski, and J.J.C.p.i.p.b. Chappell, *Extraction and analysis of terpenes/terpenoids.* 2017. **1**(2): p. 345-358.

108. Patravale, V., et al., *Nanotoxicology: evaluating toxicity potential of drug-nanoparticles*, in *Nanoparticulate Drug Delivery*. 2012, Woodhead Publishing. p. 123-155.

109. Sgouras, D. and R.J.J.o.M.S.M.i.M. Duncan, *Methods for the evaluation of biocompatibility of soluble synthetic polymers which have potential for biomedical use: 1—Use of the tetrazolium-based colorimetric assay (MTT) as a preliminary screen for evaluation ofin vitro cytotoxicity.* 1990. **1**(2): p. 61-68.

Appendix A. Raw Data
A.1 Chapter 3 Data
A.1.1 Inhibitor Experiment
A.1.1a UPLC Data (Inhibitor Experiment)

Table A1: UPLC area data for standards in inhibitor experiment. The average area of the standards was used to make the standard curve. Cycle letters represent the number of times the standard was run through the UPLC. The slope of the standard curve was found to be 32074 with an R squared of 0.9855.

	Cycle	a	b	c	d	e	f	g	Average (a-g)
PTX Standard	**0 mg/L**	0	0	0	0	0	0		**0**
	12.5 mg/L	530860	535400	344266		222506	221666		**370940**
	25 mg/L	950618	947453	857206		828078	819734	817343	**880618**
	50 mg/L	2044978	2037738	1689079	168963	1013865	1000873		**1325916**
	100 mg/L	3668206	3770754	3137480	3141435	3145018	3135128		**3333004**

Table A2: UPLC data for inhibitor experiment samples from Day 14. Each inhibitor or treatment was done in replicates of three flask. Each flask had two total culture samples taken (C1 and C2) and two media samples taken (M1 and M2). Samples showing measurable PTX were indicated and used for results. Treatments showing no measurable PTX in any samples were omitted for clarity and brevity.

Day 14 Samples				Measurable
Number	**Sample**	**Time**	**Area**	**PTX?**
Standard	*STD 0 mg/L 14*		*0*	
Standard	*STD 12.5mg/L 14*	*3.535*	*530860*	
Standard	*STD 25 mg/L 14*	*3.477*	*950618*	
Standard	*STD 50 mg/L 14*	*3.405*	*2044978*	
Standard	*STD 100 mg/L 14*	*3.37*	*3668206*	
1 - 12	All Control Samples (Day 14)			NO
Standard	*STD 12.5 mg/L*	*3.334*	*535400*	
13	MeJA 1 C1	3.327	43910	YES
14	MeJA 1 C2	3.36	0	
15	MeJA 1 M1	3.362	0	
16	MeJA 1 M2	3.318	8275	YES

17	MeJA 2 C1	3.357	0	
18	MeJA 2 C2	3.355	0	
19	MeJA 2 M1	3.172	6255	YES
20	MeJA 2 M2	3.172	4147	YES
21	MeJA 3 C1	3.353	0	
22	MeJA 3 C2	3.408	0	
23	MeJA 3 M1	3.407	0	
24	MeJA 3 M2	3.409	0	
Standard	*STD 25 mg/L*	*3.326*	*947453*	
25-36	All Verapamil Samples (Day 14)			NO
Standard	*STD 50 mg/L 14*	*3.31*	*2037738*	
37	CY 1 C1	3.337	0	
38	CY 1 C2	3.332	0	
39	CY 1 M1	3.331	0	
40	CY 1 M2	3.332	0	
41	CY2 C1	3.308	0	
42	CY2 C2	3.299	0	
43	CY2 M1	3.328	0	
44	CY2 M2	3.262	0	
45	CY3 C1	3.21	1068	YES
46	CY3 C2		0	
47	CY3 M1		0	
48	CY3 M2		0	
Standard	*STD 100 mg/L*	*3.18*	*3770754*	
Day 14 Samples		**Time**	**Area**	**Measurable PTX?**
Standard	*STD 100 mg/L*	*3.099*	*3141435*	
49	VN1 C1	3.094	7377	YES
50	VN 1 C2	3.1	0	
51	VN1 M1	3.1	0	
52	VN1 M2	3.1	0	
53	VN2 C1	3.114	0	
54	VN2 C2	3.111	0	
55	VN2 M1	~3.1	0	
56	VN2 M2	~3.111	0	
57	VN3 C1	3.107	0	
58	VN3 C2	3.102	0	
Standard	*STD 12.5 mg/L*	*3.079*	*344266*	
59	VN3 M1		0	
60	VN3 M2		0	
61-68	All Vanadate & Verapamil Samples (Day 14)			NO
Standard	*STD 25 mg/L*	*3.1*	*857206*	

69-72	All Vanadate & Verapamil Samples (Day 14)	NO

Table A3: UPLC data for inhibitor experiment samples from Day 21 following the same layout as the Day 14 table.

Day 21 Samples				Measurable
Number	**Sample**	**Time**	**Area**	**PTX?**
73	Ctrl 1 C1	3.087	1325	YES
74	CTRL 1 C2	3.075	1136	YES
75	CTRL 1 M1	3.084	1384	YES
76	CTRL 1 M2	3.088	1649	YES
77	CTRL 2 C1	3.113	26262	YES
78	CTRL 2 C2	3.108	40368	YES
Standard	*STD 50 MG/ML*	*3.082*	*1689079*	
79	CTRL 2 M1	3	12952	YES
80	CTRL 2 M2	3.082	17940	YES
81	CTRL 3 C1	3.042	962	YES
82	CTRL 3 C2	3.04	785	YES
83	CTRL 3 M1	3.04	0	
84	CTRL 3 M2	3.04	0	
85	MeJA 1 C1	3.042	447	YES
86	MeJA 1 C2	3.042	685	YES
87	MeJA 1 M1	3.039	894	YES
88	MeJA 1 M2	3.041	1222	YES
Standard	*STD 100 mg/L*	*3.053*	*3137480*	
89	MeJA 2 C1	3.037	7250	YES
90	MeJA 2 C2	3.037	2154	YES
91	MeJA 2 M1	3.04	0	
92	MeJA 2 M2	3.04	0	
93	MeJA 3 C1	3.041	4763	YES
94	MeJA 3 C2	2.974	44465	YES
95	MeJA 3 M1	3.04	0	
96	MeJA 3 M2	3.04	0	
Standard	*STD 50 mg/L*	*3.051*	*168963*	
Day 21 Samples				
Standard	*STD 0 mg/L*	*0*	*0*	
Standard	*STD 12.5 mg/L*	*3.042*	*222506*	
Standard	*STD 25 mg/L*	*3.043*	*828078*	
Standard	*STD 50 mg/L*	*3.043*	*1013865*	
Standard	*STD 100 mg/mL*	*3.041*	*3145018*	
97	VP 1 C1 (21)	3.051	38488	YES
98	VP 1 C2	3.052	767	YES

99	VP 1 M1	3.038	1957	YES
100	VP1 M2	3.037	3847	YES
101	VP2 C1	3.03	72415	YES
102	VP2 C2	3.052	4510	YES
103	VP2 M1	3.05	0	
104	VP2 M2	3.05	0	
105	VP3 C1	3.05	0	
106	VP3 C2	3.05	0	
Standard	*STD 12.5 mg/L*	*3.045*	*221666*	
107	VP3 M1	3.045	0	
108	VP3 M2	3.027	5109	YES
109	CY1 C1	3.045	0	
110	CY1 C2	3.045	0	
111	CY1 M1	3.045	0	
112	CY1 M2	3.045	0	
113	CY2 C1			
114	CY2 C2			
115	CY2 M1	3.028	5981	YES
116	CY2 M2	3.032	3714	YES
Standard	*STD 25 mg/L*	*3.038*	*819734*	
117	CY3 C1	3.038	0	
118	CY3 C2	3.038	0	
119	CY3 M1	3.038	0	
120	CY3 M2	3.038	0	
121 - 126	All Vanadate Samples (Day 21)			NO
Standard	*STD 50 mg/L*	*2.985*	*1000873*	
127 - 132	All Vanadate Samples (Day 21)			NO
133 - 137	All Vanadate + Verapamil Samples (Day 21)			NO
Standard	*STD 100 mg/L*	*2.99*	*3135128*	
137-144	All Vanadate + Verapamil Samples (Day 21)			NO
Standard	*STD 25 mg/L*	*2.987*	*817343*	

A.1.1b Coulter Counter Data (Inhibitor Experiment)

These tables show raw data collected from the Coulter Counter during the inhibitor experiments. The minimum and average bin diameters were set by the coulter counter system. In each sample, (a) represents the number of aggregates counted by the instrument that fall into the bin in the column and (b) represents the percent of aggregates of the total sample that fall into that bin size.

On each day (Day 14 and Day 21), the same Coulter Counter parameters were used. The leftmost bin column is used as a label for each bin.

Table A4: Coulter counter parameters compared to blanks on days 14 and 21.

	Coulter Counter Parameters		Blank Day 14				Blank Day 21			
Bin	Min. Bin Dia. (um)	Avg. Bin Dia. (um)	Sample 1		Sample 2		Sample 1		Sample 2	
			a	b	a	b	a	b	a	b
1	72.3	74.38925	9	15.19	13	4.73	109	0.0034	4	3.7028
2	76.4785	78.68845	1	2.06	9	3.997	49	0.0018	7	7.6696
3	80.8984	83.2361	1	2.514	7	3.794	54	0.0024	4	5.1872
4	85.5738	88.0466	3	9.203	6	3.968	39	0.002	7	10.744
5	90.5194	93.1351	3	11.23	4	3.229	14	0.0009	4	7.2668
6	95.7508	98.5179	0	0	5	4.926	22	0.0016	3	6.4507
7	101.285	104.2115	2	11.15	5	6.011	12	0.001	1	2.545
8	107.138	110.234	1	6.806	2	2.935	13	0.0013	1	3.0122
9	113.33	116.605	2	16.61	3	5.372	3	0.0004	0	0
10	119.88	123.344	1	10.14	0	0	10	0.0014	2	8.4396
11	126.808	130.4725	0	0	2	5.334	4	0.0007	1	4.9946
12	134.137	138.013	1	15.1	0	0	11	0.0022	2	11.823
13	141.889	145.989	0	0	1	3.973	4	0.001	0	0
14	150.089	154.426	0	0	0	0	8	0.0023	2	16.563
15	158.763	163.351	0	0	2	11.83	1	0.0003	0	0
16	167.939	172.792	0	0	1	7.222	0	0	1	11.601
17	177.645	182.778	0	0	1	8.813	2	0.0009	0	0
18	187.911	193.341	0	0	0	0	1	0.0006	0	0
19	198.771	204.515	0	0	0	0	2	0.0013	0	0
20	210.259	216.335	0	0	0	0	0	0	0	0
21	222.411	228.8375	0	0	0	0	2	0.0018	0	0
22	235.264	242.0625	0	0	1	23.86	0	0	0	0
23	248.861	256.0525	0	0	0	0	3	0.0039	0	0
24	263.244	270.8505	0	0	0	0	1	0.0015	0	0
25	278.457	286.504	0	0	0	0	0	0	0	0
26	294.551	303.0625	0	0	0	0	4	0.0085	0	0
27	311.574	320.5775	0	0	0	0	5	0.0126	0	0
28	329.581	339.1045	0	0	0	0	3	0.009	0	0
29	348.628	358.702	0	0	0	0	3	0.0106	0	0

30	**368.776**	**379.4325**	0	0	0	0	3	0.0126	0	0
31	**390.089**	**401.3615**	0	0	0	0	14	0.0695	0	0
32	**412.634**	**424.5575**	0	0	0	0	15	0.0881	0	0
33	**436.481**	**449.094**	0	0	0	0	23	0.1599	0	0
34	**461.707**	**475.049**	0	0	0	0	14	0.1152	0	0
35	**488.391**	**502.504**	0	0	0	0	15	0.1461	0	0
36	**516.617**	**531.5455**	0	0	0	0	10	0.1153	0	0
37	**546.474**	**562.265**	0	0	0	0	11	0.1501	0	0
38	**578.056**	**594.76**	0	0	0	0	16	0.2584	0	0
39	**611.464**	**629.1335**	0	0	0	0	27	0.5161	0	0
40	**646.803**	**665.4935**	0	0	0	0	33	0.7466	0	0
41	**684.184**	**703.9545**	0	0	0	0	31	0.8301	0	0
42	**723.725**	**744.638**	0	0	0	0	17	0.5388	0	0
43	**765.551**	**787.673**	0	0	0	0	37	1.388	0	0
44	**809.795**	**833.1955**	0	0	0	0	70	3.108	0	0
45	**856.596**	**881.349**	0	0	0	0	83	4.3617	0	0
46	**906.102**	**932.285**	0	0	0	0	195	12.129	0	0
47	**958.468**	**986.164**	0	0	0	0	468	34.453	0	0
48	**1013.86**	**1043.16**	0	0	0	0	252	21.958	0	0
49	**1072.46**	**1103.45**	0	0	0	0	104	10.726	0	0
50	**1134.44**	**1167.22**	0	0	0	0	66	8.0563	0	0

Table A5: Day 14 Coulter counter data: control and cyclosporine treatments. Flask three of the cyclosporine treatment encountered a processing error and data was not collected.

Bin	**Control Day 14**						**Cyclosporine Day 14**			
	Sample 1		**Sample 2**		**Sample 3**		**Sample 1**		**Sample 2**	
	a	**b**	**a**	**b**	**a**	**b**	**a**	**b**	**a**	**b**
	370	0.268	160	0.121	975	0.626	63	0.049	62	0.07
1	318	0.281	142	0.131	664	0.52	29	0.028	34	0.047
2	307	0.331	133	0.15	520	0.497	45	0.053	37	0.062
3	301	0.396	132	0.182	453	0.529	51	0.073	31	0.064
4	310	0.498	107	0.18	438	0.624	49	0.085	33	0.083
5	260	0.509	123	0.252	444	0.772	38	0.081	33	0.101
6	274	0.655	142	0.355	454	0.963	47	0.122	34	0.127
7	237	0.692	146	0.445	373	0.966	58	0.183	45	0.205
8	242	0.862	147	0.547	155	0.49	51	0.197	42	0.234
9	234	1.017	137	0.623	117	0.451	46	0.217	33	0.224
10	207	1.098	133	0.738	125	0.588	41	0.236	48	0.398
11	205	1.327	113	0.765	125	0.718	51	0.358	33	0.334

12	180	1.422	139	1.148	96	0.673	62	0.531	39	0.481
13	177	1.707	124	1.25	102	0.872	40	0.418	30	0.452
14	162	1.907	112	1.378	95	0.992	46	0.586	35	0.643
15	139	1.997	96	1.442	79	1.006	42	0.653	28	0.628
16	99	1.736	119	2.181	79	1.228	40	0.759	26	0.712
17	93	1.99	88	1.968	90	1.708	42	0.973	24	0.802
18	103	2.689	101	2.757	66	1.528	45	1.272	25	1.02
19	86	2.741	77	2.565	72	2.035	42	1.449	36	1.792
20	67	2.606	78	3.171	47	1.621	23	0.969	28	1.701
21	50	2.373	50	2.481	47	1.979	35	1.799	16	1.186
22	47	2.723	38	2.301	45	2.312	41	2.572	23	2.081
23	48	3.393	39	2.882	39	2.445	26	1.99	17	1.877
24	34	2.933	36	3.247	40	3.061	20	1.869	14	1.887
25	49	5.16	38	4.183	35	3.269	15	1.71	14	2.303
26	34	4.369	29	3.896	25	2.849	16	2.226	16	3.212
27	30	4.705	18	2.951	24	3.339	20	3.397	26	6.37
28	33	6.316	29	5.803	28	4.753	17	3.523	7	2.093
29	21	4.906	21	5.129	19	3.937	25	6.324	11	4.014
30	19	5.417	23	6.855	18	4.551	20	6.174	8	3.563
31	13	4.523	17	6.184	16	4.938	12	4.521	11	5.978
32	14	5.945	11	4.883	21	7.909	8	3.678	5	3.317
33	5	2.591	6	3.251	14	6.435	13	7.295	4	3.238
34	5	3.162	5	3.306	14	7.853	9	6.164	6	5.928
35	6	4.631	8	6.456	9	6.162	6	5.015	10	12.06
36	5	4.71	4	3.939	4	3.342	6	6.12	5	7.358
37	2	2.299	1	1.202	4	4.079	2	2.49	3	5.388
38	1	1.403	2	2.934	2	2.489	0	0	4	8.767
39	1	1.712	2	3.581	2	3.038	5	9.271	1	2.675
40	0	0	1	2.185	1	1.854	3	6.789	2	6.529
41	0	0	0	0	0	0	1	2.762	0	0
42	0	0	0	0	0	0	0	0	0	0
43	0	0	0	0	0	0	0	0	0	0
44	0	0	0	0	0	0	1	5.02	0	0
45	0	0	0	0	0	0	0	0	0	0
46	0	0	0	0	0	0	0	0	0	0
47	0	0	0	0	0	0	0	0	0	0
48	0	0	0	0	0	0	0	0	0	0
49	0	0	0	0	0	0	0	0	0	0
50										

Table A6: Day 14 Coulter counter data: elicited and vanadate treatments.

Bin	Elicited Day 14						Vanadate Day 14					
	Sample 1		Sample 2		Sample 3		Sample 1		Sample 2		Sample 3	
	a	b	a	b	a	b	a	b	a	b	a	b
1	37	0.021	144	0.101	27	0.137	68	0.039	51	0.037	62	0.121
2	36	0.025	102	0.088	24	0.149	67	0.047	35	0.031	36	0.085
3	38	0.032	92	0.097	29	0.22	65	0.056	31	0.033	20	0.058
4	37	0.038	118	0.151	27	0.25	68	0.072	37	0.048	22	0.078
5	47	0.059	49	0.077	23	0.26	51	0.065	47	0.075	29	0.125
6	55	0.084	33	0.063	21	0.289	59	0.092	46	0.089	32	0.169
7	41	0.077	40	0.093	25	0.421	68	0.13	43	0.102	33	0.212
8	43	0.098	28	0.08	20	0.411	58	0.135	55	0.159	30	0.235
9	42	0.117	50	0.173	26	0.651	61	0.174	56	0.198	23	0.22
10	44	0.15	35	0.148	35	1.07	47	0.163	38	0.164	30	0.351
11	42	0.175	54	0.279	20	0.746	64	0.272	46	0.242	40	0.57
12	49	0.249	49	0.309	18	0.82	55	0.285	41	0.263	32	0.557
13	46	0.285	43	0.331	23	1.278	73	0.461	47	0.368	33	0.701
14	52	0.393	57	0.535	25	1.696	54	0.417	53	0.506	32	0.83
15	36	0.332	54	0.619	19	1.573	67	0.631	41	0.478	34	1.076
16	47	0.529	48	0.671	23	2.324	68	0.781	54	0.768	29	1.12
17	39	0.536	46	0.785	10	1.233	66	0.925	53	0.921	27	1.272
18	63	1.056	58	1.208	20	3.01	55	0.941	49	1.039	26	1.495
19	45	0.921	53	1.348	16	2.939	45	0.94	37	0.957	26	1.825
20	45	1.124	43	1.334	5	1.121	62	1.58	45	1.421	24	2.056
21	41	1.25	34	1.288	10	2.736	62	1.929	41	1.58	10	1.045
22	28	1.042	29	1.34	6	2.003	51	1.936	36	1.693	12	1.531
23	29	1.317	30	1.692	8	3.26	38	1.761	31	1.779	14	2.18
24	26	1.441	26	1.79	4	1.989	39	2.205	28	1.961	12	2.28
25	17	1.15	32	2.689	9	5.462	41	2.829	24	2.051	11	2.551
26	23	1.898	30	3.076	8	5.925	27	2.274	24	2.504	12	3.397
27	22	2.216	16	2.002	2	1.808	32	3.289	23	2.928	8	2.764
28	18	2.213	24	3.666	3	3.31	31	3.889	19	2.952	10	4.216
29	15	2.25	18	3.355	5	6.732	19	2.909	16	3.034	4	2.058
30	17	3.112	21	4.777	3	4.929	26	4.858	18	4.166	5	3.14
31	14	3.128	16	4.442	1	2.005	22	5.016	12	3.389	5	3.832
32	19	5.181	19	6.438	1	2.447	9	2.505	15	5.171	4	3.741
33	11	3.661	12	4.962	2	5.974	19	6.453	11	4.628	6	6.849
34	10	4.062	11	5.552	0	0	19	7.875	9	4.621	2	2.786
35	12	5.948	13	8.007	2	8.898	16	8.094	4	2.506	6	10.2
36	7	4.235	4	3.007	1	5.429	10	6.174	9	6.883	2	4.15

37	14	10.34	6	5.505	1	6.626	5	3.767	7	6.533	1	2.532
38	13	11.71	7	7.838	0	0	7	6.437	3	3.417	4	12.36
39	9	9.897	6	8.199	1	9.869	6	6.733	6	8.341	1	3.772
40	8	10.74	2	3.335	0	0	4	5.478	3	5.09	1	4.603
41	3	4.914	0	0	0	0	2	3.343	3	6.212	0	0
42	1	1.999	1	2.484	0	0	1	2.04	3	7.581	1	6.856
43	0	0	2	6.063	0	0	0	0	1	3.084	0	0
44	0	0	0	0	0	0	0	0	0	0	0	0
45	0	0	0	0	0	0	0	0	0	0	0	0
46	0	0	0	0	0	0	0	0	0	0	0	0
47	0	0	0	0	0	0	0	0	0	0	0	0
48	0	0	0	0	0	0	0	0	0	0	0	0
49	0	0	0	0	0	0	0	0	0	0	0	0
50	0	0	0	0	0	0	0	0	0	0	0	0

Table A7: Day 14 Coulter counter data: verapamil and combined (vanadate & verapamil) treatments.

Bin	**Verapamil Day 14**						**Vanadate and Verapamil Day 14**					
	Sample 1		**Sample 2**		**Sample 3**		**Sample 1**		**Sample 2**		**Sample 3**	
	a	**b**	**a**	**b**	**a**	**b**	**a**	**b**	**a**	**b**	**a**	**b**
1	57	0.118	231	0.246	50	0.056	102	0.035	44	0.034	162	0.201
2	40	0.101	120	0.156	51	0.07	90	0.037	39	0.037	101	0.153
3	42	0.129	63	0.1	40	0.067	59	0.03	27	0.031	87	0.161
4	37	0.139	65	0.126	35	0.072	61	0.038	36	0.051	88	0.199
5	27	0.124	61	0.144	49	0.122	77	0.058	46	0.079	72	0.198
6	39	0.218	65	0.188	38	0.116	77	0.071	33	0.069	91	0.306
7	31	0.211	65	0.229	36	0.134	61	0.068	30	0.077	79	0.324
8	34	0.283	51	0.219	40	0.181	65	0.089	39	0.122	87	0.436
9	26	0.264	74	0.388	35	0.194	69	0.115	36	0.137	72	0.44
10	38	0.471	57	0.365	42	0.284	79	0.161	37	0.172	64	0.478
11	32	0.484	56	0.438	43	0.355	81	0.202	40	0.227	81	0.738
12	22	0.406	44	0.42	45	0.453	79	0.24	39	0.27	66	0.734
13	35	0.788	62	0.722	43	0.528	82	0.304	46	0.388	66	0.895
14	44	1.21	65	0.924	37	0.555	65	0.294	39	0.401	66	1.093
15	28	0.94	66	1.145	26	0.476	87	0.481	40	0.503	45	0.909
16	34	1.392	69	1.46	30	0.67	72	0.486	50	0.767	42	1.036
17	37	1.849	54	1.395	24	0.654	82	0.675	46	0.861	63	1.896
18	33	2.013	57	1.797	26	0.864	67	0.673	47	1.073	47	1.726
19	26	1.935	41	1.577	31	1.258	74	0.907	39	1.087	40	1.793
20	29	2.635	35	1.643	32	1.585	102	1.526	46	1.565	39	2.133
21	26	2.883	34	1.948	18	1.088	64	1.169	25	1.038	36	2.403

22	18	2.436	36	2.518	15	1.106	52	1.159	22	1.115	28	2.281
23	20	3.303	23	1.963	17	1.53	67	1.822	26	1.608	29	2.884
24	23	4.636	12	1.25	8	0.879	54	1.792	12	0.906	22	2.67
25	12	2.952	11	1.398	5	0.67	60	2.43	24	2.21	19	2.814
26	5	1.501	16	2.483	11	1.8	46	2.274	31	3.484	11	1.988
27	10	3.664	14	2.651	10	1.997	37	2.232	20	2.743	15	3.309
28	12	5.365	16	3.698	11	2.681	31	2.283	26	4.353	10	2.692
29	7	3.82	12	3.385	9	2.677	37	3.325	18	3.678	6	1.971
30	10	6.66	12	4.131	8	2.904	29	3.181	22	5.486	8	3.208
31	7	5.689	12	5.041	9	3.987	27	3.614	12	3.652	14	6.852
32	8	7.935	8	4.102	1	0.541	26	4.247	15	5.571	11	6.57
33	4	4.842	12	7.508	4	2.64	24	4.785	8	3.626	7	5.103
34	4	5.91	4	3.055	2	1.611	33	8.029	8	4.425	4	3.559
35	3	5.409	9	8.388	4	3.931	18	5.345	8	5.401	4	4.343
36	3	6.602	7	7.962	6	7.197	14	5.074	4	3.296	6	7.95
37	1	2.686	5	6.941	4	5.856	9	3.981	1	1.006	2	3.234
38	0	0	2	3.388	2	3.573	15	8.097	7	8.59	2	3.947
39	2	8	1	2.068	5	10.9	7	4.611	8	11.98	2	4.817
40	0	0	1	2.523	3	7.983	4	3.216	1	1.828	0	0
41	0	0	2	6.159	4	12.99	4	3.925	2	4.462	2	7.175
42	0	0	1	3.758	2	7.927	6	7.185	0	0	1	4.378
43	0	0	0	0	1	4.837	3	4.384	2	6.645	0	0
44	0	0	0	0	0	0	3	5.351	0	0	0	0
45	0	0	0	0	0	0	0	0	1	4.949	0	0
46	0	0	0	0	0	0	0	0	0	0	0	0
47	0	0	0	0	0	0	0	0	0	0	0	0
48	0	0	0	0	0	0	0	0	0	0	0	0
49	0	0	0	0	0	0	0	0	0	0	0	0
50	0	0	0	0	0	0	0	0	0	0	0	0

Table A8: Day 21 Coulter counter data: control and cyclosporine treatments.

	Control Day 21						**Cyclosporine Day 21**					
	Sample 1		**Sample 2**		**Sample 3**		**Sample 1**		**Sample 2**		**Sample 3**	
Bin	**a**	**b**	**a**	**b**	**a**	**b**	**a**	**b**	**a**	**b**	**a**	**b**
1	850	0.7484	321	0.213	1527	1.2866	154	0.0891	61	0.1012	62	0.2386
2	776	0.8087	301	0.2364	1044	1.0411	134	0.0918	61	0.1198	56	0.2551
3	734	0.9054	273	0.2537	760	0.8971	144	0.1168	62	0.1441	69	0.372
4	727	1.0614	300	0.33	575	0.8033	123	0.118	68	0.187	53	0.3382
5	637	1.1007	275	0.358	564	0.9326	101	0.1147	55	0.1791	43	0.3248
6	574	1.1739	296	0.4561	521	1.0197	118	0.1586	49	0.1888	42	0.3755
7	546	1.3217	274	0.4998	466	1.0795	129	0.2053	46	0.2098	38	0.4021

8	485	1.3896	283	0.6109	367	1.0062	104	0.1959	31	0.1673	49	0.6136
9	446	1.5124	233	0.5954	290	0.9411	105	0.2341	39	0.2492	44	0.6522
10	388	1.5573	223	0.6744	270	1.037	111	0.2929	43	0.3252	47	0.8245
11	332	1.5772	218	0.7803	193	0.8774	87	0.2717	52	0.4654	27	0.5606
12	320	1.7993	185	0.7838	229	1.2322	90	0.3326	35	0.3708	35	0.8602
13	321	2.1363	208	1.043	219	1.3947	100	0.4375	29	0.3636	37	1.0763
14	242	1.9062	163	0.9674	185	1.3945	76	0.3935	40	0.5936	36	1.2395
15	233	2.1723	147	1.0327	167	1.4899	57	0.3493	31	0.5445	26	1.0595
16	196	2.1628	147	1.2222	160	1.6895	73	0.5295	29	0.6029	29	1.3987
17	187	2.4423	127	1.2498	128	1.5998	80	0.6868	24	0.5906	27	1.5413
18	149	2.3033	102	1.1881	130	1.923	66	0.6707	29	0.8446	25	1.6892
19	148	2.7079	88	1.2132	108	1.8909	69	0.8299	26	0.8963	23	1.8394
20	124	2.6853	87	1.4196	95	1.9687	55	0.7829	22	0.8976	17	1.6091
21	89	2.2812	73	1.4099	91	2.232	53	0.893	26	1.2556	25	2.8008
22	89	2.7	71	1.623	75	2.1773	43	0.8575	15	0.8574	14	1.8564
23	74	2.6571	44	1.1904	63	2.1647	50	1.1802	17	1.1501	12	1.8834
24	74	3.1449	39	1.2489	78	3.1722	42	1.1733	18	1.4413	15	2.7864
25	53	2.666	33	1.2508	57	2.7437	45	1.488	11	1.0425	12	2.6384
26	33	1.9647	39	1.7496	42	2.3929	31	1.2132	14	1.5704	14	3.6432
27	44	3.1005	30	1.5929	40	2.6973	31	1.436	7	0.9294	9	2.7721
28	43	3.5864	24	1.5083	40	3.1925	27	1.4803	9	1.4143	7	2.5519
29	42	4.1461	25	1.8596	33	3.1174	27	1.7521	6	1.1159	2	0.863
30	29	3.3884	26	2.289	29	3.2425	20	1.5361	10	2.2014	4	2.0428
31	43	5.9465	18	1.8756	21	2.7791	24	2.1817	11	2.8661	8	4.8357
32	21	3.4373	23	2.8367	28	4.3857	31	3.3355	8	2.4671	4	2.8618
33	26	5.037	11	1.6057	18	3.337	15	1.9102	2	0.73	5	4.2339
34	15	3.4395	17	2.9372	19	4.1691	26	3.919	10	4.3202	2	2.0045
35	11	2.9854	14	2.863	16	4.1554	26	4.6385	5	2.5567	2	2.3725
36	17	5.4608	20	4.8408	21	6.4552	22	4.6454	5	3.0261	3	4.2122
37	12	4.5624	10	2.8648	10	3.6383	6	1.4995	4	2.8653	4	6.6473
38	8	3.6	7	2.3735	9	3.8756	23	6.8036	2	1.6957	0	0
39	1	0.5326	11	4.4146	10	5.0968	12	4.2014	3	3.0105	2	4.6561
40	3	1.8912	9	4.2751	5	3.0163	13	5.3871	1	1.1877	2	5.5109
41	0	0	2	1.1244	2	1.428	10	4.9048	3	4.2174	0	0
42	0	0	4	2.6617	0	0	9	5.2247	2	3.3278	3	11.58
43	0	0	1	0.7876	1	1.0003	8	5.4968	2	3.9387	1	4.5688
44	0	0	6	5.5932	2	2.3678	6	4.8795	3	6.9928	1	5.4076
45	0	0	2	2.2067	0	0	7	6.7379	3	8.2766	0	0
46	0	0	5	6.5296	1	1.6585	4	4.5571	2	6.5307	0	0
47	0	0	4	6.1827	0	0	3	4.0453	0	0	0	0
48	0	0	3	5.4884	0	0	1	1.596	2	9.1489	0	0
49	0	0	0	0	0	0	1	1.889	1	5.4143	0	0
50	0	0	3	7.6886	0	0	1	2.2358	1	6.4083	0	0

Table A9: Day 21 Coulter counter data: elicited and vanadate treatments.

Bin	Elicited Day 21						Vanadate Day 21					
	Sample 1		Sample 2		Sample 3		Sample 1		Sample 2		Sample 3	
	a	b	a	b	a	b	a	b	a	b	a	b
1	210	0.3197	129	0.2426	36	0.1424	125	0.0592	158	0.0645	36	0.1207
2	191	0.3441	93	0.207	30	0.1404	131	0.0735	125	0.0604	41	0.1627
3	173	0.3689	111	0.2924	20	0.1108	106	0.0704	125	0.0715	34	0.1597
4	166	0.419	91	0.2838	21	0.1377	100	0.0786	104	0.0704	35	0.1945
5	147	0.4392	81	0.2989	22	0.1707	77	0.0716	108	0.0865	32	0.2105
6	133	0.4703	73	0.3189	27	0.248	73	0.0804	108	0.1024	42	0.327
7	129	0.5399	80	0.4136	31	0.3371	88	0.1147	106	0.119	39	0.3594
8	108	0.535	90	0.5508	26	0.3346	72	0.111	105	0.1395	34	0.3709
9	93	0.5453	71	0.5142	31	0.4722	64	0.1168	92	0.1447	33	0.4261
10	105	0.7286	50	0.4286	25	0.4507	67	0.1447	80	0.1489	44	0.6724
11	81	0.6653	63	0.6392	22	0.4694	41	0.1048	106	0.2335	35	0.6331
12	75	0.7291	61	0.7326	31	0.7829	65	0.1967	87	0.2269	33	0.7065
13	65	0.7479	67	0.9524	25	0.7473	65	0.2328	94	0.2901	32	0.8108
14	71	0.9669	56	0.9421	37	1.3091	64	0.2713	82	0.2995	31	0.9297
15	61	0.9833	52	1.0355	29	1.2144	54	0.271	96	0.4151	48	1.7038
16	56	1.0684	43	1.0135	27	1.3382	52	0.3088	87	0.4452	36	1.5125
17	54	1.2194	47	1.3111	33	1.9359	59	0.4147	87	0.5269	19	0.9448
18	53	1.4165	39	1.2877	27	1.8747	49	0.4077	83	0.595	34	2.0011
19	27	0.8541	26	1.0161	27	2.2189	51	0.5022	72	0.6109	28	1.9505
20	48	1.7972	32	1.4801	22	2.1399	53	0.6177	60	0.6026	29	2.3911
21	34	1.5067	38	2.0803	26	2.9933	55	0.7587	60	0.7132	26	2.5373
22	25	1.3113	26	1.6847	17	2.3165	60	0.9797	68	0.9567	24	2.7721
23	21	1.3037	26	1.994	21	3.3869	50	0.9663	63	1.0491	19	2.5975
24	27	1.9839	25	2.2693	13	2.4816	45	1.0293	75	1.4782	12	1.9417
25	25	2.1742	21	2.2562	11	2.4853	39	1.0559	41	0.9564	12	2.2982
26	14	1.4411	11	1.3988	10	2.6742	27	0.8652	36	0.9939	9	2.0401
27	16	1.9494	23	3.4617	6	1.8991	31	1.1757	42	1.3725	7	1.8781
28	16	2.3072	11	1.9596	9	3.3716	25	1.1223	41	1.5858	8	2.5404
29	11	1.8775	15	3.1627	4	1.7736	35	1.8596	34	1.5565	5	1.8793
30	12	2.4242	13	3.2442	6	3.1488	35	2.201	36	1.9506	5	2.2243
31	10	2.391	13	3.8399	2	1.2423	33	2.4562	43	2.7577	7	3.6857
32	14	3.962	4	1.3984	4	2.9408	12	1.0572	29	2.2013	2	1.2464
33	8	2.6796	8	3.3103	2	1.7403	26	2.711	25	2.2461	4	2.9505
34	10	3.9645	7	3.4283	7	7.2095	15	1.8512	20	2.1267	6	5.2382
35	7	3.2847	10	5.7967	7	8.5331	18	2.6293	21	2.643	4	4.1333

36	6	3.3323	5	3.4305	6	8.6569	17	2.9391	22	3.2773	2	2.4461
37	8	5.2588	3	2.4362	0	0	19	3.888	18	3.1737	0	0
38	2	1.5561	5	4.8057	3	6.0637	17	4.1174	13	2.7129	2	3.4267
39	4	3.6835	3	3.4128	0	0	19	5.4467	13	3.211	4	8.1116
40	3	3.2698	8	10.772	3	8.4946	17	5.7681	8	2.3388	2	4.8004
41	4	5.1602	4	6.3747	1	3.3514	7	2.8111	7	2.4221	2	5.6817
42	9	13.742	2	3.7725	1	3.9667	5	2.3766	12	4.9146	1	3.3624
43	2	3.6144	2	4.4651	1	4.6949	13	7.3136	12	5.8168	0	0
44	1	2.139	2	5.2849	0	0	4	2.6635	7	4.0161	0	0
45	1	2.5317	0	0	0	0	5	3.9406	11	7.4697	0	0
46	2	5.9931	0	0	0	0	3	2.7985	3	2.4112	0	0
47	0	0	0	0	0	0	10	11.041	7	6.6591	2	15.621
48	0	0	0	0	0	0	5	6.5339	8	9.0076	0	0
49	0	0	0	0	0	0	5	7.7335	6	7.996	0	0
50	0	0	0	0	0	0	2	3.6613	3	4.732	0	0

Table A10: Day 21 Coulter counter data: verapamil and combined (vanadate and verapamil) treatments.

Bin	Verapamil Day 21						Vanadate and Verapamil Day 21					
	Sample 1		Sample 2		Sample 3		Sample 1		Sample 2		Sample 3	
	a	**b**	**a**	**b**	**a**	**b**	**a**	**b**	**a**	**b**	**a**	**b**
1	209	0.1006	110	0.1001	162	0.1219	52	0.0564	156	0.0653	49	0.06
2	178	0.1014	112	0.1207	130	0.1158	44	0.0565	146	0.0723	50	0.072
3	159	0.1072	121	0.1543	117	0.1234	32	0.0487	129	0.0756	44	0.075
4	161	0.1285	93	0.1404	91	0.1136	35	0.063	110	0.0763	55	0.111
5	119	0.1124	96	0.1715	100	0.1477	35	0.0746	123	0.101	51	0.122
6	121	0.1353	111	0.2347	89	0.1556	47	0.1185	132	0.1283	49	0.139
7	142	0.1879	102	0.2552	86	0.178	40	0.1194	113	0.13	56	0.188
8	112	0.1754	113	0.3347	95	0.2327	36	0.1272	128	0.1743	56	0.223
9	103	0.1909	93	0.326	93	0.2696	32	0.1338	127	0.2047	58	0.273
10	114	0.2501	104	0.4315	72	0.247	32	0.1583	99	0.1888	54	0.301
11	117	0.3038	96	0.4715	55	0.2233	34	0.1991	108	0.2438	37	0.244
12	94	0.2889	84	0.4883	70	0.3364	51	0.3535	111	0.2966	52	0.406
13	100	0.3638	82	0.5641	52	0.2958	30	0.2461	107	0.3384	48	0.443
14	80	0.3444	80	0.6514	64	0.4309	39	0.3787	74	0.277	74	0.809
15	96	0.4892	83	0.7999	62	0.4941	30	0.3448	81	0.3589	58	0.75
16	79	0.4765	84	0.9582	71	0.6697	26	0.3537	77	0.4038	62	0.949
17	93	0.6639	64	0.8641	48	0.5359	31	0.4991	73	0.4531	54	0.978
18	81	0.6844	71	1.1346	40	0.5286	41	0.7813	82	0.6024	49	1.051
19	86	0.86	74	1.3997	53	0.8289	33	0.7443	64	0.5565	39	0.99

20	72	0.8522	61	1.3656	52	0.9626	29	0.7742	79	0.8131	38	1.141
21	74	1.0367	63	1.6693	44	0.964	36	1.1375	78	0.9502	28	0.995
22	58	0.9617	56	1.7562	37	0.9595	27	1.0098	66	0.9516	36	1.515
23	68	1.3346	60	2.2272	44	1.3505	22	0.9739	56	0.9556	44	2.191
24	65	1.5099	49	2.1528	20	0.7266	26	1.3622	66	1.3331	33	1.945
25	57	1.5671	32	1.664	24	1.032	22	1.3643	49	1.1714	22	1.535
26	42	1.3667	36	2.2157	23	1.1705	21	1.5413	45	1.2733	24	1.982
27	35	1.3481	32	2.3311	20	1.2047	20	1.7374	52	1.7415	17	1.662
28	35	1.5956	30	2.5866	13	0.9268	11	1.131	54	2.1405	19	2.198
29	38	2.0504	25	2.5513	26	2.194	19	2.3123	33	1.5482	20	2.739
30	39	2.4906	20	2.4157	10	0.9988	19	2.7368	38	2.1101	12	1.945
31	33	2.4944	21	3.0022	19	2.2461	8	1.3639	27	1.7746	11	2.11
32	29	2.5945	10	1.6921	11	1.5391	8	1.6143	36	2.8005	12	2.725
33	41	4.3415	14	2.8038	16	2.6497	8	1.9107	29	2.6701	7	1.881
34	30	3.7599	8	1.8963	11	2.1561	8	2.2615	29	3.1603	12	3.817
35	28	4.1535	12	3.3667	9	2.088	9	3.0112	20	2.5797	4	1.506
36	16	2.8092	9	2.9886	11	3.0205	8	3.1681	23	3.5113	8	3.565
37	23	4.7796	9	3.5373	9	2.925	11	5.1558	17	3.0718	7	3.692
38	22	5.4112	10	4.652	8	3.0774	6	3.3286	16	3.4219	6	3.745
39	23	6.6957	6	3.3036	6	2.7318	4	2.6265	11	2.7845	4	2.955
40	19	6.5468	11	7.1686	8	4.3111	4	3.1087	12	3.5953	5	4.372
41	14	5.7096	5	3.8567	5	3.1891	1	0.9198	12	4.2554	1	1.035
42	16	7.7232	2	1.8259	4	3.0197	2	2.1775	13	5.4563	2	2.45
43	7	3.9993	3	3.2417	4	3.5741	4	5.1544	5	2.4839	0	0
44	5	3.3811	4	5.1158	8	8.4605	7	10.676	9	5.2918	1	1.716
45	5	4.0018	1	1.5138	5	6.2586	3	5.4156	9	6.2634	2	4.062
46	2	1.8946	3	5.375	1	1.4815	3	6.4099	5	4.1185	4	9.616
47	4	4.4849	1	2.1206	2	3.5071	3	7.5867	4	3.8997	4	11.38
48	0	0	0	0	3	6.2264	3	8.9796	3	3.4617	1	3.368
49	2	3.1414	1	2.9707	3	7.3695	0	0	2	2.7315	2	7.972
50	0	0	2	7.0323	4	11.63	1	4.1931	8	12.932	0	0

A.1.2 Paclitaxel Loading and *Taxus* Processing Experiments

A.1.2a Mass Data (Loading and Processing Experiments)

Table A11: Pre-Processing Mass Retention experiment. This table shows the masses of each sample at every point along the pre-processing steps. The same samples were analyzed for PTX concentration (Table B12).

Sample Identifier	Sample Weight g	Lyophilized Weight g	Washed Weight g	Evaporated Weight g
PTX 0 S1	0.9697			0.02
PTX 0 S2	1.0286			0.03
PTX 0 S3	1.0295			0.0313
PTX 0 L1	1.0219	0.0294		0.0281
PTX 0 L2	1.0075	0.0284		0.027
PTX 0 L3	1.0061	0.029		0.0277
PTX 0 L+W1	1.0252	0.0347	0.0032	0.007
PTX 0 L+W2	0.9443	0.0305	0.0395	0.0037
PTX 0 L+W3	1.0293	0.0327	0.018	0.0056
PTX 2 S1	1.0072			0.0314
PTX 2 S2	1.0392			0.0297
PTX 2 S3	0.9994			0.0316
PTX 2 L1	1.0098	0.0293		0.0272
PTX 2 L2	0.9269	0.0325		0.0302
PTX 2 L3	0.9164	0.0271		0.0252
PTX 2 L+W1	1.0296	0.0288	0.0647	0.0015
PTX 2 L+W2	1.0308	0.032	0.1183	0.0039
PTX 2 L+W3	0.9862	0.03	0.0823	0.003
CM S1	0.9897			0.0115
CM S2	0.9928			0.0192
CM S3	1.0385			0.0179
CM L1	1.0176	0.0142		0.0138
CM L2	0.9335	0.0168		0.0164
CM L3	1.0124	0.0189		0.0185
CM L+W1	1.0038	0.0124	0.183	0.0034
CM L+W2	1.0235	0.0153	0.1855	0.0045
CM L+W3	1.0171	0.0149	0.1164	0.004
EC S1	0.1621			0.0112

EC S2	0.2182			0.0119
EC S3	0.0821			0.0054
EC L1	0.1501	0.0085		0.0082
EC L2	0.1896	0.0092		0.0088
EC L3	0.1708	0.0066		0.0065
EC L+W1	0.0864	0.005	0.0672	0.0015
EC L+W2	0.1192	0.0072	0.1016	0.0022
EC L+W3	0.1415	0.0098	0.1358	0.0041
M S1	1.0061			0.0074
M S2	0.9888			0.0069
M S3	0.9745			0.0074
M L1	0.9366	0.0065		0.0062
M L2	0.9684	0.0072		0.0067
M L3	0.9962	0.007		0.0067
M L+W1	1.0718	0.0074	0.1947	0.0007
M L+W2	0.5955	0.0045	0.1008	0.0004
M L+W3	0.9388	0.0068	0.1715	0.0006

A.1.2b UPLC Data (Loading and Processing Experiments)

Table A12: Processing Paclitaxel Retention

Sample	Retention Time (minutes)	Area	Concentration PTX (mg/L)
PTX 0 S1	3.107	2010170	9.237234395
PTX 0 S2	3.101	2004648	9.211859422
PTX 0 S3	3.101	1376340	6.324626866
PTX 0 L1	3.101	2055659	9.446267738
PTX 0 L2	3.1	1991310	9.150567973
PTX 0 L3	3.098	2064658	9.487620396
PTX 0 L+W1	3.092	687656	3.159951474
PTX 0 L+W2	3.091	360123	1.654855342
PTX 0 L+W3	3.089	515859	2.37050125
PTX 2 S1	3.094	1793370	8.240984119
PTX 2 S2	3.096	1890110	8.685528638
PTX 2 S3	3.098	1942491	8.926232446
PTX 2 L1	3.097	1976662	9.083256746
PTX 2 L2	3.039	1921110	8.827981398
PTX 2 L3	3.094	1852639	8.513340012
PTX 2 L+W1	3.086	336858	1.547946842
PTX 2 L+W2	3.084	572074	2.628823248
PTX 2 L+W3	3.084	226758	1.042009779
CM S1	3.089	30166	0.138620322

CM S2	3.087	29508	0.135596647
CM S3	3.089	32343	0.148624182
CM L1	3.089	31706	0.145697008
CM L2	3.089	40751	0.187261047
CM L3	3.087	41032	0.188552312
CM L+W1	3.086	39046	0.179426145
CM L+W2	3.085	33182	0.152479597
CM L+W3	3.081	29782	0.136855746
EC S1	3.094	71426	0.328220351
EC S2	3.079	48180	0.221399162
EC S3	3.089	36871	0.169431476
EC L1	3.08	49284	0.226472318
EC L2	3.081	41213	0.189384053
EC L3	3.078	28970	0.133124403
EC L+W1	3.074	19108	0.087806044
EC L+W2	3.075	13510	0.062081832
EC L+W3	3.074	32914	0.15124807
M S1	3.082	21599	0.099252812
M S2	3.08	20320	0.093375487
M S3	3.073	22634	0.104008896
M L1	3.073	11548	0.053065951
M L2	3.073	17704	0.081354312
M L3	3.071	22170	0.1018767
M L+W1	3.068	27586	0.126764576
M L+W2	3.071	14086	0.064728696
M L+W3	3.07	19605	0.090089883

A.2 Chapter 4 Data

A.2.1 PicoGreen

Where:

Values of wells read fluorescence

Sample numbers indicate separate biological samples

Well numbers indicate duplicates of the same biological sample in separate wells

T values indicate the number of times the well was read by the plate reader

A.2.1a DNA Release

Table A13: Determining DNA release protocol standard curve. Where standard indicates the concentration of DNA in μg/mL. The standard curve was found to be: [fluorescence = 75890*(DNA concentration) + 6858.1] with an R-squared value of 0.9836.

Standard	3.556	1.183	0.394	0.131	0.044	0.015	0.0049	0
Well 1 T1	103350	84084	34569	21691	10225	5907	3792	3786
Well 1 T2	103989	84079	34513	20406	9218	5468	3676	3567
Well 1 T3	103829	84386	33528	19849	8898	5584	3495	3552
Well 2 T1	117392	104652	57754	23222	10278	5785	5082	4247
Well 2 T2	125078	103599	53422	21204	9616	5809	4657	4058
Well 2 T3	126514	101450	51992	20524	9211	5637	4610	3772
Average	**113359**	**93708**	**44296**	**21149**	**9574**	**5698**	**4219**	**3830**

Table A14: Determining DNA release protocol florescence readings.

Sample	PBS 1	PBS 2	PBS 3	Lysis 1	Lysis 2	Lysis 3
Well 1 T1	23770	35385	20962	9347	9415	11068
Well 1 T2	20874	33680	22243	8963	7289	10775
Well 1 T2	19788	36774	23432	7489	8222	10776
Well 2 T1	24121	33484	21084	9320	9389	10913
Well 2 T2	20975	32028	21992	8971	7569	10587
Well 2 T3	19650	34690	23176	7348	8332	10593
Well 3 T1	23730	31893	21372	9320	9467	11132
Well 3 T2	21101	31031	21900	8971	7273	10657
Well 3 T3	19992	34152	22969	7348	8089	10778
Average Fluorescence	21555.67	33679.67	22125.56	8564.111	8338.333	10808.78
DNA Conc. (µg/µL)	0.193669	0.353427	0.201179	0.02248	0.019505	0.052058
DNA Amount	0.077468	0.141371	0.080472	0.008992	0.007802	0.020823

Table A15: Determining DNA release protocol florescence readings, continued. **Data excluded from further computations due to readings outside of the standard curve range.*

Sample	Cellulase 1	Cellulase 2	Cellulase 3	Hemi. 1	Hemi. 2	*Hemi. 3**
Well 1 T1	11137	10360	9910	10705	8882	*6649*
Well 1 T2	12715	12590	10626	10399	10943	*6545*
Well 1 T2	13007	10407	11300	13674	9205	*6622*
Well 2 T1	10664	10482	10113	10676	8869	*6663*
Well 2 T2	12462	12447	10257	10220	11004	*6652*
Well 2 T3	12861	10682	11058	13455	9351	*6351*
Well 3 T1	10174	10490	9797	10786	8942	*6571*
Well 3 T2	12676	12945	10353	10648	11084	*6650*
Well 3 T3	12752	10724	11030	13726	9603	*6403*
Average Fluorescence	12049.78	11236.33	10493.78	11587.67	9764.778	*6567.333*
DNA Conc. (µg/µL)	0.068411	0.057692	0.047907	0.062321	0.038301	*-0.00383**
DNA Amount	0.034205	0.028846	0.023954	0.031161	0.019151	*-0.00192**

Table A16: Determining DNA release protocol florescence readings, continued

Sample	Macero. 1	Macero. 2	Macero. 3
Well 1 T1	9453	9950	8849
Well 1 T2	10547	8854	10100
Well 1 T2	8656	10651	8571
Well 2 T1	9491	9841	9850
Well 2 T2	10230	9016	8622
Well 2 T3	8378	10730	10055
Well 3 T1	9080	9898	
Well 3 T2	10377	9134	
Well 3 T3	8557	10817	
Average Fluorescence	9418.778	9876.778	9341.167
DNA Conc. µg/µL	0.033742	0.039777	0.032719
DNA Amount	0.016871	0.019889	0.01636

A.2.1b DNase Treatment

Table A17: Fluorescence readings from PicoGreen Assay used to develop standard curve of DNA used for comparison of lyophilized versus DNase+ versus DNase-.

Standard Curve: Flour = 39767*(Conc.) + 5286.1 R Squared = 9987				
DNA Conc. (µg/mL)	**Reading 1**	**Reading 2**	**Reading 3**	**Average Reading 1-3**
0	7241	7923	7982	7715
0.0049	4914	5045	4933	4964
0.015	6337	6268	6552	6386
0.044	6350	6237	6327	6305
0.131	12692	12916	11619	12409
0.394	19093	19044	18840	18992
1.183	49988	49578	49379	49648
3.556	147242	148086	147908	147745

Table A18: Fluorescence readings for PicoGreen Assay of lyophilized versus DNase+ versus DNase- treatments.

	Reading 1	Reading 2	Reading 3	Avg. Read 1-3	Avg. DNA (μg/mL)	Avg. DNA (μg/mL)
			Lyophilized			
Sample 1	91001	91305	91610	91305	**2.16308078**	
Sample 2	77335	78752	79497	78528	**1.84177584**	2.095118
Sample 3	94574	96092	97258	95975	**2.28049807**	
			DNase-			
Sample 1	58692	58948	58993	58878	**1.34763917**	
Sample 2	56324	54011	53483	54606	**1.24022179**	1.454679
Sample 3	76755	75519	75484	75919	**1.77617707**	
			DNase+			
Sample 1	22500	22245	21915	22220	**0.42582795**	
Sample 2	11609	11485	11031	11375	**0.15311439**	0.37045
Sample 3	27027	26306	26042	26458	**0.53240711**	

A.2.2 Flavonoid

A.2.2a Lyophilization and Wash Effect

Table A19: Data showing flavonoid assay data (absorbance (Abs.) and concentration (Conc.). Treatments included total culture samples preceding lyophilization, lyophilized samples, and samples that were lyophilized then washed. Performed on 2/27/2019

Standard curve: Abs. = 1.812*(Conc.) + 0.209 (R Squared: 0.9805)							
Standard (mg/mL)	0.000	0.100	0.200	0.400	0.600	0.800	1.000
Absorbance	0.163	0.315	0.471	0.735	1.099	1.258	1.394

Cell Type: Elicited and Treated with PTX			
Treatment	**Total Culture**	**Lyophilized**	**Lyophilized & Washed**
Sample 1 Absorbance	1.865	0.829	
Sample 2 Absorbance	1.707	0.818	0.288
Sample 3 Absorbance	1.724	0.744	0.299
Sample 1 Concentration	0.913907	0.342163	
Sample 2 Concentration	0.826711	0.336093	0.043598
Sample 3 Concentration	0.836093	0.295254	0.049669

Cell Type: Unelicited			
Treatment	**Total Culture**	**Lyophilized**	**Lyophilized & Washed**
Sample 1 Absorbance	1.5700	0.8010	0.1990
Sample 2 Absorbance	1.3300	0.6460	0.1560
Sample 3 Absorbance	1.3340	0.8140	0.2450
Sample 1 Concentration	0.7511	0.3267	***-0.00552****
Sample 2 Concentration	0.6187	0.2412	***-0.02925****
Sample 3 Concentration	0.6209	0.3339	0.0199

A.2.2b DNase Effect

Table A20: Data showing flavonoid assay data (absorbance (Abs.) and concentration (Conc.). Treatments included lyophilized samples, DNase+ treated samples and DNase- treated samples. Performed on 3/19/2019.

Standard Curve: Abs. = 1.0554*(Conc.) + 0.1816 (R Squared = 0.9977)							
Standard (mg/mL)	0	0.1	0.2	0.4	0.6	0.8	1
Absorbance	0.158	0.316	0.389	0.619	0.799	1.015	1.247

Absorbance	**Concentration (mg/mL)**	**Avg. Conc. (mg/mL)**
	DNase+	
0.272	0.085655	0.001327
0.178	-0.00341	
0.099	-0.07826	
	DNase-	
0.392	0.199356	0.118502
0.271	0.084707	
0.257	0.071442	
	Lyophilized	
0.687	0.478871	0.464658
0.699	0.490241	
0.63	0.424863	

A.2.3 Phenolic

A.2.3a Lyophilization and Wash Effect

Table A21: Data showing phenolic assay data (absorbance (Abs.) and concentration (Conc.) for cells. Treatments included total culture samples preceding lyophilization, lyophilized samples, and samples that were lyophilized then washed. Performed on 2/27/2019

Standard Curve: Abs. = 5.3042*(Conc.) + 0.0856 (R Squared: 0.9937)							
Standard (mg/mL)	0.000	0.200	0.150	0.100	0.075	0.050	0.025
Absorbance	0.070	1.112	0.916	0.603	0.531	0.347	0.203

Cell Type: Elicited and Treated with PTX			
Treatment	**Total Culture**	**Lyophilized**	**Lyophilized & Washed**
Sample 1 Absorbance	1.324	0.510	0.106
Sample 2 Absorbance	1.121	0.562	0.097
Sample 3 Absorbance	1.317	0.480	0.116
Sample 1 Concentration	1.167	0.400	0.019
Sample 2 Concentration	0.976	0.449	0.011
Sample 3 Concentration	1.161	0.372	0.029
Cell Type: Unelicited			
Treatment	**Total Culture**	**Lyophilized**	**Lyophilized & Washed**
Sample 1 Absorbance	0.998	0.990	0.075
Sample 2 Absorbance	0.976	0.587	0.090
Sample 3 Absorbance	1.177	0.642	0.103
Sample 1 Concentration	0.860		
Sample 2 Concentration	0.839	0.473	0.004
Sample 3 Concentration	1.029	0.524	0.016

A.2.3b DNase Effect

Table A22: Data showing phenolic assay data (absorbance (Abs.) and concentration (Conc.). Treatments included lyophilized samples, DNase+ treated samples and DNase- treated samples. Performed on 3/19/2019.

Standard Curve: Abs. = 5.0667*(Conc.) + 0.1036 (R Squared = 0.9862)							
Standard (mg/mL)	0	0.025	0.05	0.075	0.1	0.15	0.2
Absorbance	0.057	0.214	0.399	0.535	0.634	0.806	1.121

Absorbance	**Concentration (mg/mL)**	**Avg. Conc. (mg/mL)**
	DNase+	
0.08	-0.02328	
0.072	-0.03118	-0.0295
0.069	-0.03414	
	DNase-	
0.077	-0.02624	
0.069	-0.03414	-0.0269
0.083	-0.02032	
	Lyophilized	
0.452	0.343746	
0.775	0.662431	0.5598
0.786	0.673284	

A.2.4 UPLC

Table A23: UPLC standard curve made for decellularization. Standard runs 1 and 2 were averaged to develop a standard curve, and the y-intercept was set to zero.

Standard Curve: Area = 28010*Conc.			
Standard Run Number	**Standard Concentration (mg/L)**	**Retention Time (Minutes)**	**Area**
1	6.25	2.959	191008
1	12.5	2.941	322323
1	25	2.94	696187
1	50	2.942	1434778
2	6.25	2.966	179350
2	12.5	2.982	316460
2	25	2.985	677031
2	50	2.988	1392753

Table A24: UPLC data for paclitaxel retention through decellularization process in samples treated with DNase, samples treated with buffer only, and lyophilized cells only.

Treatment	**Sample Number**	**Ret. Time (mins)**	**Area**	**PTX Conc. mg/L**
DNase+	Biomass 1	2.948	158351	0.707
	Biomass 2	2.956	157802	0.704
	Biomass 3	2.952	144573	0.645
	Supernatant 1	2.952	517184	2.308
	Supernatant 2	2.959	503952	2.249
	Supernatant 3	2.966	607290	2.710
DNase-	Biomass 1	2.967	155209	0.693
	Biomass 2	2.966	195529	0.873
	Biomass 3	2.97	147898	0.660
	Supernatant 1	2.973	434382	1.939
	Supernatant 2	2.975	580060	2.589
	Supernatant 3	2.974	495015	2.209
Untreated	Lyoph. 1	2.981	1497062	6.681
	Lyoph. 2	2.981	1244450	5.554
	Lyoph. 3	2.983	1450753	6.474

A.3 Chapter 5 Data

A.3.1 Biomass Release Experiment

A.3.1a UPLC Data (Biomass Release)

Table A25: UPLC standard curve made for release studies. Standard runs were averaged to develop a standard curve, and the y-intercept was set to zero.

Standard Curve: Area = 17206*(PTX Conc.)			
Run Number	PTX Standard Concentration (mg/L)	Retention Time (mins)	Area
1	50	3	919515
2	50	3.008	901975
3	50	3.005	795590
1	25	3.001	476498
2	25	3.003	471127
3	25	3.006	464069
1	12.5	3.001	123410
2	12.5	3.004	124360
1	6.25	3.001	31848
2	6.25	3.006	31190

Table A26: UPLC Data for PTX release from decellularized biomass. Where PTX concentration was determined from the UPLC standard curve, then PTX (mg/sample) was corrected to the volume of the sample taken.

Sample Type	Sample Number	Hour	Retention Time (mins)	Area	PTX Conc. (mg/L)	PTX mg/sample
Supernatant (850 uL)	1	1	2.999	84788	0.615976985	0.000724679
	2	1	2.993	72912	0.529698942	0.000623175
	3	1	2.995	91665	0.665937754	0.000783456
	1	6	2.998	34120	0.247878647	0.000291622
	2	6	2.998	30206	0.219443799	0.000258169
	3	6	2.999	43479	0.315870917	0.000371613
	1	12	2.997	10768	0.078228525	9.20336E-05
	2	12	2.996	13789	0.100175811	0.000117854
	3	12	2.999	17401	0.126416657	0.000148725
	1	24	3	4340	0.031529699	3.70938E-05
	2	24	3	4714	0.034246774	4.02903E-05
	3	24	2.998	6124	0.044490294	5.23415E-05
	1	48	3.001	1342	0.009749506	1.147E-05

	2	48	2.998	1735	0.012604615	1.4829E-05
	3	48	2.995	2139	0.015539637	1.82819E-05
	1	72	2.996	157	0.00114059	1.34187E-06
	2	72	3	547	0.003973904	4.67518E-06
	3	72	2.996	842	0.006117052	7.19653E-06
	1	144	0	0	0	0
	2	144	0	0	0	0
	3	144	0	0	0	0
	1	192	0	0	0	0
	2	192	0	0	0	0
	3	192	0	0	0	0
	1	240	2.998	90023	0.654008776	0.000769422
	2	240	2.998	1371	0.009960188	1.17179E-05
	3	240	2.996	269	0.00195426	2.29913E-06
Biomass Remainder	1	-	3	636	0.004620481	4.62048E-06
	2	-	3.002	314	0.002281181	2.28118E-06
	3	-	2.995	600	0.004358945	4.35894E-06

A.3.1b Sample Release Analysis

Table A27: Sample analysis of release profile development for biomass into BSA (mass of PTX released in mg). Hour 1 samples are directly from UPLC data, converted to mg/mL. Following time points were calculated by subtracting the mass of PTX left over from the previous sample (Hour 1, where 0.85 mL was sampled, 0.15 mL remained) from the concentration measured at that time point.

	Sample Number			Average	Standard
Hour	**1**	**2**	**3**	**(1-3)**	**Deviation**
1	0.000615977	0.000529699	0.000665938	**0.000603871**	6.89214E-05
6	0.000155482	0.000139989	0.00021598	**0.000170484**	4.01554E-05
12	2.90868E-09	6.72592E-05	7.9036E-05	**4.87661E-05**	4.26387E-05
24	1.97954E-05	1.92204E-05	2.55278E-05	**2.15145E-05**	3.48745E-06
48	5.02005E-06	7.4676E-06	8.86609E-06	**7.11791E-06**	1.94672E-06
72	0	2.08321E-06	3.78611E-06	**1.95644E-06**	1.89623E-06
144	0	0	0	**0**	0
192	0	0	0	**0**	0
240	0	9.96019E-06	1.95426E-06	**3.97148E-06**	5.27762E-06

A.3.2 Alginate Release Experiment

Table A28: UPLC Data for PTX release from decellularized biomass and free PTX from alginate microbeads. Where PTX concentration was determined from the same UPLC standard curve as the biomass release experiment, then PTX (mg/sample) was corrected to the volume of the sample taken.

Sample Number	Hour	Ret. Time (mins)	Area	PTX Conc. (mg/L)	PTX mg/sample
Biomass 1	1	2.998	63577	0.46188103	0.001358474
Biomass 2	1	2.997	60789	0.441626468	0.001298901
Biomass 3	1	3.001	63162	0.458866093	0.001349606
Biomass 1	6	3.002	40902	0.29714925	0.000873968
Biomass 2	6	3.001	38525	0.279880565	0.000823178
Biomass 3	6	2.999	34969	0.254046554	0.000747196
Biomass 1	12	3	14386	0.104512961	0.000307391
Biomass 2	12	3.004	9754	0.070861909	0.000208417
Biomass 3	12	2.999	15297	0.111131291	0.000326857
Free PTX 1	1	3.001	24752	0.179820993	0.000528885
Free PTX 2	1	3	20979	0.152410496	0.000448266
Free PTX 3	1	3.002	19739	0.143402011	0.000421771
Free PTX 1	6	3.001	15491	0.112540683	0.000331002
Free PTX 2	6	2.999	14556	0.105747995	0.000311024
Free PTX 3	6	2.999	2135	0.015510578	4.56193E-05
Free PTX 1	12	3.001	403	0.002927758	8.61105E-06
Free PTX 2	12	3	1834	0.013323841	3.91878E-05
Free PTX 3	12	3	738	0.005361502	1.57691E-05

Appendix B. Program Protocols
B.1 PicoGreen

Protocol description

Protocol name ..... PicoGreen_JMC

Protocol number ..... N/A

Name of the plate type ..... NUNC 96 Well Black 265301

Number of wells in the plate ..... 8 X 12

Height of the plate ..... 15.0 mm

Offset of the wells ..... 10.885 mm, 14.753 mm

Distance between wells ..... 8.994 mm, 8.980 mm

Number of repeats 3

Delay between repeats ..... 0 s

Measurement height ..... 18.00 mm

Protocol notes .....

Shaking duration ..... 5.0 s

Shaking speed ..... Fast

Shaking diameter ..... 0.10 mm

Shaking type ..... Linear

Repeated operation ..... Yes

Name of the label ..... PicoGreen_JMC

Label technology ..... Prompt fluorometry

CW-lamp filter name F485

CW-lamp filter slot A5

Emission filter name F535

Emission filter slot A5

Measurement time ..... 0.1 s

Emission aperture ..... Normal

CW-lamp energy 65535

Second measurement CW-lamp energy . 0

Emission side ..... Above

CW-Lamp Control ..... Stabilized Energy

Excitation Aperture ..... N/A

Plate map of plate 1: Varies with trial

A | M M M M M M M M M M M M

B | M M M M M M M M M M M M

C | M M M M M M M M M M M M

D | M M M M M M M M M M M M

E | M M M M M M M M M M M M

F | M M M M M M M M M M M M

G | M M M M M M M M M M M M

H | M M M M M M M M M M M M

Protocol created by .....

Protocol creation date 7/13/2017

Protocol last edited by ..... awerner

Protocol last edited 1/25/2019

Instrument serial number: 7895

Assay ID: 19266

Measured on ..... 1/25/2019 2:18:18 PM

Appendix C. Product Information

C.1 Cell Lines

Taxus chinensis: 21260C

Taxus cuspidata: 48-82-A

C.2 Chemicals and Reagents

Sucrose (Caisson Laboratories, Smithfield UT)

Gamborg-B5 (PhytoTechnology Laboratories, Lenexa KS)

Benzyl adenine (Sigma-Aldrich, St. Louis MO)

1-napthalenacetic acid (Sigma-Aldrich, St. Louis MO)

Ascorbic acid (Fisher Scientific, Hampton NH)

Citric acid (PhytoTechnology Laboratories, Lenexa KS)

L-glutamine (Caisson Laboratories, Smithfield UT)

MeJA: methyl jasmonate (Sigma-Aldrich, St Louis MO, 392707)

Cyclosporine A (Cayman Chemical, Ann Arbor MI, 12088)

Verapamil: (+ -) - verapamil hydrochloride (Acros Organics, Geel (Belgium), 329330010)

Vanadate: sodium orthovanadate (MP Biomedicals, Solon OH, 218058)

Glycerol (Thermo Fischer Scientific, Waltham MA, A16205-0D)

Sodium chloride (Sigma-Aldrich, St Louis MO, S5886)

Sodium azide (Acros, New Jersey, 19038-1000)

Hemicellulase (Sigma-Aldrich, St Louis MO, H-2125)

Cellulase (bioWORLD, New York NY 21500003-1)

Macerozyme (ICN Biomedicals Inc, Aurora OH, 152340)

Triton X-100 (Laboratory Grade, Sigma-Aldrich, St Louis MO, 9002-93-1)

PBS: phosphate buffered saline (Fisher Scientific, Hampton NH, BP2944-100)

DNase: Deoxyribonuclease I from bovine pancreas, 2000 units/mg (Sigma-Aldrich, St. Louis MO, D5025)

DPBS: Dulbecco's PBS (DPBS) (Thermo Fisher Scientific, Waltham MA, 14080-055)

Paclitaxel (Alfa Aesar, Ward Hill, MA)

Quant-iT™ PicoGreen™ dsDNA Assay Kit (Thermo Fisher Scientific, Waltham MA, P11496)

Sodium carbonate (Fischer Scientific, Hampton NH, S263-500)

Sodium nitrite (Acros, New Jersey, 42435-5000)

Aluminum chloride (Sigma-Aldrich, St Louis MO, 7784-13-6)

Sodium hydroxide (Sigma-Aldrich, St Louis MO, 1310-73-2)

Catechin: (+)- catechin (hydrate) (Cayman Chemical, Ann Arbor MI, 70940)

Hoechst Stain (Hoechst 33342, Tocris Bioscience, Bristol United Kingdom, 5517)

Paraformaldehyde (PFA) (Acros, New Jersey, 30525-89-4)

Bovine serum albumin (BSA) (Sigma-Aldrich, St Louis MO, 9048-46-8)

Sodium alginate (Willpowder, Miami Beach FL)

Calcium chloride ($CaCl_2$) (Willpowder, Miami Beach FL)

C.3 Instruments and Products

Shelf lyophilizer (VirTis BenchTop Pro with Omnitonics, SP Scientific, Stone Ridge, NY)

Evaporative centrifuge (Vacufuge plus, Eppendorf, Hamburg Germany)

Sonicator (Aquasonic 75HT, VWR, Radnor PA)

Coulter Counter: Multisizer 3™ Coulter Counter (Beckman, Brea CA)

0.5 mm diameter zirconium silicate beads (Next Advance, Troy NY)

Bullet Blender (Next Advance, Troy NY) Model: 24 Gold

Mechanical homogenizer: (BioSpec Products, Inc., Bartlesville OK, Tissue Tearor™)

UPLC: (Waters, Milford MA, Acquity UPLC H-Class)

Fluorescent Plate Reader: Victor3 1420 Multilabel Plate Reader (PerkinElmer, Waltham, MA)

Colorimetric Plate Reader: (Accuskan Go, Fisher Scientific, Hampton NH)

Microscope: Nikon Eclipse E600 MVI, Avon MA

Shaker (New Brunswick Scientific Co. Inc, Edison NJ, Model G24)

Centrifuge: (Eppendorf, Hamburg Germany, Model 5418R)